Republic of Iraq
Ministry of Higher Education
and Scientific Research
Diyala University
College of Sciences

Ferroelectric Ferromagnetic composite materials

A Thesis
Submitted to the Council of College of Science
University of Diyala in Partial Fulfillment
of the Degree of M.Sc. in Physics

By

Ali Ahmed Hassan

(B.SC. in physics 2013)

Supervised By

Prof. Dr. Thaseen H. Mubarak

Asst. Prof . Dr. Sabah M. Ali

2017 A.D 1438 A.H

Examination Committee Discussion

We certify that we have read this thesis entitled (**Ferroectric Ferromagnetic Composite Materials**) and we examined the student (**Ali ahmed Hassan**) on its content and in what is related with it, and in our opinion it meets the standard of a thesis for the degree of Master of Science in Physics .

Signature :
Name : Dr. Nadir F. Habobi
Title: Professor
Date:
(Chairman)

Signature:
Name : Dr. Nabil A. Baker
Title: Professor
Date:
(Member)

Signature :
Name : Dr. Aulfat A.Mahmood
Title:Assistant Professor
Date:
(Member)

Signature:
Name : Dr. Tahseen H. Mubarak
Title: Professor
Date:
(Supervisor)

Signature:
Name : Dr. Sabah M. Ali
Title:Assistant Professor
Date:
(Supervisor)

Approved by the dean of the college of Science / University of Diyala .

Signature:
Name :Prof. Dr. Tahseen H. Mubarak
Date:

CERTIFICATION

We certify that the thesis entitled (Ferroelectric Ferromagnetic composite materials) has been prepared under our supervision at the University of Diyala / College of Science / Department of Physics as a partial fulfillment of the requirements for the Degree of Master of science in Physics.

Signature:
Name: D. Tahseen H. Mubarak
Title: Assistant Professor
Date: / / 2017

Signature:
Name: D. Sabah M. Ali
Title: Assistant Professor
Date: / / 2017

In view of the available recommendation, I forward this thesis for debate by the examining committee.

Signature:
Name: Dr.Ziad Tariq Khuthair
Chairman of the Department of physics: Assistant professor
Date: / / 2017

يَقولُ تعالى عَزَّوجَلَّ:

بسم الله الرحمن الرحيم

وَيَسْأَلُونَكَ عَنِ الرُّوحِ قُلِ الرُّوحُ مِنْ أَمْرِ رَبِّي وَمَا أُوتِيتُم مِّنَ الْعِلْمِ إِلاَّ قَلِيلاً ﴿85﴾

صدق الله العظيم

سورة الإسراء
{85}

الآية

ACKNOWLEDGEMENT

Praise is for almighty Allah, the most merciful and compassionate , the creator of the universe, who enable me to complete this research successfully and overcome all difficulties.

I would like to express my sincere gratitude to my supervisors ***Assist Prof. Tahseen Hussein Mubarak, Ph.D.and Assist Prof. Sabah Mohamad Ali***, ***Ph.D.*** who granted me the opportunity to do this study. I am indebted to them for their suggestions and valuable remarks.

Special thank are extended to the ***Dean of the College of Science***, D. ziad Tariq Khuthair all the ***staff of the Department of Physics*** for their assistance.

Finally, I would also express my deep sense of gratitude to my **parents** and **family** my **brothers, sister** and for their unlimited encouragement and support.

My dearest friends ***Zaid Hameed, Shahlaa Monther, Chiua Hasseeb , Duraid Mahdi,Adnan Ali and Abdulwahhab Hameed .***

Ali A. H.

DEDICATION

To the three pillars of my life: my God, my father and my mother. Without you, my life would fall apart. I might not know where the life's road will take me, but Walking with You:

My God, through this journey has given me Strength.

My Father, I would like to lift your forehead high in response your grace to me.

My Mother, if love was a human it shall be you, thanks for your faith in me.

My brothers and friends, the source of my happiness and tranquility

Thanks for inspiring. We made it…

Ali A. H.

ABSTRACT

In the present study, $BaTiO_3$+$CuFe_2O_4$ composite materials were synthesized using sol-gel auto combustion chemical method, in which pre-synthesized Barium Titanate was combined with the copper ferrite, using Titanium oxide, Barium nitrate, Ferric nitrate , Citric acid, Copper nitrate Tri hydrate and ammonium solution. $BaTiO_3$ was burn on (800˚C) for 3hour then it out the oven and mixing in strung again, put in crucible and burned at 1200˚C and cooled at room temperature. $CuFe_2O_4$ was burned in (200-220˚C) and cooled at room temperature, then Calcine at (400°C) for three hours. This process was repeated to obtain ferrimagnetic and ferroelectric composites [x$BaTiO_3$+(1-x)$CuFe_2O_4$] with different weight fractions (x= 0, 0.1, 0.2, 0.3, 0.4, 0.5, 0.6, 0.7, 0.8, 0.9, 1) .Then composite powders with different weight, burn each mix at 800˚C for three hours. Then composite powder with different weight percent were milled and pressed into pellets 1.2cm, and then darken at 950˚C for three hours.

The Structural, electrical and dielectric properties of $BaTiO_3$+$CuFe_2O_4$ composite materials nanopowders have been studied using FTIR, XRD, AFM, SEM and LCR-meter analysis.

FTIR-spectra of $BaTiO_3$+$CuFe_2O_4$ composite materials powders calcined at deferent temperatures (950˚C) where shown Fourier transform infrared model barium titanate nanoparticles prepared having packets within the scope of the (522 cm^{-1}) to (547 cm^{-1}) belonging to the association of Aoxgen- metal (titanium), it featured packages within the scope of the (459 cm^{-1}) to (584 cm^{-1}) belonging to the association of oxygen - a metal (copper), as well as packages have emerged within the range (550-

600 and 400-450cm^{-1}) belonging to the association of oxygen - a metal (titanium - copper)..

The chemical phase analysis that has been used X-ray diffraction measurement device XRD confirms be copper ferrite ($CuFe_2O_4$ spinel powder), Barium Titanate (Barovskait) and materials overlapped between them. Where the study of X-ray diffraction showed that the crystal size increases with increasing temperature calcination powder (copper ferrite). While finding that the crystal size increases with the concentration of Barium Titanate decrease concentration (copper ferrite) and also found that the lattice constant decreases (at least) with the increase concentration Barium Titanate. The theoretical ferrite powder density decreases with increase Barium Titanate content.

From SEM micrographs, cobalt ferrite showed particle size is less than 100nm, also noted an increase in the particle shapes with increasing calcination temperatures. AFM figures proved that the particle size is very small, homogeneous and in the range of nano size.

Electric and dielectric properties were studied in all pelletized and sintered samples at temperature 950^0C, and the frequency range of (50 Hz – 5MHz).

AC Resistivity of all samples (sintered at 950^0C) have been measured as a function of frequency and found it decreases with increase in frequency. Dielectric constant (ε_r'), the loss tangent (tanδ) and the loss factor (ε_r'') are calculated from capacitance data, and showed that the dielectric parameters decreases with increasing frequency. This behavior is typical of ferrites as explained by Koop's model, conductivity increased with increase Barium Titanate content in $BaTiO_3$+$CuFe_2O_4$ composite materials, dielectric loss were change between increase and decrease with increase Barium Titanate, while conductivity increases with frequency increase.

Table of Contents

LIST OF FIGURES

LIST OF TABLES

LIST OF SYMBOLS

Symbol	Definition	Unit
f	Voltage frequency	Hz
P	Polarization	C/m^2
q	Electric charge	C
N	Number of dipoles per unit volume	$1/m^3$
d	distance	Mm
E	Electric field	V/cm
ε_o	Permittivity of vacuum ($8.85x10^{-12}$)	F/m
ε_r	Relative permittivity (dielectric constant)	---
C_o	Vacuum capacitance	F
C	Capacitance of dielectric material	F
ε	Permittivity of the dielectric material	F/m
X_c	Impedance of capacitor	Ω
ω	Angular frequency ($2\pi f$)	$Rad.s^{-1}$
φ	Phase angle	Degree
δ	Loss angle	Degree
I_a	Active current (resistive current)	A
I_r	Reactive current (capacitive current)	A
ε_r'	Real dielectric constant	---
ε_r''	Imaginary dielectric constant	---
tanδ	Tangent loss angle	---
Q	Quality factor	
α	Thermal Coefficient to Dielectric losses Factor	K^{-1}
T	absolute temperature	°K
UP	Unsaturated polyester	---

β	**Is the broadening of diffraction line measured at half its max.**	**rad**
D	**Crystallite Size**	**Nm**
a	**Lattice constant**	**A□**
ℓ	**Thickness**	**M**
A	**Area**	**m^2**
(hkl)	**Miller indices**	**-**

List of Abbreviations

SEM	**Scanning electron microscope**
XRD	**X-ray diffraction**
HRXRD	**High rselution X-ray diffraction**
TEM	**Transmission electron microscope**
HRTEM	**High rselution Transmission electron microscope**
TMAH	**Tetramethylammonium hydroxide**
FESEM	**Field Emission Scanning electron microscope**
CTAB	**Hexadecy trimethylammonium bromide**
TGA	**Thermo-gravimetric analysis**
EDS	**Energy dispersive spectrometry**
MPS	**Methacryloxy propyltrimethoxy silane**
FTIR	**Forrier Transform Infrared**
FWHM	**Full Width at Half Maximum**
T_N	**Neel Temperature**
T_C	**Curie Temperature**
ICDD	**International Centre for Diffraction Data**
JCPDS	**Joint Committee on Powder Diffraction Standards**
LCR	**Inductance(L), Capacitance(C), and Resistance(R)**

1.1 Introduction

The science of nanotechnology is the study of the phenomena and processed materials in terms of the balance of atomic, molecular and molecules, these characteristics an significantly different from those on a large scale in the advantages [1]. The reason that makes sense to regulate nanotechnology as a separate category is that materials, nanotechnology work differently from bulk materials [2], as the basis of nanotechnology depended on the rearrangement of atoms to make new molecules with new specifications and planned. Nano-scale material appears properties that differ from the properties in micron-sized bulky due to the large surface area [3]. When the specific surface area increases, rates of interaction of particles increase. This means that the inverse proportionality between particle size and specific surface area. Nano-size materials particle be few compensation atoms compared to bulk particles and this leads easily to link the materials. Nano-sized materials possess little surface stability and average highest binding energy per atom because of low consistency [4, 5]. The goal of knowing the nanotechnology and how to be entered in the field of manufacturing including devices and systems with accurate sizes and compositions for generating important functions and characteristics of new and better results shows us this technical feature [6]. There are many applications for nanotechnology and we can set then at figure (1-1). Recently, many applications depended on magnetism and magnetic materials, [7] and one of the materials has electrical and magnetic properties are ferrites. Ferrites are polycrystalline magnetic oxides that can be described by the general chemical formula "$XO \bullet Fe_2O_3$" in which X is a divalent ion such as Co^{2+} or Mn^{2+} [8]. In new fields, many applications found for ferrites in nanocrystalline form like magnetically guided drug

delivery, magnetic resonance imaging (MRI), catalyst, humidity and gas sensors. [9-11]

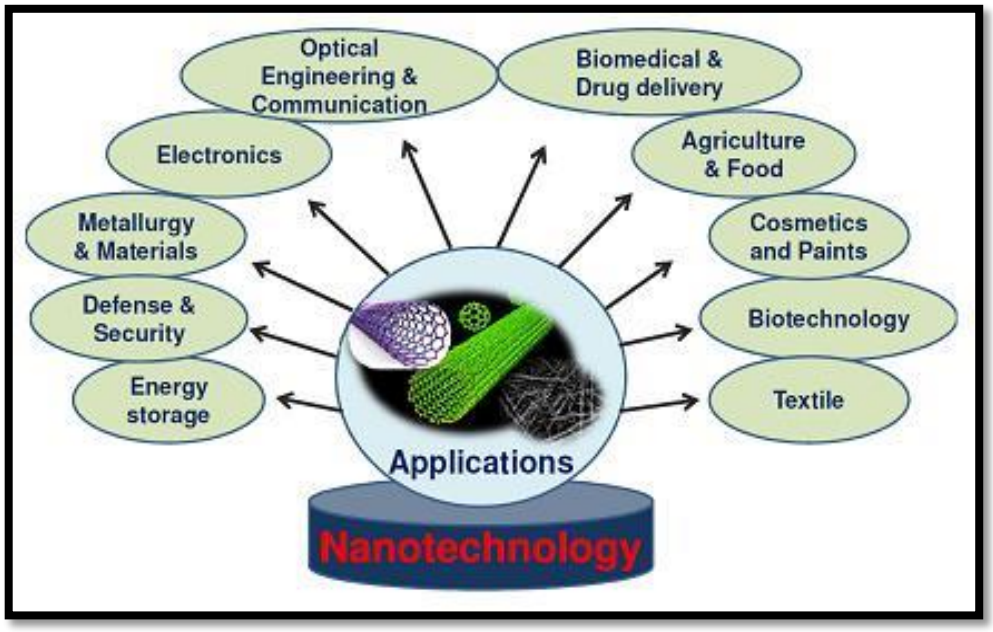

Fig (1-1): Applications of nanotechnology

One of the important categories of types of ferrite is copper ferrite which is a good magnetization, coercive force is high contrast and high magnetic field (HA) as well as premium chemical constancy and also corrosion resistance [12] .copper ferrite powder with a tight particle size distribution is to be a benefit of the media as the registration of high density and lack of size because it is usually desirable to dramatically increase the absorption of information storage and limit the issuance of the medium fuss [13, 14]. The copper ferrite is an inverse spinel with the general formula $CuFe_2O_4$, where the Cu^{+2} commute some of the iron cations in the structure [15, 16] . Its structure is like the magnetite, so far with partly various of chemical and physical properties due to the existence of copper. The metal was found in an uncovered ore dump, on the monarchy of Consolidated Rambler Mines confined near Baie Verte, New found land[17, 18]. It can

be used in a large number of applications like gas sensing ,catalytic,Li-ion batteries,high density magnetoelectric register devices, colour imaging, bioprocessing, magnetic refrigeration and ferrofluids[19-24]. Moreover, $CuFe_2O_4$ conduct it is a major significance due to high thermal stability, high electric conductivity and high catalytic efficiency for O_2 progression from alumina–cryolite system used for aluminum fabrication [25]. Barium titanate is a ferroelectric oxide is subject a transition from a ferroelectric tetragonal phase to a paraelectric cubic phase when heating above 120 °C due to its low loss and high dielectric constant characteristics. It has been used in applications, like capacitors, multilayer capacitors doped barium titanate has been found a wide application in PTC theorist and piezoelectric devices semiconductors, semiconductors, and has become one used of the most important ferroelectric ceramics[26,27]. There is a new class of physical properties of composite materials called "product Properties". After the notion of productive property as submited from before Van Suchtelen, a proper combination of magnetostrictive material , piezoelectric material can allow altitude to the magneto-electric effect. The composites exhibiting a magneto-electric impact are described as magneto-electric composite. Its impact in such composites leads to the strain induced at the ferrite juncture being mechanical connected to a stress induce in the ferroelectric juncture. Conjugation results in an electrified voltage [28,29].Ferrites are mixed metal oxides with iron(III) oxide as main component. Ferrites crystal in three crystal types: spinel (cubic crystal structure where Me¼Fe, Mn, Mg, Ni, Zn. Cd, Co, Cu, Al or a mixture of these), garnet (cubic crystal structure where Me¼Y, Sm, EU, Gd, Th, Dy, Ho, Er, Tm.or Lu) and magnetoplumbite type (hexagonal crystal structure where Me¼Be or Sr) [30]. Preparations and properties of a bulk composite such as $BaTiO_3$–$Ni_{0.5}Zn_{0.5}Fe_2O_4$, PLZT– $Ni_{0.5}Zn_{0.5}Fe_2O_4$, $BaTiO_3$–$CoFe_2O_4$, $xNiFe_2O_4$–(1-

x)$BaTiO_3$ have been recently reported [30,31]. The main problem in preparing of these composite materials is possible reaction at the interfaces between the ferroelectric and magnetic phases during sintering. Therefore, the optimization of sintering process should be performed in order to obtain di-phase composite material of desired composition. The preparation method and properties of composite materials containing barium titanate (BT) as a ferroelectric phase and Copper ferrite (CF) as a magnetic phase is presented in this work.

As a matter of fact, there have been a few attempts made to overcome this obstacle, such as spark plasma sintering technique,[32]. FM/FE core-shell precursors and powder in-soil wet chemistry method. [32,33]. They are either expensive or relatively complicate. More importantly, for Pb-free FE/FM composites (e.g., $BaTiO_3$ based composites) those often require high calcination temperature and thus possess high inter-phase reactive activity, their effects are so far not as good as those observed in $Pb(ZrTi)O_3$ based composites[32-35]

1.2 Literature review

A composite made from two or more constituent materials with a difference of chemical properties or physical when collecting articles and so material it produces different properties of individual components as the individual substances shall be separate and distinct within the final composition and be a favorite for many reasons, and advantage materials are stronger and lighter and also less expensive compared to traditional point of view[36]. Many of the earlier researchers may have collected articles for various compounds as the following :

In 2000, MAHAJAN et al [37], studied dielectric behavior, conductivity and magneto-electric effect in copper ferrite–barium titanate composites. Composites of $CuFe_2O_4$ and $BaTiO_3$ were prepared using a conventional ceramic double sintering process. The presence of both phases was confirmed by X-ray diffraction. The variations of resistivity and (thermo emf) with temperature in these samples were studied. All the composites showed (n-type) behavior. The variation of dielectric constant (ε□) in the frequency range was between 100 Hz to 1 MHz and with the temperature at constant frequency were studied. The conduction phenomenon was explained on the basis of a small Polaron mobility model. Also confirmation of this phenomenon was made with the help of A.C conductivity measurements. The static value of the magneto-electric conversion factor, i.e. d.c. $(ME)_H$ was studied as a function of intensity of the magnetic field. The maximum value of the ME coefficient has been observed in 75% phase Ferroelectric compound.

In 2002, MAHAJAN et al [38], studied dielectric behavior and magnetoelectric effect in cobalt ferrite $CoFe_2O_4$– $BaTiO_3$ composites and their electrical properties. Cobalt Ferrite(CF) combining with Barium Titanate(BT) composites were prepared using(conventional ceramic double sintering methods) with various compositions by using measurements (XRD,L.C.R meter). It was confirmed that presence of two phases in composite materials using(X-ray diffraction). The D.C resistivity, A.C conductivity, dielectric constant (ε□) and loss tangent tan (δ)and thermo emf as a function of temperature in the temperature range 300 K to 600 K were measured. Where the frequencywas between ranged 100 Hz to 1 MHz and also with the temperature at a constant frequency of 1 KHZ has been studied. It was discussed the nature of conductivity on the

basis of a small Polaron mobility model. The study has a fixed value of the magneto-electric conversion factor as a function of magnetic field.

In 2003, Arya et al. [39], studied dielectric behavior properties of nanometer sized(Barium Strontium Titanates(BST)) prepared by(the polymerization citrate precursor method). Since these oxides were found with a cubic structure, which is retained until after heating at 800 ºC. Particle size is almost nanoscale reasonably stable. They found that the dielectric constant of sintered of these oxides decreases from 510 for $BaTiO_3$(BT) to 190 for $SrTiO_3$(ST) at 100 KHz.

In 2004, Xiwei Qi et al [40], studied dielectric behavior, magnetic and electric properties of ceramic ferroelectric–ferromagnetic composite(xPMZNT·(1 –x) NiCuZn), in which x varies as (0, 0.1, 0.2, 0.4, 0.6, 0.9, and 1.0) using a standard ceramic technique.

In 2005, J. G. Wan et al [41], studied structure,magnetic and electric properties of Magneto-electric $CoFe_2O_4$–$Pb(Zr,Ti)O_3$ composite thin films .The Magnetoelectric (ME) $CoFe_2O_4$–$Pb(Ti, Zr)O_3$ composite thin films have been prepared by a spin-coating technique and sol-gel motheds and spin-coating technique . The use of X-ray diffraction and scanning electron microscopy was noted that there is a gathering of atoms and the separation of the phases of the $Pb(Zr,Ti)O_3$ and $CoFe_2O_4$ phases in the thin films. Ferroelectric test unit, Vibrating sample magnetometer , and magnetoelectric measuring device were used to describe the ferroelectric and magnetic properties, likewise the ME effect of the films. It turns out that each of the films exhibit magnetic properties of ferroelectric good, as well as the impact of ME. It is noted the initial presence of magnetoelectric high voltage coefficient of the film.

In (2007) , Cui et al [42], prepared Nb-doped $BaTiO_3$ nanocrystalline powders and ceramics by a simple sol–gel process, using $H_3[Nb(O_2)_4]$ as a precursor. The powders and ceramics were characterized by XRD, SEM and TEM, while dielectric properties of the ceramics were also determined. The results indicated that the powders synthesized by sol–gel process were in nanometer scale, which were mainly composed of cubic $BaTiO_3$ with small amount of $BaCO_3$.

In 2007, A. KUMAR RAY [43],studied the synthesis and characterization of $BaTiO_3$ powder prepared by combustion synthesis process. This study described a simple low temperature combustion synthesis method of barium titanate powders. XRD diffraction pattern of $BaTiO_3$ calcined in air at (600,700,800,900℃),the peaks become sharped and the phase pure BaTiO3 is found at 900℃ through citrate precursor method. Further, the oxidation of citrate precursor by HNO_3 was accompanied by the evolution of CO_2 , NO_2 and water vapour and the gas evolution helped the product to result in a fine-grained structure. Citric acid and HNO_3 presented in the solution play the key role for the synthesis of shaped barium titanate at a low temperature. The average particle size of $BaTiO_3$ at different temperatures was calculated using Scherrer's formula and it was found to be around 24nm. Scanning electron micrograph of this powder considerable amount of a nanorod formed.

In (2008),**Ramajo et al. [44],** synthesized and studied $BaTiO_3$ powder from the Pechini method. The synthesis of $BaTiO_3$ starts at 150ºC by the thermal dehydration of organic precursors. The usual inevitable formation of barium carbonate during the thermal decomposition of the precursor could be retarded at lower calcination temperatures and optimized heating rates. The organic precursors were treated at temperatures between 200 and 400◦C. Samples were then calcined at 700 and 800 ◦C for 4 and 2 h,

respectively. The resulted ceramic powders were characterized by gravimetric and differential thermal analyses, X-ray powder diffraction and infrared spectroscopy. It was found that depending on the heating rate and final temperature of the thermal treatment, high amounts of $BaCO_3$ and TiO_2 could be present due to the higher concentration of organics in the final calcination step.

In 2008 Habib et al. [45], synthesized and studied barium titanate ($BaTiO_3$) nanopowder using two TiO_2 powder precursors with different particle sizes and barium hydroxide via hydrothermal route. They studied the effect of temperature, time and particle size on barium titanate using transmission electron microscopy (TEM), scanning electron microscopy (SEM) and X-ray diffraction (XRD) techniques. TEM observation of low reaction temperature samples (60◦C) supports in situ transformation or short range dissolution precipitation reaction mechanism. The fine grained TiO_2 (~25 nm) precursor reacted faster than coarse grained TiO_2 (~110–125 nm) precursor. The phase of the obtained $BaTiO_3$ in all samples was found to be cubic.

In 2008, K. Kamishima et al [46], studied the simple process synthesis of $BaTiO_3$–$(Ni,Zn,Cu)Fe_2O_4$ Ceramic Composite. Ceramic composites (2Ni 0.41 Zn 0.41 Cu 0.18 Fe_2O_4 –$BaTiO_3$) were successfully prepared by a direct solid-state reaction of raw materials ($BaCO_3$, CuO, α-Fe_2O_3, NiO, TiO_2 , and ZnO). The X-ray diffraction (XRD) and electron probe micro analysis (EPMA) measurements were performed on these samples and it is confirmed that the composites consist of spinel ferrite and $BaTiO_3$ phases. The composites are so homogeneous that the ferrite and $BaTiO_3$ grains do not react with each other and have radius in the range of 1–5 μm. Hexagonal $BaTiO_3$ (h -$BaTiO_3$) can be made in this composite form with a sintering temperature of 1200 °C, although h -$BaTiO_3$ can be usually synthesized above 1460 °C. The freezing-point depression of

$BaTiO_3$ takes place due to the mixing with the spinel ferrite, which may result in the formation of h -$BaTiO_3$ at a low temperature of 1200 °C.

In 2010, Ramana et al [47],studied and prepared the ferromagnetic-dielectric $Ni_{0.5}Zn_{0.5}Fe_{1.9}O_4-\delta/PbZr_{0.5}2Ti_{O.48}O_3$ particulate composites electric, magnetic, mechanical, and electromagnetic properties.Novel ferromagnetic-dielectric particulate composites of $Ni_{0.5}Zn_{0.5}Fe_{1.95}O_{4-\delta}$ (NZF) and PbZr0.52TiO.48O_3(PZT) were by using the conventional ceramic method. The presence of two phases in composites was confirmed by XRD technique. The variations of dielectric constant with frequency in the range of 100 kHz–1 MHz at room temperature and also with temperature at three different frequencies (50 kHz, 100 kHz, and 500 kHz) were studied. Detailed studies on the dielectric properties were done to confirm the magnetoelectric interaction between the constituent phases may that be resulted in various anomalies in the dielectric behaviour of the composites. It is proposed that interfaces play an important role in the dielectric properties, causing space charge effects and Maxwell-Wagner relaxation, particularly at low frequencies and high temperatures.

In 2011, Khamkongkaeo et at [48], studied frequency-dependent magnetoelectricity of $CoFe_2O_4-BaTiO_3$ particulate composites. $CoFe_2O_4$-$BaTiO_3$ particulate composites were prepared by wet ball milling method,and their magnetoelectric (ME) effect was studied as a function of their constituents and modulation frequency. The results show that the ME coefficient increases as a function of modulation frequency from 400 to 1000 Hz and the ME characteristics of ME curves are also modified because the electrical conductivity of the $CoFe_2O_4$ phase is sensitive to the increase in frequency between 400 and 1000 Hz. The third phase $Ba_2Fe_2O_5$ formed during the sintering tends to reduce the ME effect.

In 2012, Bhuiyan et al [49],the Synthesis and Characterization of Barium Titanate ($BaTiO_3$) Nano particle. Barium titanate (BaTiO3) nanoparticles were synthesized via an electrochemical route from Ti metal plate at room temperature. Structural, compositional and optical properties were characterized by XRD, SEM, EDX, FTIR, UV- Vis and photoluminescence (PL) spectroscopy. TheX-ray diffraction (XRD) confirmed the preferential growth of $BaTiO_3$ nano particles that width is ~15 nm in the (110) orientation. The SEM image shows the synthesized BaTiO3 were nanowires in shape. The EDX measurements confirm that the composition of the samples was Ba, Ti and O elements. UV – V is Spectroscopy shows absorption peak at ~330 nm. PL measurements reveal an intense and broad band at around the green colour emission region.

In 2012, Joshi et al [50], studied the synthesis and dielectric behavior of nano-scale Barium Titanate. In this study, an effort has been made to synthesize nano-scale barium titanate powder by sol-gel and hydrothermal methods. Characterization of the synthesized Barium Titanate is conducted by using X-ray diffraction for crystallite size,Transmission Electron Microscopy for particle size and scanning electron microscopy for surface morphology. It is observed that the powders prepared by Sol-gel and hydrothermal routes have almost similar average crystallite size of 34 ± 2 nm. Electrical properties such as dielectric constant, dielectric dissipation factor and electrical resistivity have also been measured. Hydrothermal process has enabled the synthesis of material with higher dielectric constant of 4000 compared to the Sol-gel route value of 1600. The dielectric dissipation factor is measured and found to be less 0.3 than a wide range of frequencies for powders generated using both processes.

In 2013, Bochenek et al [51],studied the Ferroelectric–Ferromagnetic composites based on PZT type powder and ferrite Powder. A ferroelectric-

ferromagnetic composites based on PZT powder have been obtained in presented work. The main aim of combination of ferroelectric and magnetic powders was to obtain material showing both electric and magnetic properties. Ferroelectric ceramic powder (in amount of 90%) was based on the doped PZT type solid solution while magnetic component of the composite was nickel-zinc ferrite Ni_{1-x} $Zn_xFe_2O_4$ (in amount of 10%). The synthesis of components of ferroelectric-ferromagnetic composite was performed using the solid phase sintering. Final densification of synthesized powder has been done using free sintering. For obtained of ferroelectric-ferromagnetic composites the XRD, the microstructure, EDS, dielectric, magnetic, internal friction and electrical hysteresis loop investigations were performed. Obtained results showed the correlations between the magnetic subsystem and the electrical subsystem of the ferroelectric-ferromagnetic composites. Such properties of obtained composites give the possibility to use them in memory applications of new type.

In 2014, Haffer et al [52],studied the synthesis notion of a nanostructured of $BaTiO_3$/ $CoFe_2O_4$ composite across multiferroics. The mixture of a periodically ordered, nanostructured composite consisting of $BaTiO_3$(BT) and $CoFe_2O_4$(CF) was presented. In a first step, mesoporous $CoFe_2O_4$(CF)was prepared by the structure, replication method (Nanocasting) using [Mesoporous KIT-6 silica as a structural fungus]. Subsequently, BT was created inside the pores of CF by the citrate route, give rise to in a well - ordered composite material of jointly phases. The two components are known for their distinct Ferroic properties, namely Ferrimagnetism (CF) and Ferroelectricity (BF), on the ranking. Therefore, this proof of synthesis concept offers new Point of views in the invention of composite materials with Multiferroic properties.

In 2015, Alexander et al[53],studied magnetic and crystal properties of multiferroic composites [(x)MFe_2O_4 + (1-x)$BaTiO_3$],where (M = Ni, Co). Multiferroic composites of [$(BaTiO3)_{1-x}$ + $(CoFe_2O_4)_x$] with x = 0.2, and 0.4[(1-x)$BaTiO_3$ + (x)$NiFe_2O_4$]with x = 0.2, 0.3 and 0.4 and[$(CoFe_2O_4)_x$ + $(BaTiO_3)_{1-x}$] with x = 0.2, and 0.4 [(x)$NiFe_2O_4$ + (1-x)$BaTiO_3$] with x = 0.2, 0.3 and 0.4 have been synthesized by mixing $CoFe_2O_4$ ($NiFe_2O_4$) spinel and $BaTiO_3$ piezoelectric. Distribution of Co (Ni) ions on 8a and 16d positions of the spinel lattice (space group F d-3m) is determined by (neutron powder diffraction). The Magnetic structure of wave vector of the spinal structure is (k = 0). The dielectric permittivity of the composites was measured in the frequency range (102 – 105 Hz).Where the dielectric permittivity decreased with low frequencies from(~940 for x = 0.2 to ~360 for 0.4).

1.3 Applications of ME composites

The device, the electric composite is classified into three types based on the magneto:

1) The device using ferroelectric and magnetic properties separately.
2) The device that employingthe magnetic and ferroelectric properties, but without any ME interaction.
3) The device whose action is based on ME effect The Faraday phase invertors operating in the microwave region, Also the reversing optical modulators and the optical processors came under the devices of the second type and the first type, which is not considered significant in the present text. The third type of devices is based on the ME effect. It is the tool for the conversion of energy from magnetic to the electric form. The gyrator was proposed by Tellegen [54] using the ME materials, as well as Austin suggested some species of an applications of ME material, Respectively, Optical diodes, Amplification, ME data storage and

switching, Spin wave generation, Modulation of amplitudes, polarizations and phases of optical waves and Frequency conversion [54].

1.4 Objective of the reseach

1- Preparing $BaTiO_3$, $CuFe_2O_4$ nanoparticle and composite [$(BaTiO_3)_{x+}$ $(CuFe_2O_4)_{1-x}$] with different composition where, x takes a value (0.1 to 0.9) by using sol-gel auto-combustion method.

2- Studying the structural properties using XRD, AFM, SEM and FTIR for some powder that calcined at the different temperatures.

3- Studying the dielectric properties as a function of frequency in the range 50 Hz-5MHz for all samples.

2-1 Introduction

This chapter demonstrates the theoretical part which includes the explanation of Multiferioc Materials it is defined as two or more of the main ferroic orders like ferroelasticity,ferromagnetism and ferroelectricity , the two previous being the most important. Although present technologies incorporate both ferro-magnetic and -electric materials and have been for a long time, no known materials presentation these properties at room temperature . Hence $BaTiO_3$ and $CuFe_2O_4$ were considered as suitable constituents in terms of ferroelectric and ferrimagnetic properties. In spite of no reports on $BaTiO_3$+$CuFe_2O_4$ composite synthesized using sol-gel auto combustion chemical method, we tried to synthesize and study structural, and dielectric characteristics of this material system.This $BaTiO_3$ is combined with $CuFe_2O_4$ during its synthesis using sol-gel auto combustion chemical method .

2-2 Ferroelectrics

It is a state of certain non-conducting crystals or dielectrics that when an external electric field, cause reverse electrical polarity that shows the crystal. Rochelle salt ($KNaC_4H_4O_6$•$4H_2O$) is the first ferroelectric material that was prepared more than 400 years ago. Firstly, because of easy preparation of Rochelle salt made it interesting for the study, but its solubility made it technologically barren [55] . Discovery of barium during World War II was the first jump technology in ferroelectricity. Steatite, mica, TiO_2, $MgTiO_3$ and $CaTiO_3$ were used materials for capacitors before the discovery of barium titanate, barium titanate was widely used for capacitors due to the dielectric constant is more than 1100 and compared to the previously reported materials is very high [56]. On the basis of symmetry operations, the ferroelectricity of crystals were explained. 32

different ways can be joined in symmetry operations, resulting in 32 different crystal classes.

The 32 point groups were categorized into: (a) Crystals with identical center and contains 11 point groups that were assorted as centrosymmetric and don't show polarity, (b) crystals without center of symmetry and contains 21 point groups that were assorted as non-centrosymmetric, these classes can be divided into two classes: piezoelectric and pyroelectric. Ferroelectrics are subclass of piezoelectric and pyroelectric [57], have the polarization identical to the polarization of pyroelectric but the variance between them that the polarization of ferroelectrics is reversed through the use of external electric field [58] . Four subcategories in the group of ferroelectric materials: tungston Bronze, pyrchlore, layer structure and pervskite group.

The mineral name of calcium titanate is perovskite, it has cubic structure. Ferroelectricity is characteristics of compound with distorted perovskite structure [59] .The ferroelectrics materials were had important characteristic called ferroelectric Curie point (Tc). At a temperature above Tc, the crystal does not exhibit ferroelectricity; on the other hand, when the temperature is below Tc, the crystal exhibits ferroelectricity. If the temperature decreases to Curie point, transition phase structural of ferroelectric materials from a paraelectric to a ferroelectric and this temperature of the phase transition called the Curie temperature Fig.2-1 [60,61]. Ferroelectric materials have many applications such as:

1- radio and communication filters.

2- ultrasonic transducers.

3- communication filters and radio.

4- medical diagnostic transducers and piezoelectric sonar.

5- ferroelectric thin film memories etc.[62,63].

2-2-1 $BaTiO_3$

Chemical formula: $BaTiO_3$

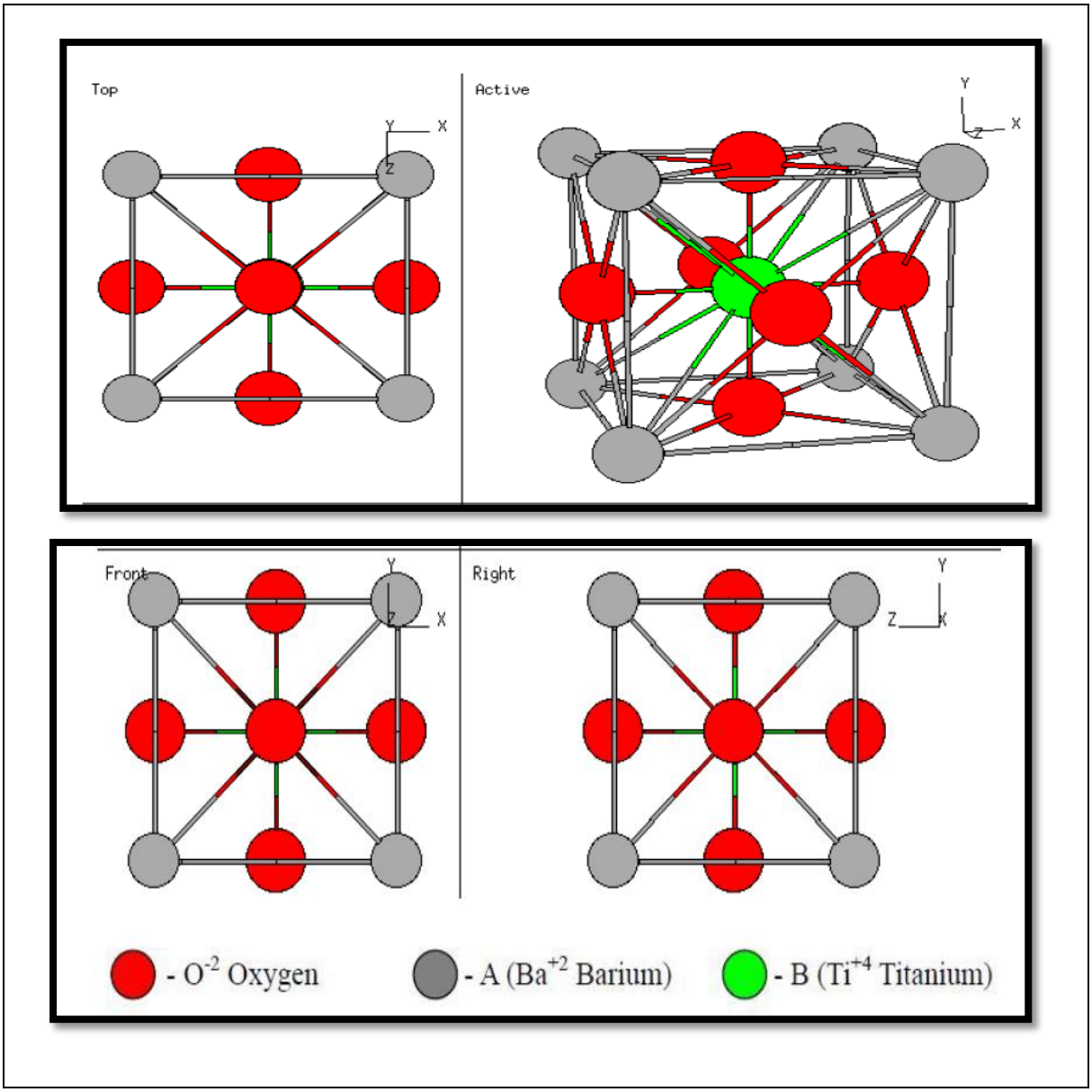

Fig.2-1 Perovskite Structure[64]

2-2-1 -1 The prototypical Ferroelectric of $BaTiO_3$

The observation of ferroelectric behavior in $BaTiO_3$ made it first and probably the most extensively investigated of all ferroelectrics and is basically due to the properties of its polymorphs. The discovery led to the availability of dielectric constant (**κ**) up to 2 orders of magnitude, greater than that had been known before. Reasons that made BaTiO3, a curious field of study:

- Relatively simple crystal structure
- Ferroelectric at room temperature (θc=120°C)
- Durable
- Easily prepared in the form of thin film, single crystal, or polycrystalline ceramic [65] .

2-2-1-2 Crystal Structure

The Ba^{2+} and O^{2-} forms a face centered cubic arrangement with Ti^{4+} occupying the octahedral interstices. $BaTiO_3$ exhibits para-electricity and an isotropic di-electricity due to the high symmetry of its cubic phase. When cooled below θc , there is a change in structure from cubic phase to distorted tetragonal with the displacement of positive and negative charge centers within the sub-lattice as show in Fig.2. 2 [66]. Due to this, a dipole moment parallel to one of the cubic axes of original phase arises and this spontaneous polarization generated in the tetragonal structure leads to piezoelectric and ferroelectric behavior.

Transformations:

Rhombohedral(<-90°C), Orthorhombic(<0°C), Tetragonal(<120°C), Cubic(>120°C)

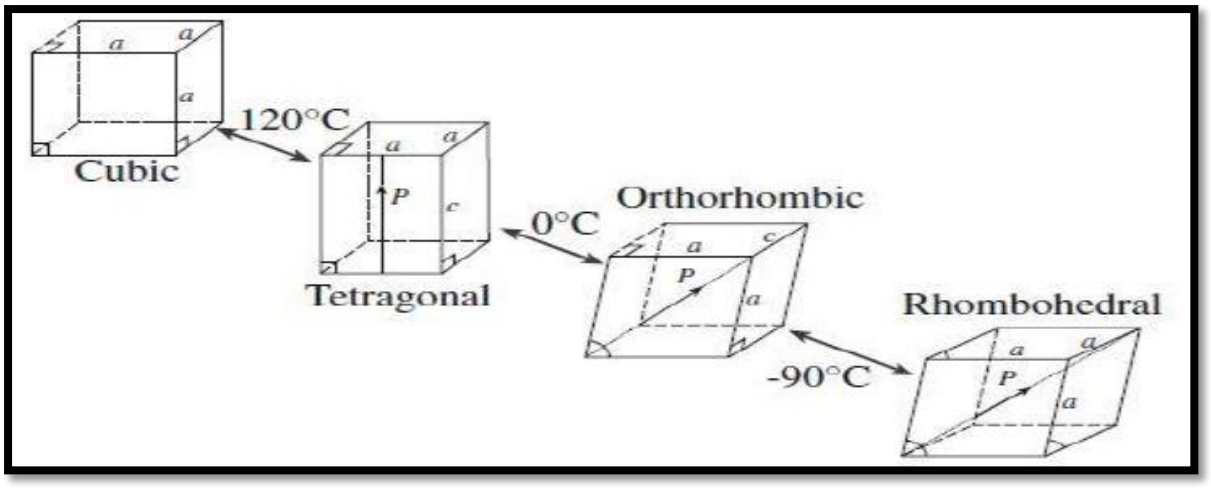

Fig. 2.2: $BaTiO_3$ Polymorphs showing direction of polarization [66]

However $BaTiO_3$ is rarely used in its pure form, solid-solution with an iso-structural compound is used to broaden the θc as well as shifting it to the lower temperatures.

(Ex: solid solution of $BaTiO_3$ and $SrTiO_3$) [66].

The firing of $BaTiO_3$ ceramics in an inert atmosphere (argon) , without sacrificing densification can lead to a dramatic increase of both the dielectric constant and dissipation factor of the samples[67].

2-2-1-3 Properties of $BaTiO_3$

It is Ferroelectric,by inclusion ,piezoelectric and also para-electric material as well as hysteresis loop for polycrystalline $BaTiO_3$ ceramic has a lower Pr and higher Ec than the single crystal. Fusion degree amounting is 1625°C and density is 6.02 g/cc. demeanor as tanδ and dielectric changes with frequency. Proving that the high values of the dielectric constant is in perfect stability to room temperature in the extent of high-grading [66].

- Solid solution can be formed
- Grain size can be reduced

- Induction of mechanical stresses in thin films

So study of all these aspects are of great importance to enhance the applicability.

2-2-1-4 Applications of $BaTiO_3$

$BaTiO_3$ being a dielectric ceramic is used for capacitors (Disk capacitors, MLCC etc.). Also as a piezoelectric material it is used for transducers and microphones. The Curie point of $BaTiO_3$ is 120 °C and its spontaneous polarization is about 0.15 C/m^2 at room temperature [68]. Polycrystalline $BaTiO_3$ exhibits positive temperature co-efficient, making it useful for thermistors and self-regulating electric heating systems.

2-2-1-5 Major Research on $BaTiO_3$

The recent advances relating to electronic devices modeled from $BaTiO_3$ show the trend of improved performance with continuous miniaturization. For MLCCs, this means enhanced capacitance per unit volume of the component. This can be achieved by increasing the number of active layers to 200–400 and by lowering the dielectric layer thickness below 2–3μm [69]. For capacitors, important properties such as break down voltage and DC leakage are dependent on the pore defects, layer thickness and grain size. The effective thickness of dielectric layer is expected to be several, e.g. at least 3–5, grains. Therefore $BaTiO_3$ powders with particle size in nanometer- range, a large surface area with high homogeneity are required to achieve good sinterability as well as fine grained microstructure in sintered ceramics.

2.3 Ferrimagnetic materials

In physics, a ferrimagnetic material is one that has populations of atoms with opposing magnetic moments, as in antiferromagnetism; however, in ferrimagnetic materials, the opposing moments are unequal and a spontaneous magnetization remains[70]. This happens when the populations consist of different materials or ions (such as Fe^{2+} and Fe^{3+}). Ferrimagnetism is exhibited by ferrites and magnetic garnets. The oldest known magnetic substance, magnetite (iron (II, III) oxide; Fe_3O_4), is a ferrimagnet; it was originally classified as a ferromagnet before Néel's discovery of ferrimagnetism and antiferromagnetism in 1948 [71].

Some ferrimagnetic materials are YIG (yttrium iron garnet), cubic ferrites composed of iron oxides and other elements such as aluminum, cobalt, nickel, manganese and zinc, hexagonal ferrites such as $PbFe_{12}O_{19}$ and $BaFe_{12}O_{19}$, and pyrrhotite, $Fe_{1-x}S$ [72].

2.3.1 Effects of temperature

Ferrimagnetic materials are like ferromagnets in that they hold a spontaneous magnetization below the Curie temperature, and show no magnetic order (are paramagnetic) above this temperature. However, there is sometimes a temperature below the Curie temperature at which the two opposing moments are equal, resulting in a net magnetic moment of zero; this is called the magnetization compensation point. This compensation point is observed easily in garnets and rare earth-transition metal alloys (RE-TM). Furthermore, ferrimagnets may also have an angular momentum compensation point at which the net angular momentum vanishes. This compensation point is a crucial point for achieving high speed magnetization reversal in magnetic memory devices [73].

2.3.2 Properties

Ferrimagnetic materials have high resistivity and have anisotropic properties. The anisotropy is actually induced by an external applied field. When this applied field aligns with the magnetic dipoles, it causes a net magnetic dipole moment and causes the magnetic dipoles to precess at a frequency controlled by the applied field, called Larmor or precession frequency. As a particular example, a microwave signal circularly polarized in the same direction as this precession strongly interacts with the magnetic dipole moments; when it is polarized in the opposite direction the interaction is very low. When the interaction is strong, the microwave signal can pass through the material. This directional property is used in the construction of microwave devices like isolators, circulators and gyrators. Ferromagnetic materials are also used to produce optical isolators and circulators. Ferrimagnetic minerals in various rock types are used to study ancient geomagnetic properties of Earth and other planets. That field of study is known as paleomagnetism [73].

2.3.3 Molecular ferrimagnets

Ferrimagnetism can also occur in molecular magnets. A classic example is a dodecanuclear manganese molecule with an effective spin of S = 10 derived from antiferromagnetic interaction on Mn (IV) metal centers with Mn (III) and Mn (II) metal centers [74].

2.3.4 Copper ferrite

The Cu-Fe-O system is of long-standing interest in solid-state physics, mineralogy, ceramics and metallurgy. By virtue of its magnetic and semiconducting properties, copper ferrite ($CuFe_2O_4$) and its solid solutions with other ferrites are widely used in the electronic industry [75]. Copper ferrite is one of the important spinel ferrites MFe_2O_4 because it exhibits

phase transitions, changes semiconducting properties, shows electric switching and tetragonality variation when treated under different conditions in addition to interesting magnetic and electrical properties with chemical and thermal stabilities [76]. It is used in a wide range of applications in gas sensing [77], catalytic applications [79], Li-ion batteries [80] high density magneto-optic recording devices, color imaging, bioprocessing, magnetic refrigeration and Ferro's fluids[81]. Moreover, CuFe2O4 assumes great significance because of its high electric conductivity, high thermal stability and high catalytic activity for O_2 evolution from alumina–cryolite system used for aluminum production [82]. $CuFe_2O_4$ is known to exist in tetragonal and cubic structures. Under slow cooling Cu-ferrite crystallizes in a tetragonal structure with lattice parameter ratio c/a of about 1.06. Tetragonal phase of Cu-ferrite has an inverse spinel structure with almost all Cu^{2+} ions occupying octahedral sublattice, whereas Fe^{3+} ions divide equally between the tetrahedral and octahedral sub lattices [83]. The tetragonal structure is stable at room temperature and transforms to cubic phase only at a temperature of 360°C and above due to Jahn–Teller distortion. The distortion is directly related to the magnetic properties. The cubic structure possesses a larger magnetic moment than that of the tetragonal one, because there are more cupric ions (Cu^{2+}) at tetrahedral sites in a cubic structure as compared to that in the case of tetragonal structure [84].

2-4 Multiferroism

The expression multiferroism has been described materials that two or all three of ferroelectricity, ferromagnetism and ferroelasticity happen in the same phase [85]. This means that the materials have a spontaneous magnetization, polarization and deformation which can be reoriented by an applied magnetic field, electric field and applied stress respectively.

The simultaneous presence of these three or even two in the selfsame step are rarein nature. In spite of magnetism and ferroelectricity resort to preclude one another, there are several methods in which these properties reside and such systems are known as magnetoelectric [86,87]. A magnetoelectric materials has a casual magnetization that can be converted by using magnetic field, a casual polarization that can be converted by using electric field and often conjugation amidst the two. This has unlock a modern usherette route in technology where we have extra degree of freedom for manipulating the job [88,89] .Mostly in store materials ferroelectric polarization and magnetization are exercised to encode duple input of FeRAMs and MRAMs. Hence these amalgamations of FeRAMs and MRAMs offers a non-volatile magnetic stock pilling arrangement because it exercises alow-power electrical write procedure and non-destructive magnetic read procedure. Relationship between multiferroic and magnetoelectric materials obtained .The nickel iodine boracite was chiefied magnetoelectric material reported [90].

Later on, many multiferroic boracite composie have been prepared [91,92]. However all of them have complex structures with many atoms and more than one formula unit per unit cell.

Generally, the multiferroics are categorized in two groups: (1) type I multiferroics[86]. This group of Multiferroics contains those perovskite in which ferroelectricity and ferromagnetism have different sources (cations at A-site and B-site respectively). Type I Multiferroics are further classified in many subclasses on the basis of origin of ferroelectricity, ferroelectricity due to shifting of B-cation [86]. ferroelectricity due to lone pairs [87],ferroelectricity due to charge ordering[89],and geometric ferroelectricity [90]. (2) Type II Multiferroics (Magnetic Multiferroics) the materials in which the ferroelectricity is originated from magnetism and

implies strong magnetoelectric coupling [86], this type divide in two categories. spiral type [87] and collinear magnetic structures [92].

2-5 Ferri-ferro composites

Ferroelectric/ferrimagnetic (FE/FM) composite ceramics are of much interest due to their outstanding and tailorable multiferroic properties in comparison with rare single-phase multiferroics[93–96].They may be utilized to develop various multifunctional devices such as magnetoelectric and inductance-capacitance (LC) integrated devices[93–96]. However, in these co-fired systems, detrimental interfacial interaction between the two phases usually takes place, rendering the intrinsic properties of both phases significantly deteriorated[96]. For example, impurities are easily formed in FE/FM ceramics due to inter-diffusion of atoms and interfacial reaction[96–99]. Such interaction would induce high concentrations of defects in both phases, which contributes considerably to the high conductivity and dielectric loss (tanδ) of FE/FM composite ceramics prepared by traditional ceramic method[99]. Besides, it is also considered as one of the most important causes those are responsible for the much lower experimental magnetoelectric property of FE/FM composite ceramics than that predicted[96]. Obviously, it is critical to improve the chemical compatibility of the constituent phases at high temperatures and depress effectively the unfavorable interfacial interaction in order to obtain highquality FE/FM composite ceramics[99-103].

As a matter of fact, there have been a few attempts made to overcome this obstacle, such as spark plasma sintering technique,[103]. FM/FE core-shell precursors and powderin-sol wet chemistry method.[104-106]. They are either expensive or relatively complicate.

More importantly,for Pb-free FE/FM composites (e.g., $BaTiO_3$ based composites) those often require high calcination temperature and thus

possess high inter-phase reactive activity, their effects are so far not as good as those observed in Pb(ZrTi)O_3basedcomposites[103-106]. For instance, $BaTiO_3/Ni_{0.5}Zn_{0.5}Fe_2O_4$ (BTO/NZFO) ceramic composites prepared by these methods exhibit low permittivity (100–500 at 1 kHz) and/or high tangent loss (0.2 at 1 kHz) when NZFO content is around 0.3[105,106].Therefore, their dielectric/electric properties need to be further improved or recovered.In this paper, a simple method that takes advantage of nano ferrite precursors synthesized by combustion method is demonstrated to be substantially valid to recover the outstanding intrinsic dielectric/electric properties of $BaTiO_3/Ni_{0.5}Zn_{0.5}Fe_2O_4$ composites through introducing interfacial barrier for conduction as well as for ionic inter-diffusion. As a matter of fact, it has been reported the dielectric loss and conductivity of single NZFO ceramics can be significantly reduced by taking such NZFO fine powders as precurcors.[107].It was attributed to fine grain size and interfacial amorphous phase formed which acts as barrier for hopping conduction between NZFO grains. Thereafter, we considered it would be also contributable most probably to recover the electric properties of BTO/NZFO ceramic composites, which are typical FE/FM composite ceramics needing calcination at relatively high temperature.

2-5-1 Electrical properties of spinel ferrites

Spinel ferrites materials have low electrical conductivities when compared to other magnetic materials and hence they find wide use at microwave frequencies. Spinel ferrites, in general are semiconductors with their conductivity lying in between 10^2 and 10^{-11} Ohm^{-1} cm^{-1}. The

conductivity is due to the presence of Fe^{2+} and the metal ions (Me^{3+}). The presence of Fe^{2+} results in n-type behaviour and of Me^{3+} in p –type behaviour. The conductivity arises due to the mobility of the extra electron orther positive hole through the crystal lattice. The movement is described by a hopping mechanism, in which the charge carriers jump from one ionic site to the other. In such a process the mobility of the jumping electrons or holes are found to be proportional to $e^{-E/kT}$ where E- the activation energy, k-Boltzmann's constant, T- the temperature in degree absolute.

2-5-2 Dielectric properties of spinel ferrite

The dielectric property of ferrite is important to physicists. These properties are not constant; they can change with frequency, orientation, mixture, and pressure and molecule structure of the material. A material is said to be dielectric if it has the ability to store energy when an external electric field is applied. If an ac sinusoidal voltage source is placed across the same capacitor, the resulting current will be made up of a charging current and a loss current that is related to the dielectric constant. Here we are interested only in the dielectric constant (έ) of the material and the loss (tanδ) . Dielectric constant (έ) describes the interaction of a material with an electric field. The relative dielectric constant is given by equation $\varepsilon_r = \varepsilon / \varepsilon_0$ .The complex relative dielectric constant is given by equation (2-1).

$$\varepsilon_r = \frac{\varepsilon'}{\varepsilon 0} = \frac{\varepsilon - j\varepsilon''}{\varepsilon 0} \qquad \text{……(2-1)}$$

Where ε_0 is the dielectric constant of free space, which is equal to 8.854×10^{-12} f/m .The real part of dielectric constant **(ε_r)** is a measure of how much energy from an external electric field is stored in a material. The imaginary part of the dielectric constant (ε'') is called the loss factor [108].

2-5-3 Composition and structure of ferroelectrics

2-5-3-1 Chemical composition

The group of compounds which can be described by the general formula ABO_3 has the type designation $E2_1$ where the B ions of smaller radius are surrounded by the anions in a octahedral form and A ions of larger radius have 12 –fold co-ordination with anions. Unit cell is as shown Fig 2.3.

2-5-3-2 Crystal structure of ferroelectrics

Structure of ferroelectrics is Perovskite. It structures consist of 12 coordinated A^{+2} atoms on the corner, octahedral (O^{-}) ions on the faces and the tetrahedral B^{+4} in the center. The simple cubic perovskite structure of ABO_3 and its unit cell is as shown in fig 2.3(a). Depending on ionic radii and polarizibilites, pervoskite family may belong to the cubic, tetragonal, rhombic and monoclinic crystal system. According to the geometric requirement of Goldsmith (1927), pervoskite structure can only be formed when correlation, $t= \frac{rA+rB}{\sqrt{2}(rA+r0)}$ exist between the ionic radius. Here, the tolerance factor has value $0.85<t<1.05$,for cubic structure,but $0.8>t<1.3$ for orthorombic the ratio of ionic radius is $0.41< \frac{rb}{r0} <0.73$ and $\frac{rb}{r0} >0.73$ where r_A ,r_B and r_O are radius of A ,B and O atoms respectively.

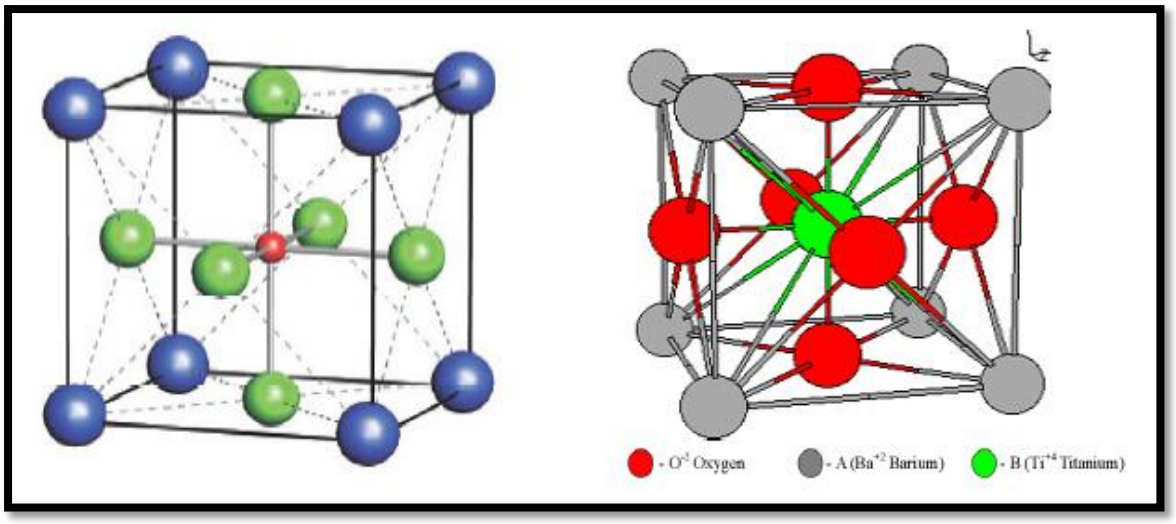

Fig 2-3: The simple cubic perovskite structure of ABO_3 and its unit cell

Tertragonal $BaTiO_3$,Tc= 1200 ^{0c},Ti-displacement=0.125Å Ti-O short =1.83Å,Ti-O long= 2.21Å , Ba^{2+} displacement=0.067Å. $BaTiO_3$ is one of the first simple structures to exhibit compounds with ferroelectric properties and is still probably the most important ferroelectric prototype. Perovskite structure has the curious property that the central tetrahedral B^{+4} atoms do not touch its coordination neighbors in violation of Pauling rule. This allows small displacement of the distortion of the structure and the reduction of symmetry giving rise to ferroelectricity. The perovskite cubic structure and ferroelectric tetragonal of barium titanate is as shown in fig2.3. In perovskite structure BaTiO3,barium are located at corners, the titanium ion is located at the center and oxygen ions are located at the face center of the cubic lattice cell .Each barium ion is surrounded by 6 oxygen ions and each oxygen is surrounded by 4 barium and 2 titanium ions. Barium titanate is in its tetragonal (ferroelectric) phase at room temperature and will transform into cubic (paraelectric) phase above its Curie temperature (Tc =1200℃). In tetragonal ferroelectric two types of domain in boundaries exist at 90^0 and 180^0 [109].

2-5-3-3 Electrical properties

Ferroelectric semiconductors display a number of properties not inherent in common semiconductors owing to the spontaneous polarization and to the phase transition at Curie temperature [110]. One of these properties is the posistor effect (PTC effect) that shows up a growth in resistivity of a ferroelectric material with temperature when it passes from the ferroelectric phase into paraelectric phase. Ferroelectric materials are bad conductor but when temperature increases conductivity increases according to relation which is characteristics of semiconductor.

$$\delta = K^{e-E/RT} \quad \text{.....(2-2)}$$

Where, δ = the conductivity K= a material constant, T=the temperature in deg K, E= the activation energy. It is interest to note that the activity in energy of conductivity of the non-polar paraelectric state (1.75eV=40cal/mole) substantially exceeds that of a crystal in the ferroelectric state (1.15eV=26cal/mole) [111].

2-5-3-4 Dielectric properties of ferroelectrics

ferroelectric has been defined as a dielectric having spontaneous polarization which can be reversed in sign. It must have polar structure with no center of symmetry. In changing the direction of polar axis the structure must pass through an intermediate polar stage and the polar structure is a distortion of this more symmetrical form. The structure of ferroelectric material becomes less distorted as the temperature increases and undistorted at and above a temperature called the Curie point. The dielectric susceptibility (χ_e) of a dielectric material is a measure of how easily it polarizes in response to an electric field. The dielectric constant (ε') of the material is defined as the constant of proportionality relating an electric field E to the induced dielectric polarization P such that $P=\varepsilon_o \chi_e E$

where ε_o is the dielectric constant of free space The susceptibility of a medium is related to its relative permittivity (ε_r) by relation, $\chi e = \varepsilon_r - 1$. Foe vaccum $\chi_e = 0$ and electric displacement D is related to the polarization density P [112].

Dielectric constant (ε_r) is a combined contribution of four polarization:atomic polarization (ε_a), ionic polarization (ε_i), dipolar polarization (ε_d) and space charge (ε_s)[113]. Thus $\varepsilon_r = \varepsilon_a + \varepsilon_i + \varepsilon_d + \varepsilon_s$. All of the useful properties of ferroelectric ceramics are related in some manner to their response with an electric field, the electrical behavior of these materials is important to their successful application in dielectric, piezoelectric, pyroelectric, or electro optic devices. Ferroelectrics are, in general, characterized by (1) higher dielectric constants (200–10000) than ordinary insulating substances. (2) Relatively low dielectric loss (0.1%–7%) (3) High specific electrical resistivity ($>10^{13}$ Ω-cm) [114].

3-1 Introduction

This chapter includes practical steps for the preparation three series of spinel ferrites samples with general formula [$xBaTiO_3+(1-x)CuFe_2O_4$] by (using sol-gel auto combustion chemical method), also this chapter includes the explanation method of measurements for the study of the physical properties, and the explanation of the laws relating to the measurement of structural properties, bulk density, method of X-ray diffraction and Scanning Electron Microscopy (SEM) to determine structures of samples.

3-2 Raw materials

In this study, many chemicals were used. Some of them were used for synthesis $CuFe_2O_4$ and others were used for synthesis $BaTiO_3$. The table (3-1) illustrated all these chemicals.

Table (3-1) Chemicals Used

Chemical material	Formula	%Purity
Copper nitrate trihydrate	$Cu(NO_3)_3.3H_2O$	**98%**
Citric acid	$C_6H_8O_7.H_2O$	**98%**
Iron (III) nitrate	$Fe(NO_3)_3.9H_2O$	**97%**
Barium nitrate	$Ba(NO_3)_2$	**98%**
Titanium oxide	TiO_2	**97%**

3-3 Tools and equipment

The laboratory testing needs to tools and devices for the purpose of preparation of solutions and standard reagents and other solutions necessary for conducting experiments, for example (Sensitive balance, Spatula, Beakers, Hot plate with magnetic stirrer, pH meter, Pipette, Oven for drying, Electric furnace to calcine and distille water device) .

3.3.1 Balance

We have used sensitive balance with high degree of sensitivity of four digits, type "GÖTTINGEN ", Max. 210 gm, Germany origin .

3.3.2 Magnetic Stirrer

This heater is used to the material heat that cannot be heated on flames such flammable material is also used in experiments that need to control the temperature of any that determine the degree of heat required to heat, Type " Wisestir " work at 20 A and 50/60 Hz, made by "DAIHAN" Scientific Co. Ltd., Korea's origin as shown in figure.

Figure (3-1) Magnetic Stirrer

3-4 Finding the molecular weight of the used substances in the preparation

The molecular weight of the involved materials in the installation is calculated in terms of the atomic weight of materials and explain below:

$Fe(NO_3)_3.9H_2O = 55.84+3(14+48) + 9(18) = 403.84g/Mol$

$C_6H_8O_7.H_2O$ = (12.011 x6) + 8(1) + 16 (7) +2(1)+16=210.14g/Mol

$Ba(NO_3)_2$ = (137.32) + 2(14+48) = 261.32 g/Mol

$Cu(NO_2)_3.3H_2O$ = (63.54) + 3(14+48) + 3(18) = 303.54g/Mol

TiO_2 = (47.86) + (2x16) = 79.86g/Mol.

3-5 Preparation of copper ferrite powders CuFe2O4

CuFe2O4 was prepared by[sol-gel auto combustion methods] using $Cu(NO_3)_2.3H_2O$, $C_6H_8O_7.H_2O$ and $Fe(NO_3)_3.9H_2O$. Two solutions prepared, one a solution prepared for mixed (29.9g) of $Cu(NO_3)_2.3H_2O$ and (100g) of $Fe(NO_3)_3.9H_2O$ with 80ml deionized water (so1) and the other contains a solution of citric acid prepared by dissolving (78g) in 50ml deionized water (sol 2). (Sol 2) was added drop wise into the (sol1). Add drops of ammonium solution to the mixed solution under stirring until pH of mixed solution =7. Then the mixed solution was stirred by stirring at 60˚C for 30min then heating solution at 80˚C until getting gel. Dried gel at 120˚C in oven and burned at 200-220˚C and cooled at room temperature.

3-6 Preparation of Barium titanite powders $BaTiO_3$

$BaTiO_3$ was prepared by [sol-gel auto combustion methods] using $Ba(NO_3)_2$ and TiO_3. One solution prepared, this solution prepared for mixed (36.8g) of $Ba(NO_3)_2$ and (11.25g) of TiO_3 with 50ml deionized and kept under stirring for about1hours. The resultant was heated at 50˚C under stirring, then increasing the temperature to 90˚C until getting gel. The gel of $BaTiO_3$ was obtained and washed with deionized water and dried in oven at 120˚C. Out of the oven and put on strung and well milled and then placed in the clean crucible and burn at 800˚C for 3hour then it out the oven and mixing in strung again, put in crucible and burned at 1200˚C and cooled at room temperature.

3-7 Preparation of Ferri-ferro composite ceramics [xBaTiO3+(1-x)CuFe2O4]

$BaTiO_3$ nanopawder with different weight mixed with different weight of $CuFe_2O_4$ nanopawder, blended well with ground them together to get composite [$xBaTiO_3$+(1-x)$CuFe_2O_4$] with different weight, burn each mix at 800˚C for three hours. Then composite powder with different weight percent were milled and pressed into pellets 1.2cm, and then darken at 950˚C for three hours. Fig (3-2) shows the sol-gel auto combustion We have used the scheme to illustrate the way in which is obtained powders with nanoscale structure as set out below.

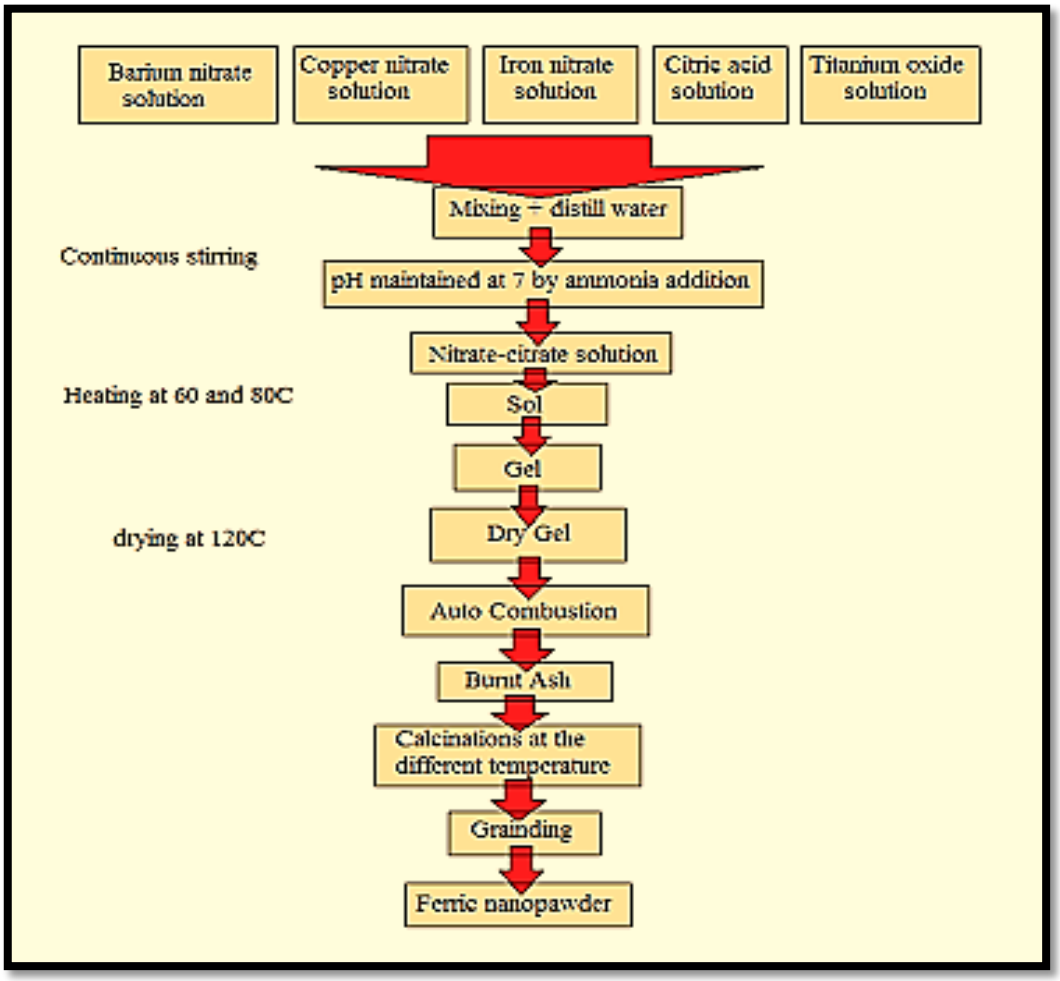

Fig (3-2) flow chart representation all steps of preparation methods composite [xBaTiO3+ (1-x) CuFe2O4]

3-8 Measurements and testing

3-8-1 X-ray diffraction technique

This technique is used to determine the crystalline phase of all synthesized materials. This technique used to examine the crystal structure of synthesized CuFe2O4, BaTiO3 and [xBaTiO3+(1-x)CuFe2O4] by using the X-ray diffraction (A Shimadzu-XRD-6000 with Nickel- cooper filter (Cu Kα, λ=1.5406 A°).

Fig (3-3) XRD microscopy

3.8.1.1Calculation of Crystallite Size From X-ray Diffraction

Shearer equation used to calculate the crystal size after the completion of the preparation of materials technology, X-ray diffraction as described below **[125]**:

$$D = 0.9\,\lambda / \beta \cos\theta \quad \text{---------- (3-1)}$$

Where
D = crystallite size .
λ = wavelength of the radiation (1.54 **A°**) .
θ = Bragg's angle .
β = full width of the peak at half maximum.

3-8-2 Atomic Force microscopy

Atomic force microscopy was used to image the surface to topography of nano$CuFe_2O_4$, $BaTiO_3$ and [xBaTiO3+ (1-x) CuFe2O4] that calcinated at different temperature. AFM was performed using advanced angstrom (AA3000) model made USA. In DR: Abdul-Kareem al Samaraii lab.

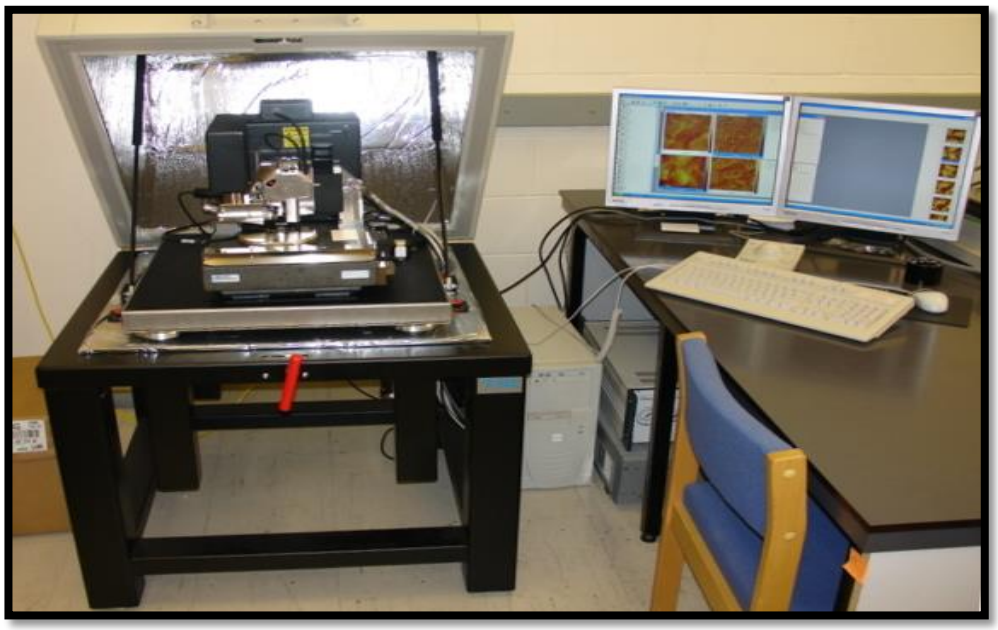

Fig (3-4) AFM microscopy

3-8-3 Scanning Electron Microscopy (SEM)

In this study, we used SEM model inspect S50 from FEI company (Field Emission Inc. company) at technology university-Nanotechnology center of our samples. SEM was used to study the morphology and topography of nano$CuFe_2O_4$, $BaTiO_3$ and [xBaTiO3+(1-x)CuFe2O4] samples that calcinated at different temperature.

Fig (3-5) SEM microscopy

3-8-4 Fourier transform from Infrared spectroscopy

Fourier transform infrared spectroscopy (SHIMADZU-8400S FTIR spectrophotometer (Japan) was used to confirm the synthesized the nano nano$CuFe_2O_4$, $BaTiO_3$ and composite [xBaTiO3+(1-x)CuFe2O4] samples.

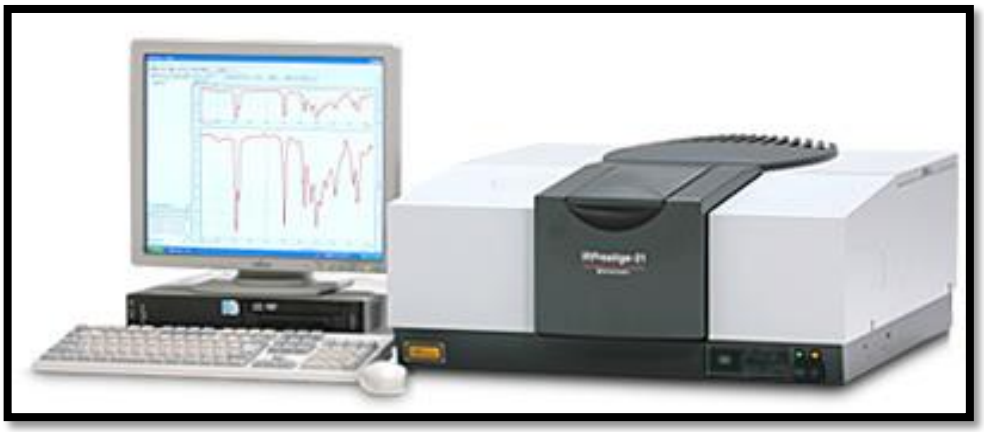

Fig (3-6) FTIR spectroscopy

3.8.5 LCR meter

The type of LCR meter is an Agilent impedance analyzer an American origin; its range of frequency is (50Hz-5MHz), as shown in the figure (3-7).

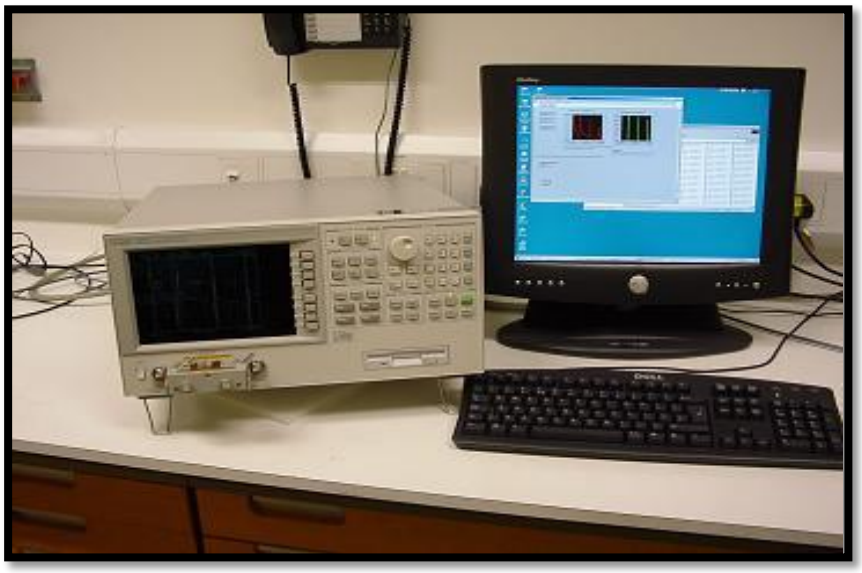

Figure (3-7) : LCR meter used in electrical measurement

3.9 Electric Tests

3.9.1 Dielectric Constant

The dielectric constant which is measured by an LCR meter connected to a computer that the sample which puts between the poles and makes sure that the poles touch the sample surface [126].

LCR system is used for o the purpose of measuring the capacity of the disc samples at different frequencies. Dielectric constant data have recorded on the computer's screen via mathematic formulas that studied previously..

3.9. 2 Dispersion Factor (Tangent Loss)

The Tangent Loss was measured by LCR meter, which connected to a computer the sample puts between the poles and makes sure that the poles touch the sample surface. Dispersion factor data have recorded on the computer's screen via mathematic formulas that studied previously..

3.9.3 Electrical resistivity

This is the electrical resistance of a ferrite core, having a constant cross-sectional area and its unit is the ohm-cm. In the present work, the surface of the pellets is cleaned by grinding with SiC paper in order to remove any contamination and then used to study the room-temperature resistivity; the silver paste is used to coat the polished pellets to provide electrical contacts. AC -resistivity is measured by a two-probe method using an LCR meter.

3.10 Samples Preparation

Samples can be composed of 11 sample processing, where the samples with thickness of 1-3 mm in diameter ring is 1.2 cm, the inner surface boundaries coated with oily and with a thin layer and the reason for this is to prevent the adhesion between the mold and the article prepared, after the completion of the installation of the mold and cleaning in well it is placed on a flat surface to be ready to cast the prepared materials (composites) and composite materials as its general formula [$xBaTiO_3+(1-x)CuFe_2O_4$], shown in figure (3-8).

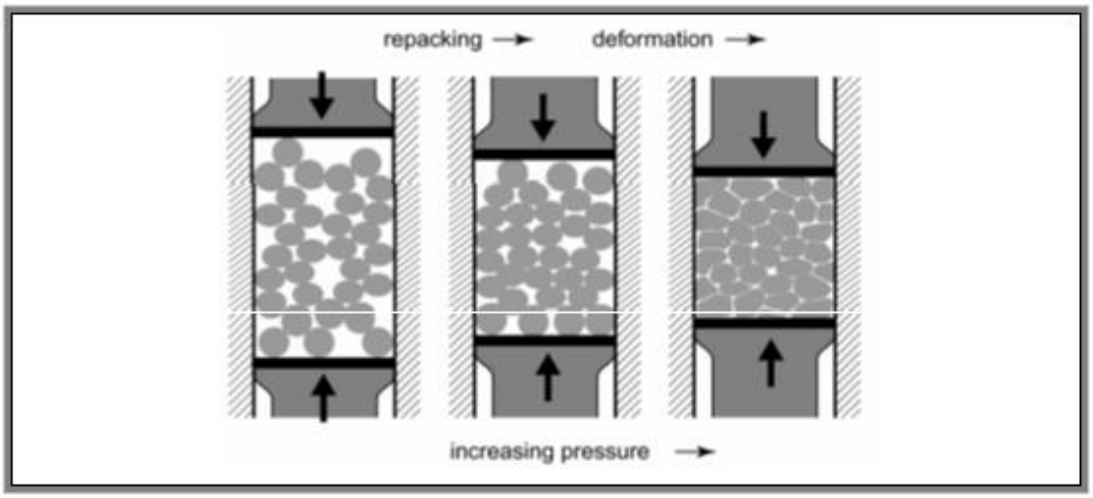

Figure (3-8) Mechanism of powder consolidation [126].

3.10.1 Bulk samples

In the current study,a special(mold) with mechanical machine called (Torna) has been made by the reseacher himself as it shown in figure (3-5).This mold used to press the powder or to prepared the bulk where the nanoparticle (nano powders) positioned inside the mold and placed under the press device for pressuring and pressing of each samples shown in Table (3-2).by 500 - 700 psi with holding time of 30 seconds for pressing of each sample with daimater (1.2cm) and thikness (1-3mm).A

hollow mold disk and pressed strongly and led us out suitable disk,shown in figure(3-9).

Figure (3-9) molds

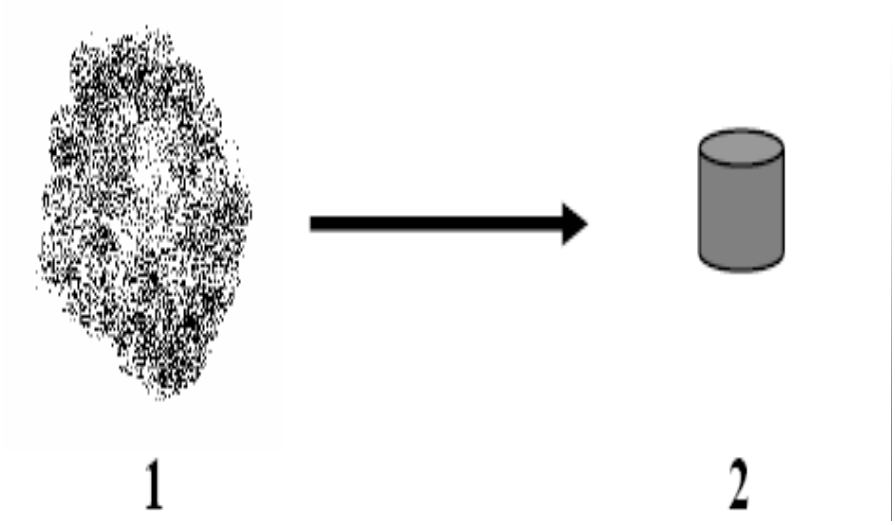

Figure(3-9) Transformation of powder to compact sample

3.10.2 Proportions of the Composition

The prepared samples and take the required formula which are given in table (3-2).

Table (3-2) Symbols of **$[(BaTiO_3)_x+(CuFe_2O_4)_{1-x}]$** prepared

Sample	Chemical formula
B_0	**CuFe2O4**
B1	**$(BaTiO3)_{0.1}$ + $(CuFe2O4)_{0.9}$**
B2	**$(BaTiO3)_{0.2}$ + $(CuFe2O4)_{0.8}$**
B3	**$(BaTiO3)_{0.3}$ + $(CuFe2O4)_{0.7}$**
B4	**$(BaTiO3)_{0.4}$ + $(CuFe2O4)_{0.6}$**
B5	**$(BaTiO3)_{0.5}$ + $(CuFe2O4)_{0.5}$**
B6	**$(BaTiO3)_{0.6}$ + $(CuFe2O4)_{0.4}$**
B7	**$(BaTiO3)_{0.7}$ + $(CuFe2O4)_{0.3}$**
B8	**$(BaTiO3)_{0.8}$ + $(CuFe2O4)_{0.2}$**
B9	**$(BaTiO3)_{0.9}$ + $(CuFe2O4)_{0.1}$**
B10	**BaTiO3**

3.11 Equipment (mold)

here are many types of equipments used in powder compacting. Such as the molds. A mold is designed for the manufacture of samples in the form of pellet in diameter (12mm) and thickness(1-3mm) and the weight of the sample is (1-1.3)g . It uses hydraulic press with a pressure of 500-700 psi,

3.12 Sintering

The (brown) cores are loaded on refractory plates (copper ferrite) and sintered at temperature of (200 °C) depending on the ferrite grade for three hours.The samples will be shrinkage in a linear and volume. The sintering can be done in tunnel kilns having a fixed temperature in box kilns. Ferrites are usually made by sintering them at the sintering temperature so that the

reactions take place between the carefully mixed raw materials, mostly oxides or carbonates, which lead to ferrite formation where O_2 exchange between ferrite and the furnace atmosphere affects its magnetic, electrical and mechanical properties. figure (3-7) shows the ceramic method of ferrite preparation

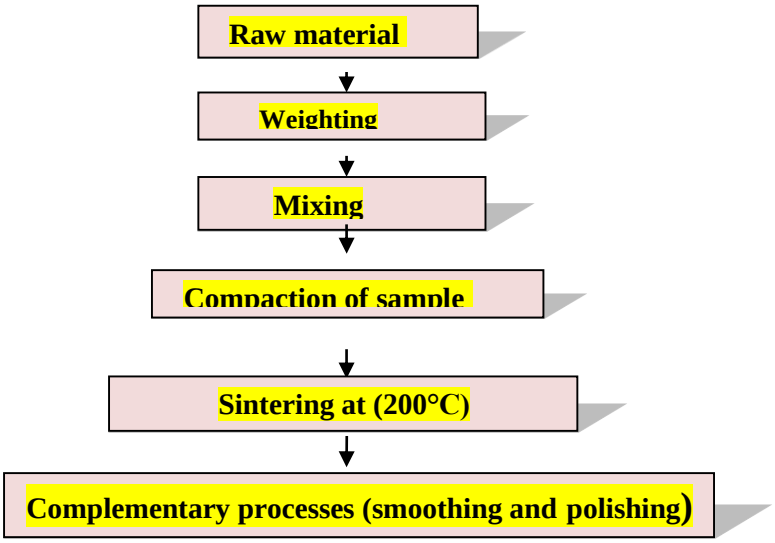

Figure (3-10) Method for ceramic composite preparation

4.1 Introduction

In this chapter will be presented the result and discussion of the preparation of $BaTiO_3$, $CuFe_2O_4$ and composite $[BaTiO_3)_x + (CuFe_2O_4)_{1-x}]$, where (x= 0 - 1] were prepared by(sol-gel auto combustion processes) as nano sized of their particles. Structural properties and electric properties were studied by using LCR meter, SEM, AFM, FTIR and XRD.

4.2 Cu-ferrite and Barium titanite powders results

The $BaTiO_3$ and $CuFe_2O_4$ was prepared using(sol-gel auto combustion method). The synthesized samples were characterized by FTIR, XRD, SEM and AFM, for their structure and morphology characterized.

4.2.1 X-ray diffraction

The crystalline phase of the auto-combustion synthesized nano$BaTiO_3$ was analyzed by XRD. Figure (4.1) shows pure phase of $BaTiO_3$ formation when calcined at 1200°C. Sharp peaks appear at (100), (110), (111), (200), (211) and (220) [117]. The size of the BT crystals was calculated through the well-known Scherrerís equation and the average crystal size was found to be (27.5nm).

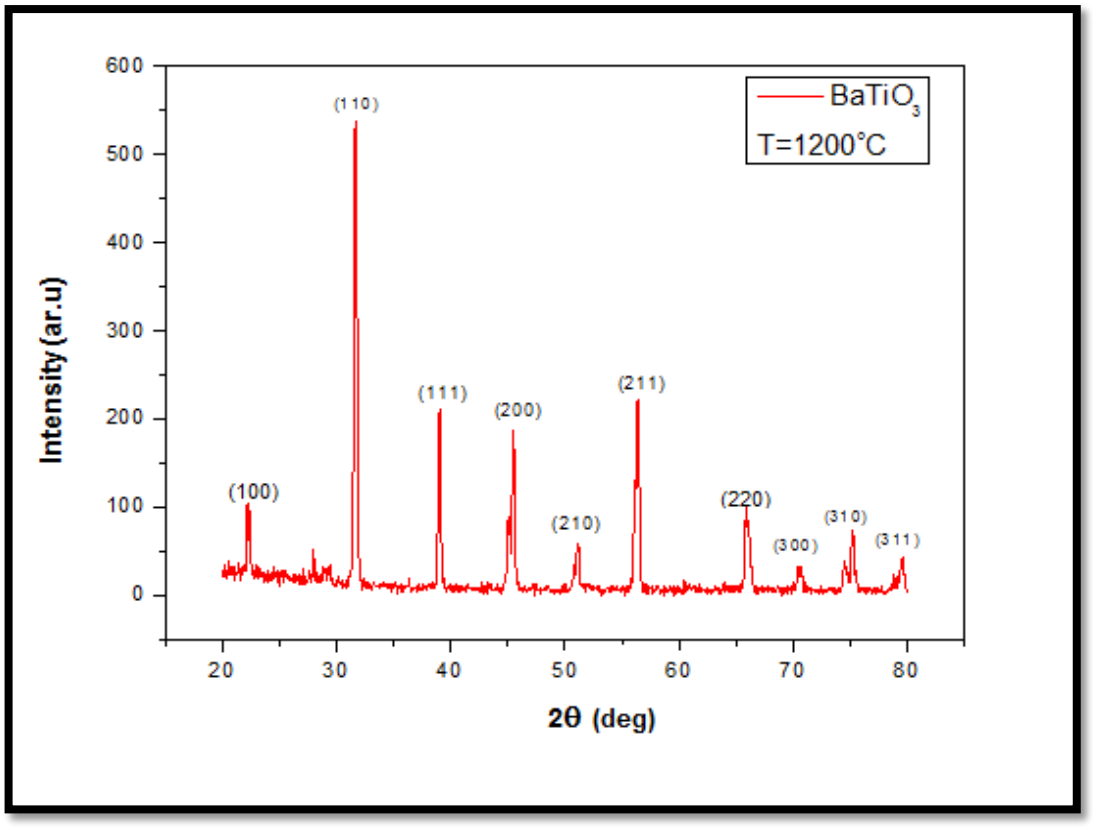

Figure (4-1) XRD of the pure phase of $BaTiO_3$ calcined at 1200°C

Fig (4-2) and (4-3) obtain XRD patterns of nano $CuFe_2O_4$ calcined at 200°C and 400°C respectively. The calcined samples show the reflection peaks at (220), (222), (311), (400), (420), (511), (440) planes which indicates the presence of single phase $CuFe_2O_4$ with spinel cubic structure impure phase of α-Fe_2O_3 is occurs naturally as hematite at (220) [118] .The result is obtained that the diffraction peaks become sharper and increase in intensity as when increase temperature. This increase in intensities of all the peaks may be back to the increase in grain growth with the increase in the temperature. The size of the $CuFe_2O_4$ crystals was calculated through the well-known Scherrerís equation and the average crystal size was found to be (29.35nm) at 200°C and (30.16nm) at 400°C. [119] .

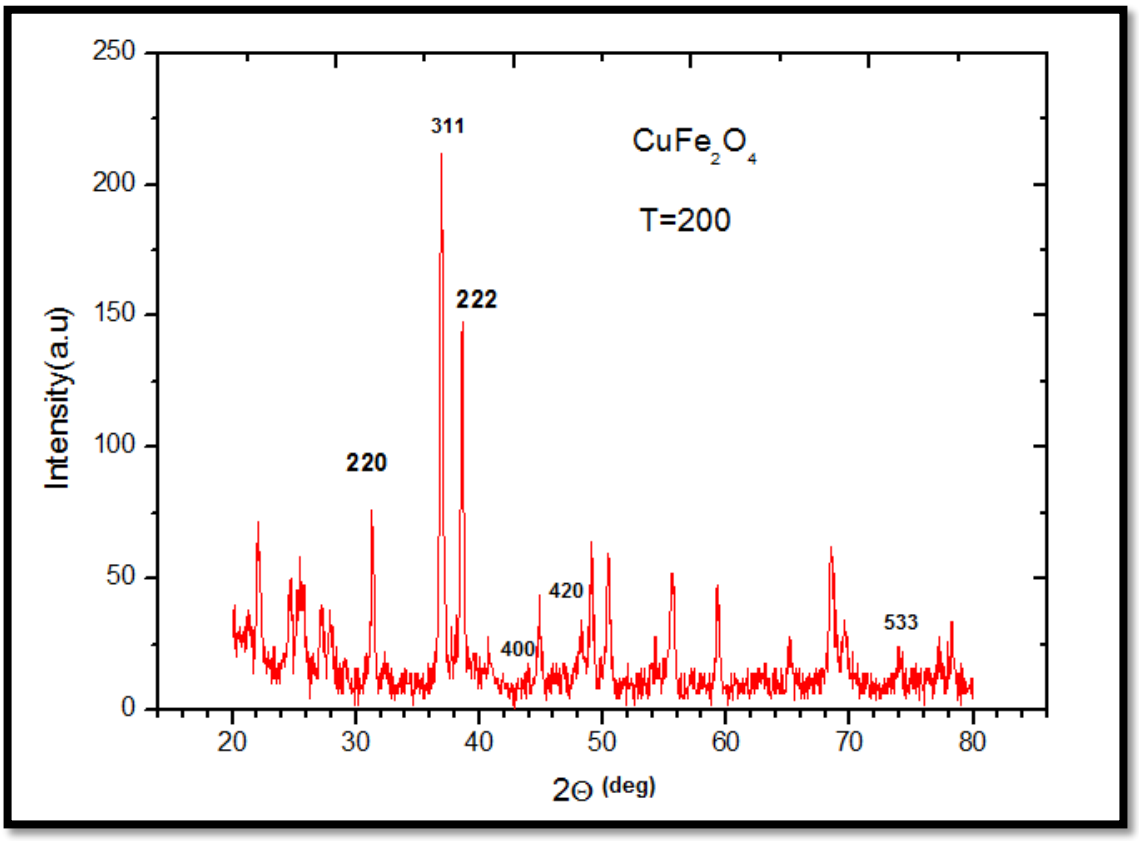

Fig (4-2) XRD patterns of nano $CuFe_2O_4$ calcined at 200˚C

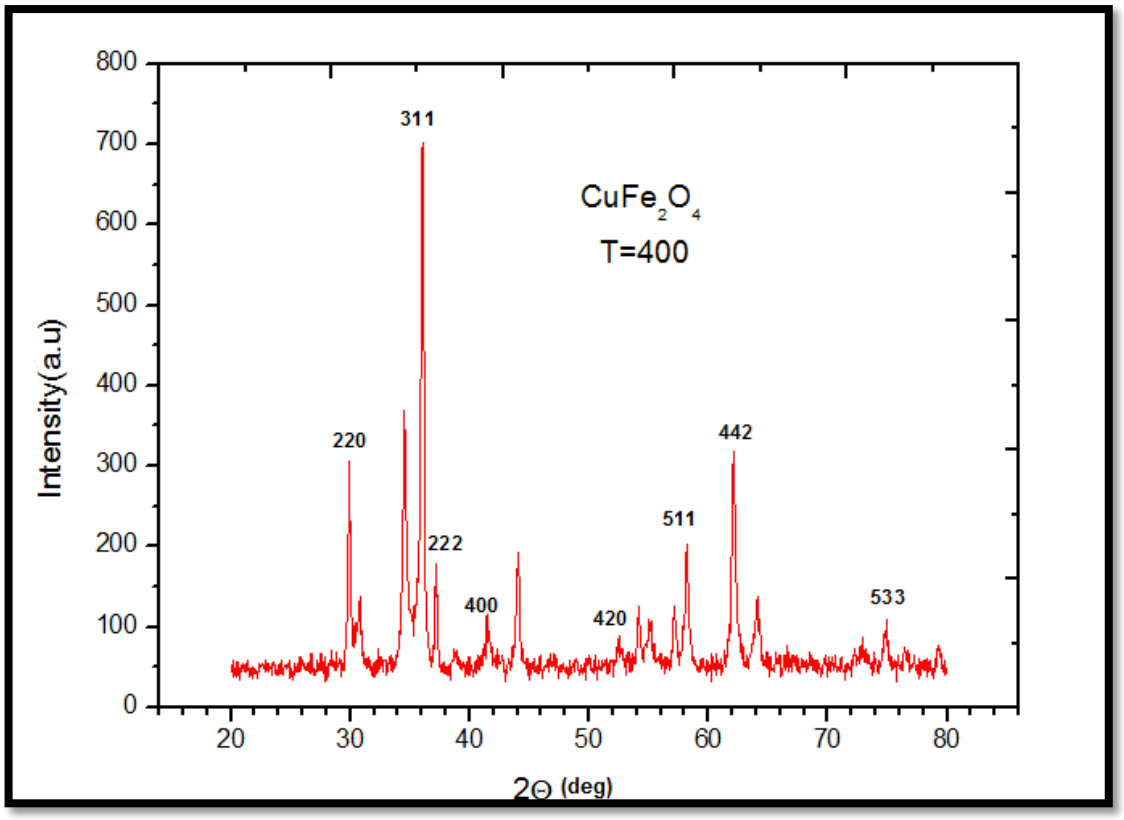

Fig (4-3) XRD patterns of nano $CuFe_2O_4$ calcined at 400°C

4.2.2 Crystallite size, lattice constant and theoretical densities

The broadening peak in the XRD patterns obtains fine crystalline size of the $BaTiO_3$ and $CuFe_2O_4$ particles using Sherer equation (4-1):

$$D = K\lambda/\beta Cos\theta \quad .....(4–1)$$

Where K is Scherrer's constant, λ is wavelength β is the FWHM in radians and θ is peak position [120]. In fig (4-1), (4-2) and (4-3) shows the highest peak is (311) and found that the particle size of the samples in the nano sized and agree with the result and found increase crystalline size of $CuFe_2O_4$ when increase temperature. The lattice constant (a) was calculated by indexing the XRD patterns using equation (4-2).

$$\mathbf{a=d_{hkL}(h^2+k^2+L^2)^{1/2} \ldots\ldots\ldots\ldots (4\text{-}2)}$$

The X-ray patterns were used to calculate the density for cubic structure

$$dx = ZM/Na^3 \quad \text{. ……. (4-3)}$$

The x-ray density for the prepared specimen was calculated from Where (Z) is the number of molecules per unit cell (Z= 8) for cubic spinel ferrites, (M) is the molecular weight and (N= 6.022x 10^{23} /mol) is Avagadro's number, all these show in table (4-1).

Table (4-1) crystalline size crystalline size, lattice constant, volume of unit cell, densities of of $BaTiO_3$ and $CuFe_2O_4$

Sample	2θ (deg)	(hkl)	FWHM (deg)	d (Å)	Lattice constant a (Å)	V (a)3	Crystalline size(nm)	dx (gm/cr
$BaTiO_3$(1200˚C)	31.675	110	0.287	2.822	3.990	63.535	27.59942	**0.01**
$CuFe_2O_4$(200˚C)	36.923	311	0.285	2.432	8.064	524.3866	29.35901	**6.06**
$CuFe_2O_4$(400˚C)	36.050	311	0.277	2.489	8.253	562.1284	30.16419	**5.65**

4.2.3 Fourier Transforms Infrared (FTIR)

FTIR-spectra of $BaTiO_3$, $CuFe_2O_4$ and composite $(BaTiO_3)_x + (CuFe_2O_4)_{1-x}$ are recorded at different temperature in the range of (400-4000) cm^{-1}, the obtained results are shown in figure (4-4 to 4-6).

Figure (4-4) shows FTIR spectrum of $BaTiO_3$. FTIR spectrum showed several types of vibration at (3028, 2360, 2341 and 2331) cm^{-1}, was assigned to stretching and in-plane deformation vibration mode of OH group. The absorption bands showed near 1653 cm^{-1} are due to organic impurities. Bands showed near 1419 cm^{-1} and 1134 cm^{-1} are due to C-O bonded to the Ti ions while the two bands showed at 547 and 522 cm^{-1} was assigned to the Ti-O. [121]

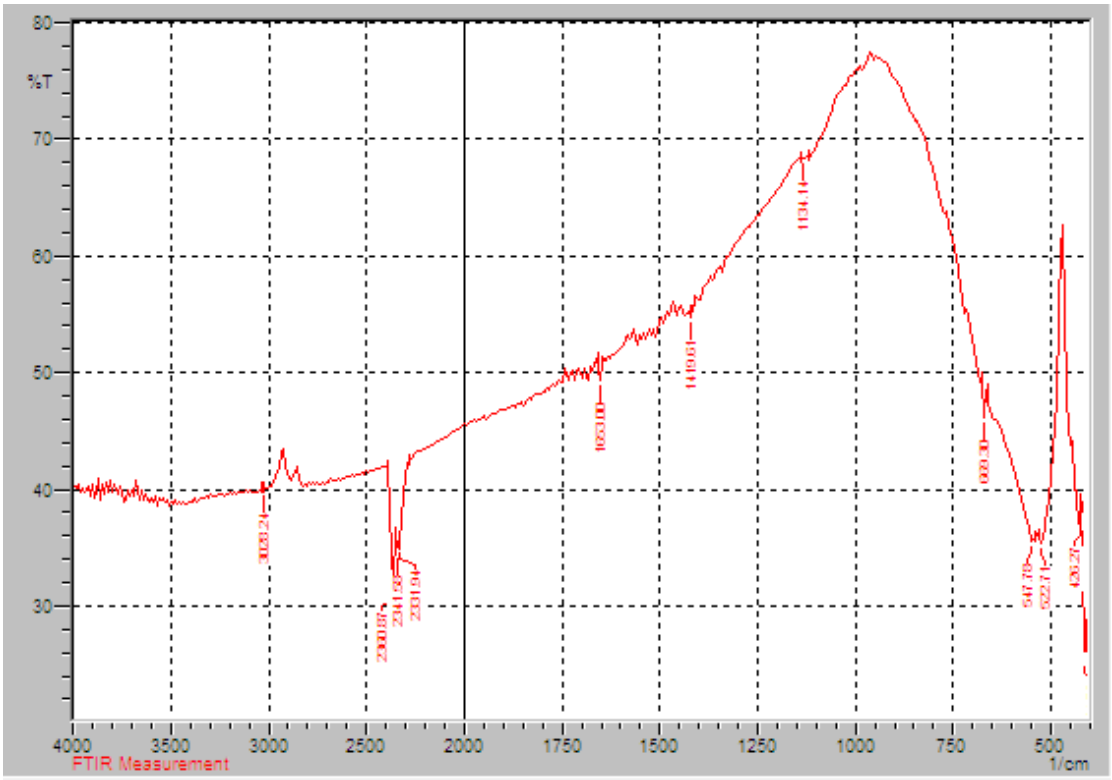

Figure (4-4) FTIR spectrum of BaTiO3

Fig (4-5) obtained FTIR of $CuFe_2O_4$ prepared at 200°C. Two main metal oxygen shows of all spinals of $CuFe_2O_4$ at approximately 400 – 600 cm^{-1}, which identify to the octahedral and tetrahedral sites of positive ions of $CuFe_2O_4$ respectively. Recorded that the higher absorption band ~584 cm^{-1} corresponds to the actual vibrations of tetrahedral complexes and the lower absorption band at ~459 cm^{-1} is back to the vibrations of octahedral complexes. The different values of absorption peaks for octahedral and tetrahedral complexes of $CuFe_2O_4$ because the different values of $Fe^{3+} – O^{-2}$ space for octahedral and tetrahedral sites [122].Two broad bands appear at 3429 and 3211 cm^{-1} was assigned to OH group. A lot of bands of unwanted materials appear at this temperature back to carbon chain that appear during burn.

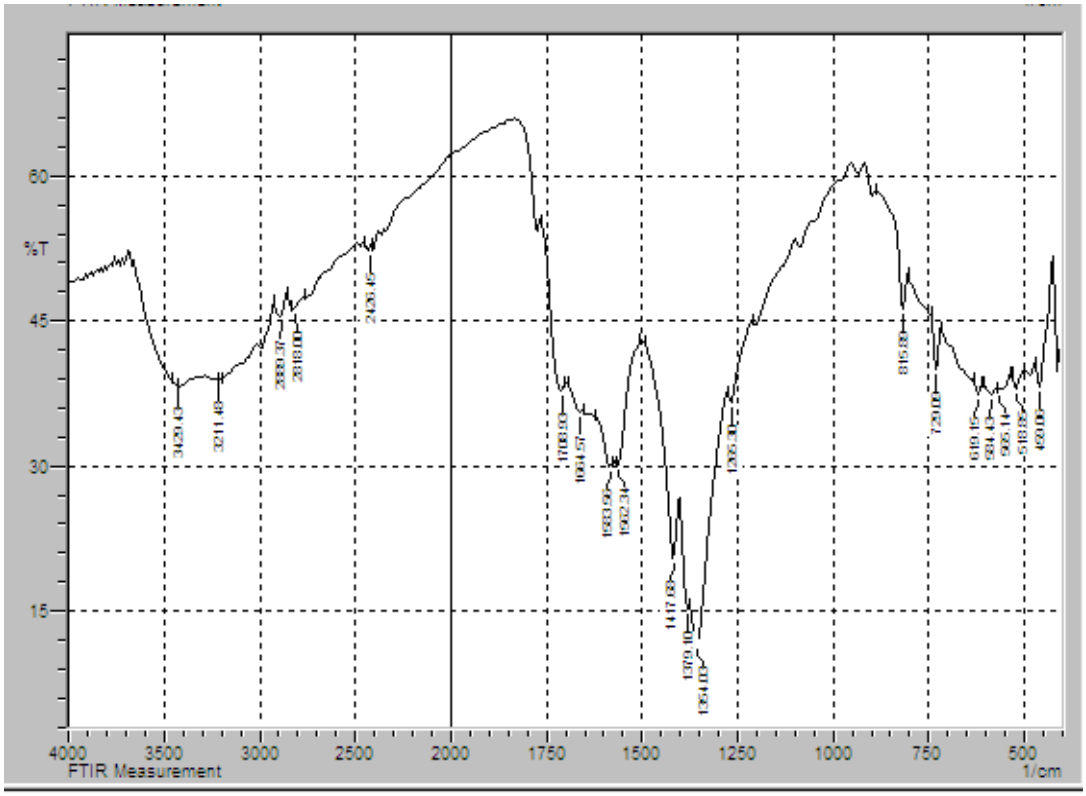

Fig (4-5) FTIR of CuFe2O4 prepared at 200˚C

Fig (4-6) obtained FTIR of CuFe2O4 prepared at 400˚C. It has been when increase the temperature cause shift of $Fe^{3+} – O^{-2}$ towards lower frequency because to occupy of Cu^{+2} at B-site. Also appear band at 3076cm-1 back to OH group[123].

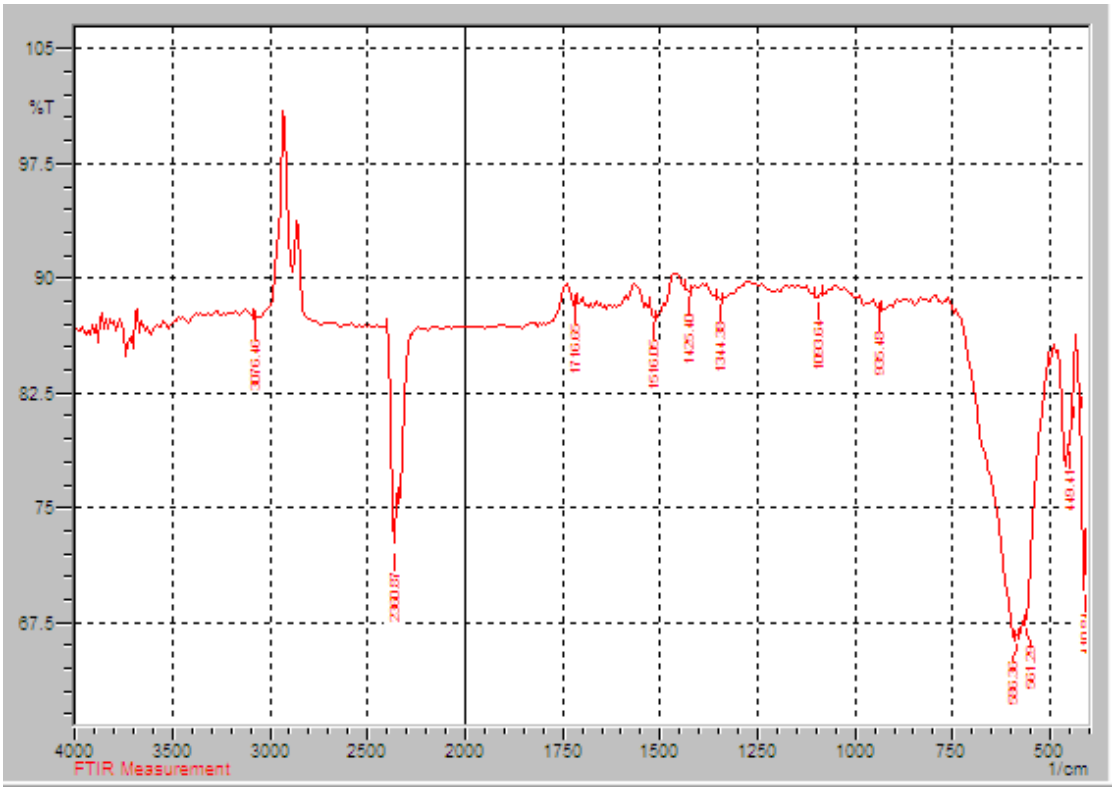

Fig (4-6) FTIR of CuFe2O4 prepared at 400◦C

4.2.4 Scanning Electron Microscope (SEM)

The morphological studies of the nano BaTiO3 and $CuFe_2O_4$ powder were carried out using a scanning electron microscope (SEM). The SEM images of the $BaTiO_3$ and $CuFe_2O_4$ samples prepared using sol gel auto combustion method are shown in figures respectively. Fig (4-7) shows the morphology of barium titanate powder. It can be observed that barium titanate powder particles are nearly spherical and many agglomerations due to lack of good crushing after drying gel.

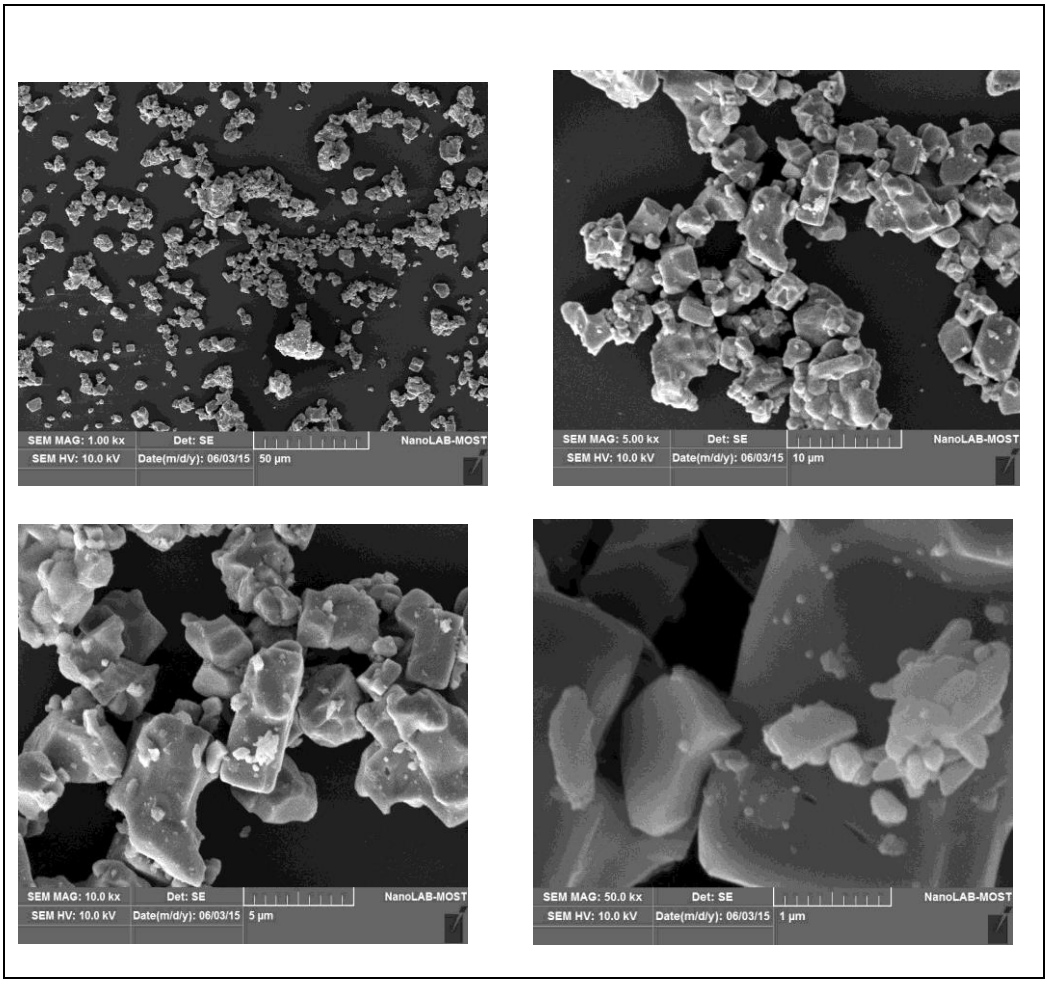

Fig (4-7) SEM of $BaTiO_3$

Fig (4-8) shows SEM of nanoparticles of $CuFe_2O_4$. It can be observed particles are spherical and found many agglomerations.

Fig (4-8) SEM of $CuFe_2O_4$

4.2.5 Atomic Force Microscope (AFM)

Atomic force microscopy (AFM) is a good technique to study the morphology, size, distribution and surface roughness of samples prepared. Fig (4-9) which obtains image AFM of BaTiO3 calcined at 200˚C, with an area (size = 2063x2017nm) and ability analytical (pixels = 448.438). Where fig (4-9-a) obtains to AFM image in (3D), it obtains structure, shape of grains while fig (4-9-b) obtain to AFM image in (2D) and it found the average roughness is (1.44 nm) and RMS (Root mean square) is 1.69 nm

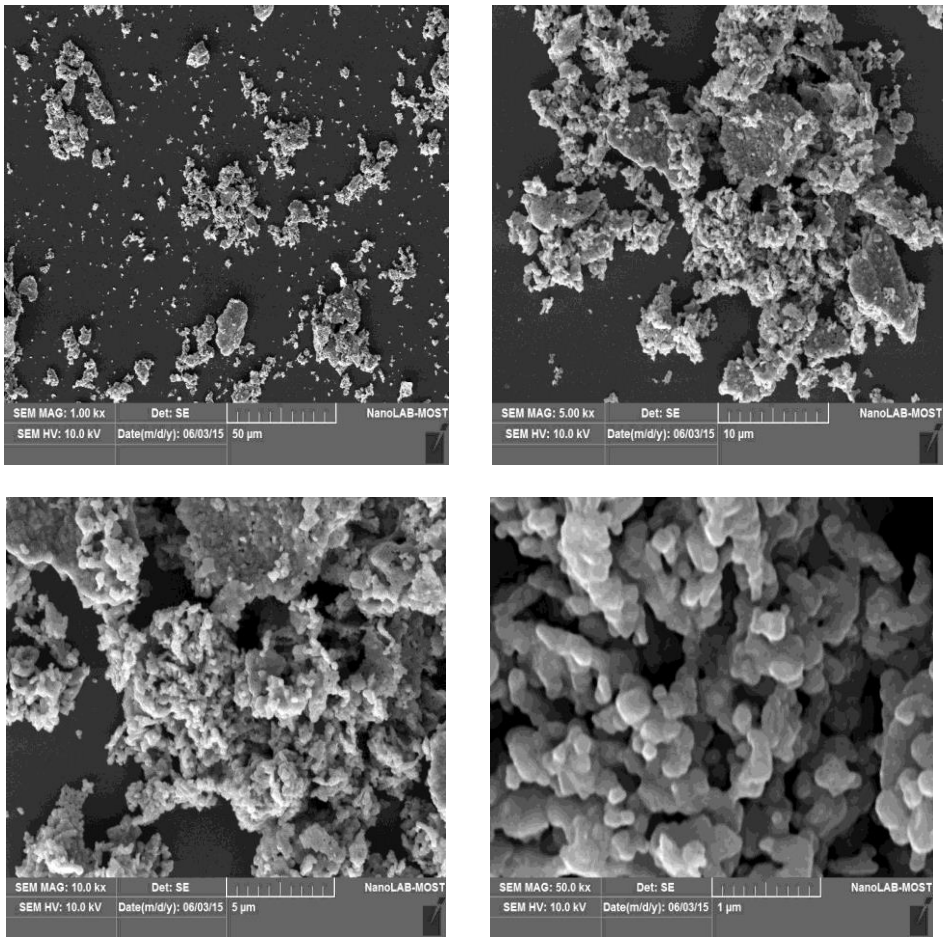

and fig (4-9-c) obtains distribution chart and it found that the average diameter of particle size of $BaTiO_3$ is 97.68 nm.

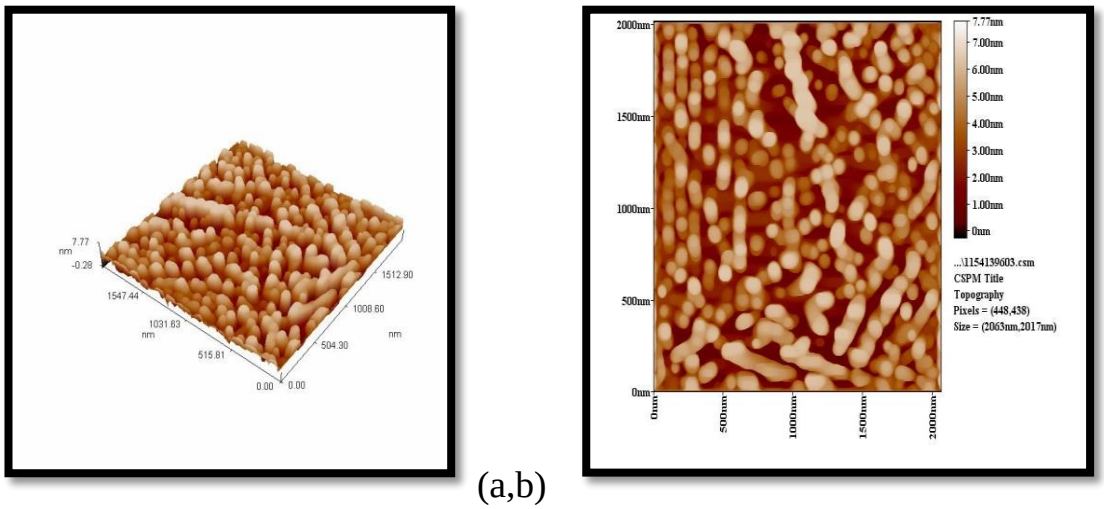

(a,b)

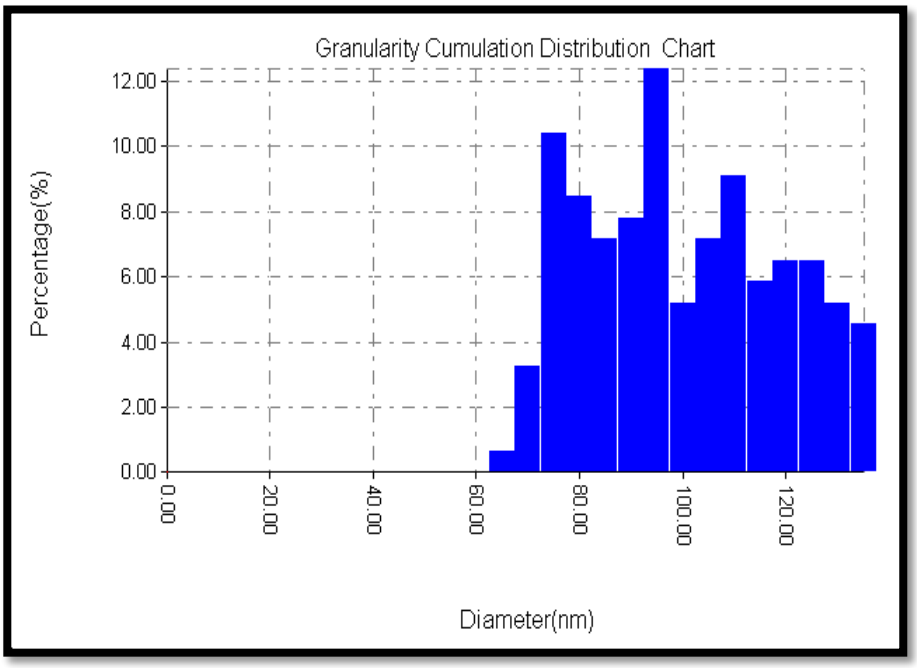

(c)

Fig (4-9) AFM of BaTiO3 calcined at 200°C

Fig (4-10) which obtains image AFM of $CuFe_2O_4$ calcined at 400°C, the area (size = 2045x2054nm) and ability analytical (pixels = 444.446). Where fig (4-10-a) obtains to AFM image in (3D), it obtains structure, shape of grains while fig (4-10-b) obtain to AFM image in (2D) and it found the average roughness is (1.17 nm) and RMS (Root mean square) is

1.36 nm and fig (4-10-c) obtains distribution chart and it found that the average diameter of particle size of $CuFe_2O_4$ is 91.88 nm.

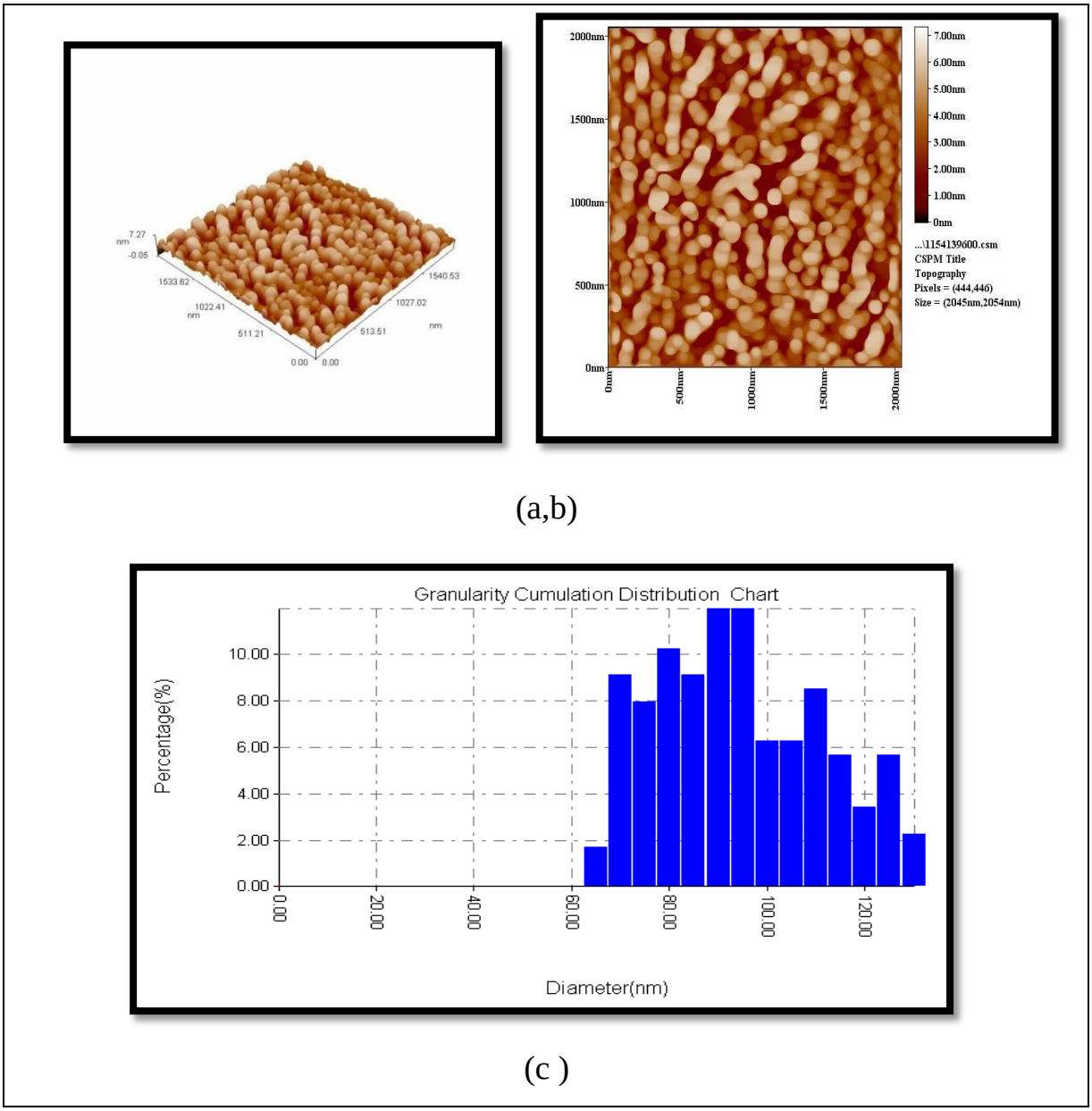

Fig (4-10) AFM of $CuFe_2O_4$ calcined at 400°C

4.3 $CuFe_2O_4$ / $BaTiO_3$ composite samples results

4.3.1 X-ray diffraction patterns

The crystalline phase of the auto-combustion synthesized nano $(BaTiO_3)_x + (CuFe_2O_4)_{1-x}$ was analyzed by XRD. The XRD spectrum related to the calcined $(BaTiO_3)_x + (CuFe_2O_4)_{1-x}$ ferrite powder, where x = 0.2, 0.4, 0.6,0.8 as shown in fig (4-11 to 4-14). As the barium content is increased, the diffraction peaks show considerable broadening which illustrates that crystalite size becomes smaller with the increment of barium content. The wider peak of $(BaTiO_3)_x + (CuFe_2O_4)_{1-x}$ for x=0.8 proved the smallest crystallite size among all the compositions. The average crystallite was found (37.72, 35.42, 32.99, 32.78nm) as (0.8, 0.6, 0.4, 0.2) displays the formation of spinel cubic – perovskite mixed structure. It is also observed that the peak intensity of the higher intensity peak of ferrite (311) plane decreases as the ferrite composition decreases and the peak intensity of higher intensity peak of ferroelectric (101) plane increases with increase in ferroelectric composition in the composites.

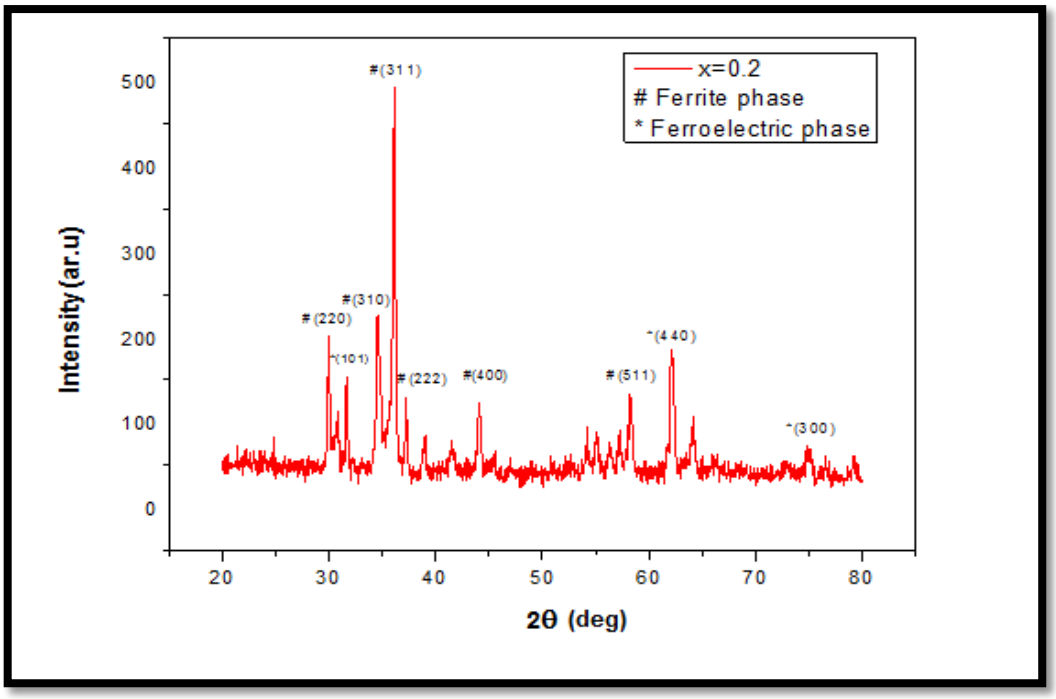

Fig (4-11) The XRD spectrum related to the calcined $(BaTiO_3)_x + (CuFe_2O_4)_{1-x}$ ferrite powder, where x = 0.2

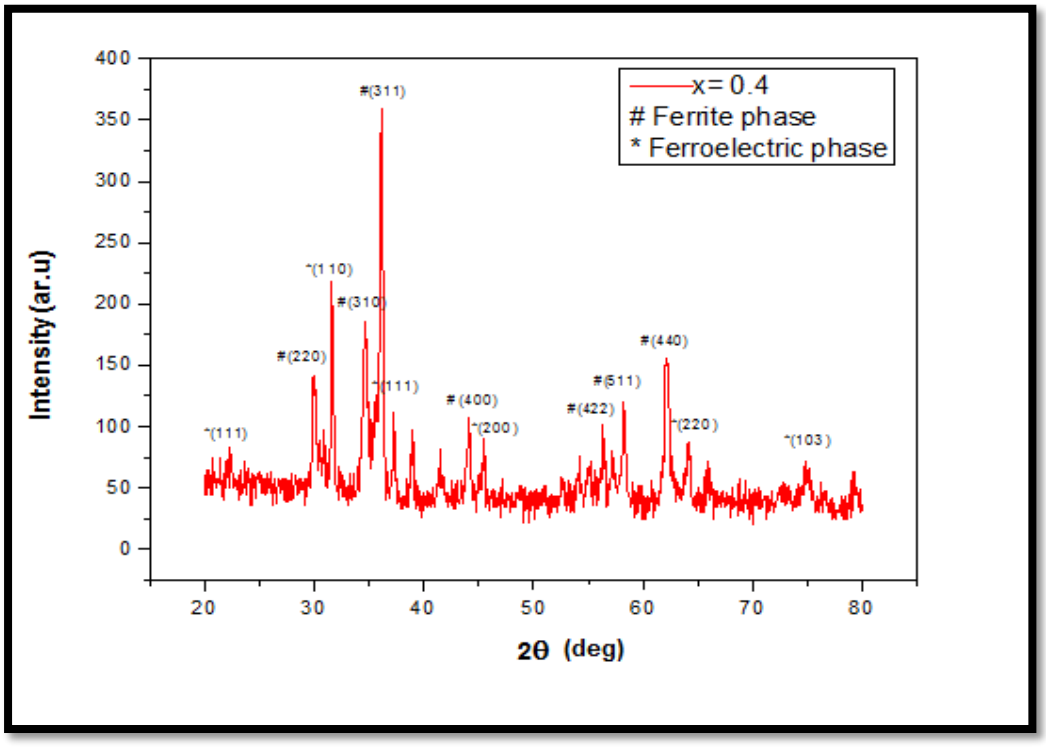

Fig (4-12) The XRD spectrum related to the calcined $(BaTiO_3)_x + (CuFe_2O_4)_{1-x}$ ferrite powder, where x = 0.4

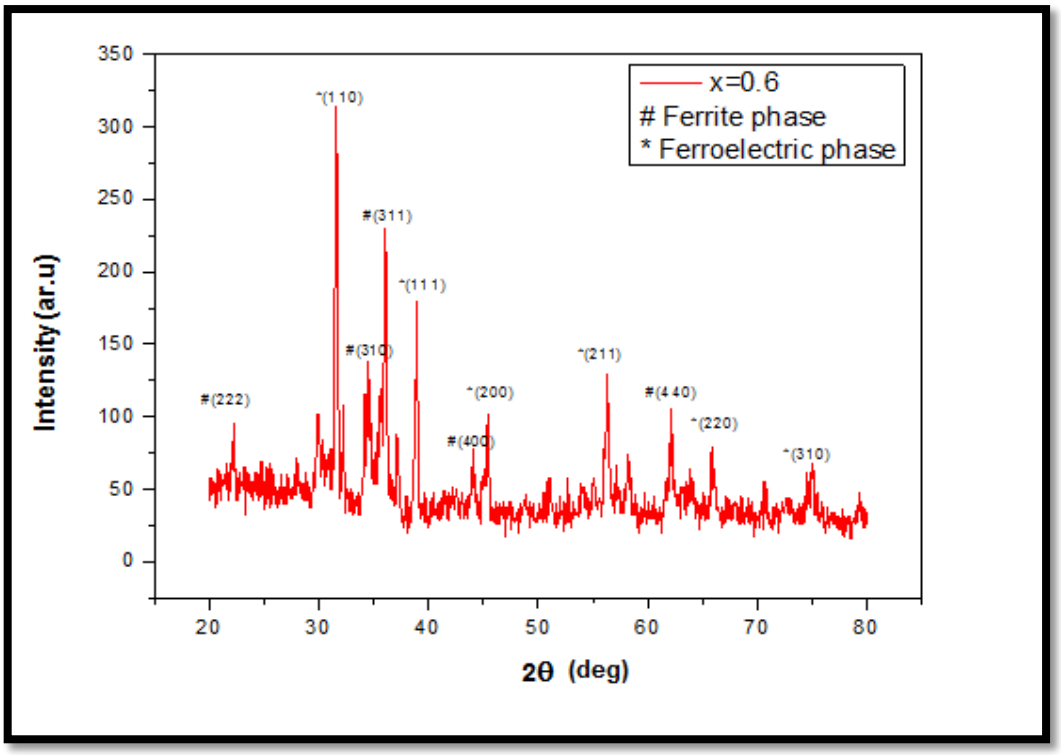

Fig (4-13) The XRD spectrum related to the calcined $(BaTiO_3)_x + (CuFe_2O_4)_{1-x}$ ferrite powder, where x = 0.6

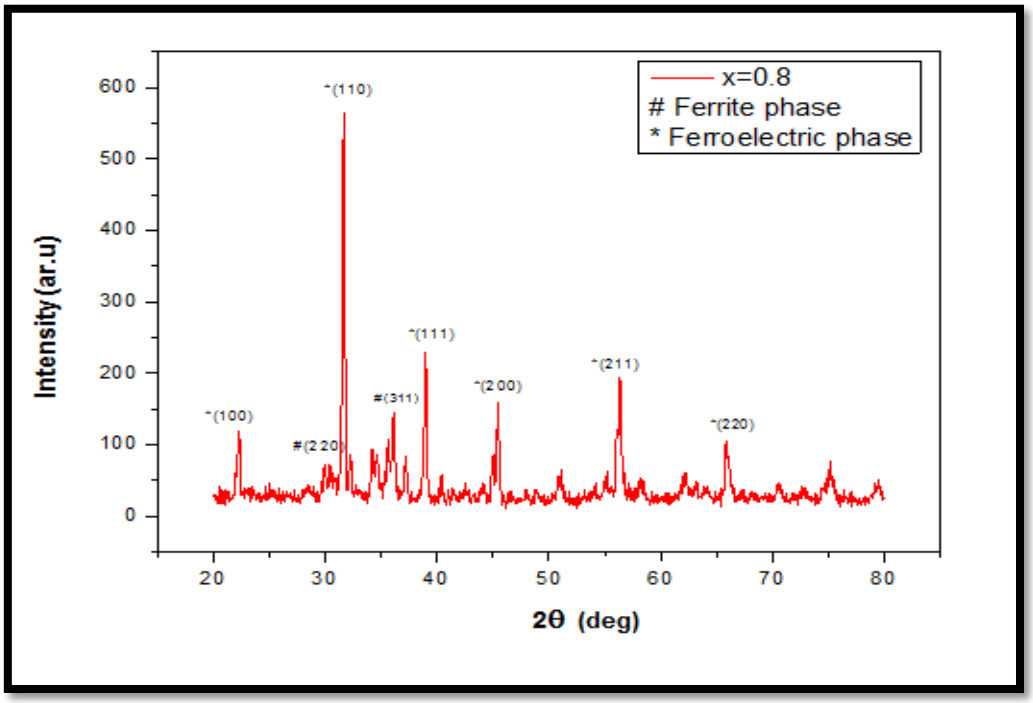

Fig (4-14) The XRD spectrum related to the calcined $(BaTiO_3)_x + (CuFe_2O_4)_{1-x}$ ferrite powder, where x = 0.8

4.3.2 Crystallite size, lattice constant

As the barium content is increased, the diffraction peaks show considerable broadening which illustrates that crystalite size becomes smaller with the increment of barium content. The wider peak of $(BaTiO_3)_x + (CuFe_2O_4)_{1-x}$ for x=0.8 proved the smallest crystallite size among all the compositions. The average crystallite was found (37.72, 35.42, 32.99, 32.78nm) as (0.8, 0.6, 0.4, 0.2) respectively. Where table (4-2) show crystalline size, lattice constant, volume of unit cell, densities of $(BaTiO_3)_x + (CuFe_2O_4)_{1-x}$.

Table (4-2) crystalline size of show crystalline size, **lattice constant, volume of unit cell** of $[(BaTiO_3)_x+(CuFe_2O_4)_{1-x}]$.

$(BaTiO_3)_x+(CuFe_2O_4)_{1-x}$	2θ (deg)	(hkl)	FWHM (deg)	d (Å)	Lattice constant a (Å)	V (a)3	Crystallin size(nm)
X=0.2	36.127	311	0.2215	2.484	8.236	558.6618	**37.72**
X=0.4	36.127	311	0.294	2.484	8.236	558.6618	**35.42**
X=0.6	31.593	110	0.2503	2.829	4.000	64.0098	**32.99**
X=0.8	31.645	110	0.2519	2.825	3.994	63.7387	**32.78**

4.3.3 X-ray density and Porosity

The values of X-ray density (dx) of the ferrite Nano powders show in table (4-3) and their density depend upon the lattice constant, also these table show Green density, Bulk density and porosity of ferrite nanoparticles . The bulk density of the present samples is calculated by using simple mass – volume relation and the obtained values are listed in **Table (4-3)** . The calculated values of X-ray density show increase in the value of 'dx' with an increase in the percentage of ferroelectric phase in composite up to

x=0.4 after that for x=0.6 decreases and again from x=0.8 increases. The values of calculated bulk density are shown in **Table (4-2)**. The values of porosity are also listed in **Table (4-3)** .

Table (4-3) X-ray density (dx), Green density, Bulk density and porosity of $[(BaTiO_3)_x+(CuFe_2O_4)_{1-x}]$

$(BaTiO_3)_x+(CuFe_2O_4)_{1-x}$	x-ray density (gm/cm^3)	Green density (gm/cm^3)	Bulk density (gm/cm^3)	Porosity
X=0.2	5.659	2.88668	3.631	**0.358**
X=0.4	5.631	2.85267	3.278	**0.417**
X=0.6	48.903	3.23857	3.454	**0.929**
X=0.8	48.851	3.48143	3.712	**0.924**

4.3.4 FTIR

FTIR-spectra of composite [x $BaTiO_3$+ (1-x) $CuFe_2O_4$] is recorded at different value of (X= 0.4 and 0.8) at temperature 1200˚C in the range of (400-4000) cm^{-1}, the obtained results are shown in figure (4-15), (4-16).

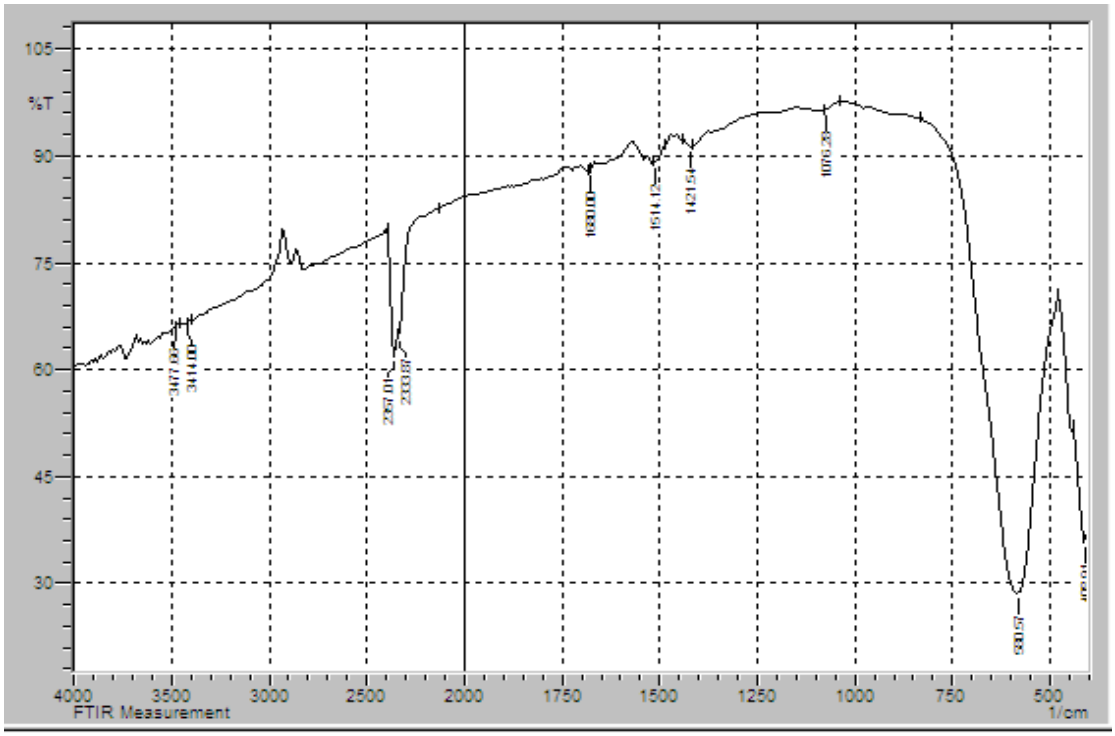

Fig (4-15) FTIR-spectra of composite [x $BaTiO_3$+ (1-x) $CuFe_2O_4$] at X=0.4

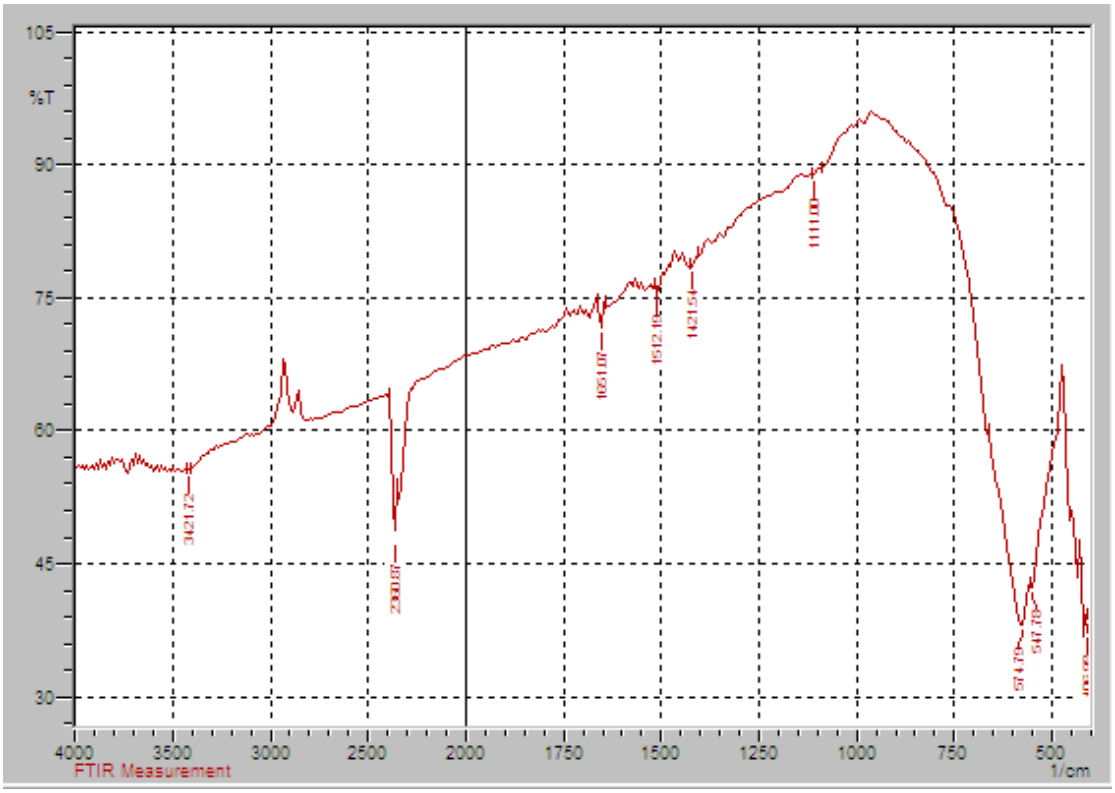

Fig (4-16) FTIR-spectra of composite [x $BaTiO_3$+ (1-x) $CuFe_2O_4$] at X=0.8

Fig (4-15) shows FTIR spectrum of (X=0.4) composite BaTiO3+$CuFe_2O_4$. Spectrum showed several types of vibration at 408, 580, 1421, 1680, 2333 and 3414 cm^{-1}. The spectrum gives stretching in the range 550-600 and 400-450cm^{-1} due to sensitivity to changes in the interaction between oxygen and cations (M-O) in octahedral and tetrahedral positions in composite and spectrum at 3414 and 2333cm^{-1}, was assigned to stretching and in-plane deformation vibration mode of OH group while in fig (4- 16) shows FTIR spectrum of (X=0.8) composite BaTiO3+$CuFe_2O_4$ when increase the temperature cause shift of $Fe^{3+} – O^{-2}$ towards lower frequency.

4.3.5 SEM

The morphological studies of the nano composite $(BaTiO_3)_x + (CuFe_2O_4)_{1-x}$ powder were carried out using a scanning electron microscope (SEM). The SEM images of the composite $(BaTiO_3)_x + (CuFe_2O_4)_{1-x}$ sample prepared using sol gel auto combustion method at temperature 1200˚C are shown in figure (4-17). It is spherical particles with agglomeration.

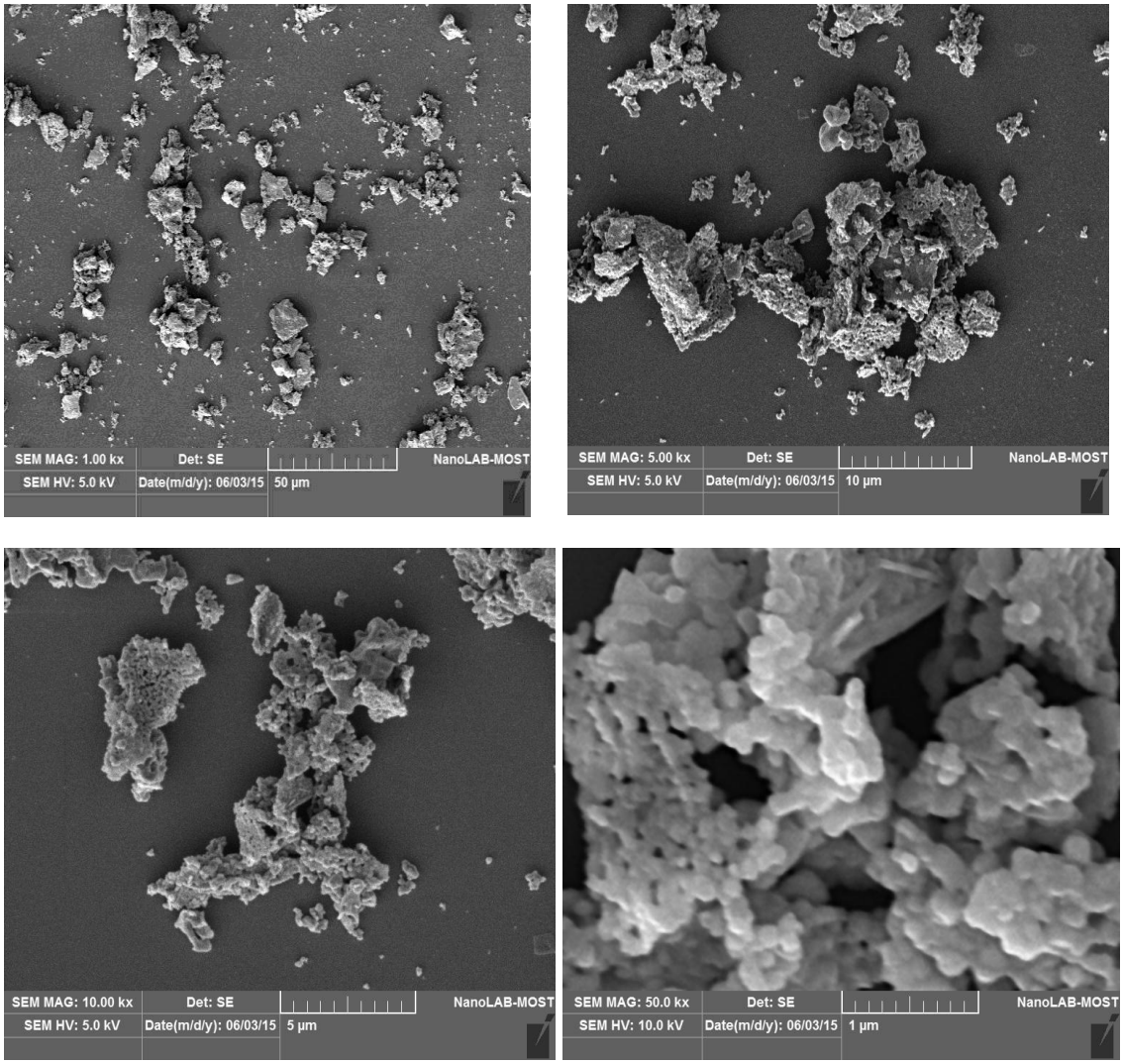

Fig (4-17) The SEM images of the composite $(BaTiO_3)_x + (CuFe_2O_4)_{1-x}$

4.3.6 AFM

Fig (4-18) which obtains image AFM of $(BaTiO_3)_x + (CuFe_2O_4)_{1-x}$ when x= 0.4 calcined at 1200˚C, the area (size = 2045x2036nm) and ability analytical (pixels = 444.442). Where fig (4-18-a) obtains to AFM image in (3D), it obtains structure, shape of grains while fig (4-18-b) obtain to AFM image in (2D) and it found the average roughness is (0.117 nm) and RMS (Root mean square) is 0.898 nm and fig (4-18-c) obtains distribution chart

and it found that the average diameter of particle size is 95.28 nm.

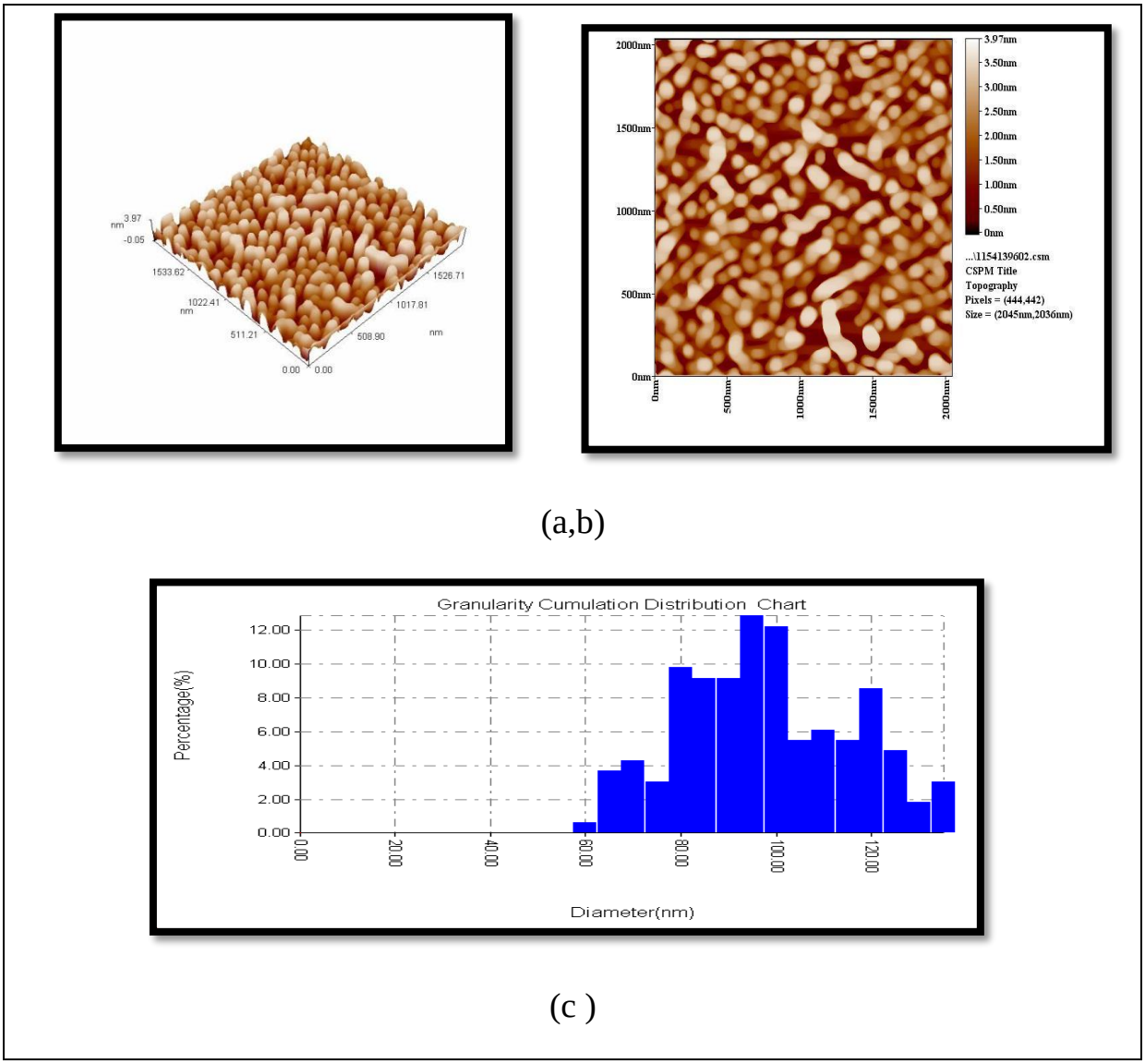

Fig (4-18) AFM of $(BaTiO_3)_x + (CuFe_2O_4)_{1-x}$ when x= 0.4

Fig (4-19) which obtains image AFM of $(BaTiO_3)_x + (CuFe_2O_4)_{1-x}$ when x= 0.8 calcined at 1200C, the area (size = 2026x2054nm) and ability analytical (pixels = 440.446). Where fig (4-19-a) obtains to AFM image in (3D), it obtains structure, shape of grains while fig (4-19-b) obtain to AFM image in (2D) and it found the average roughness is (1.08 nm) and RMS (Root mean square) is 1.24 nm and fig (4-19-c) obtains distribution chart and it found that the average diameter of particle size is 87.80 nm.

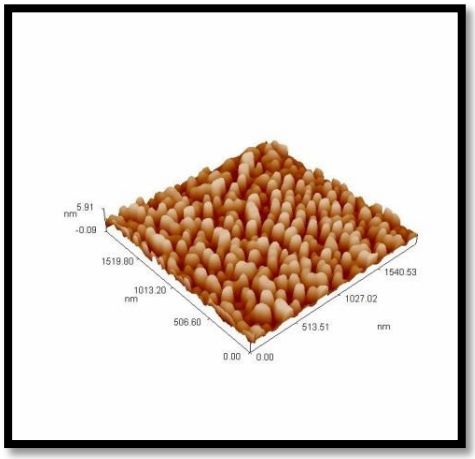

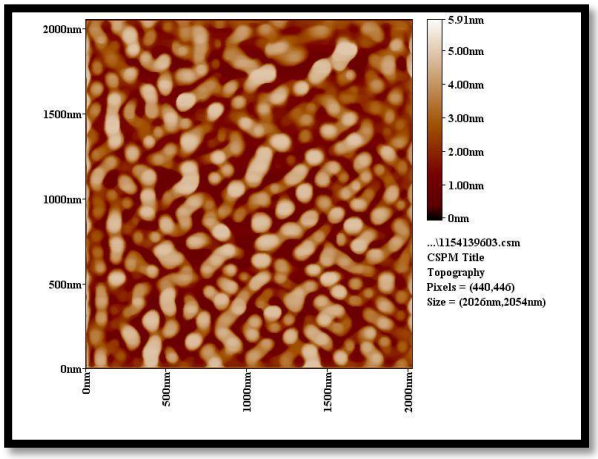

(a,b)

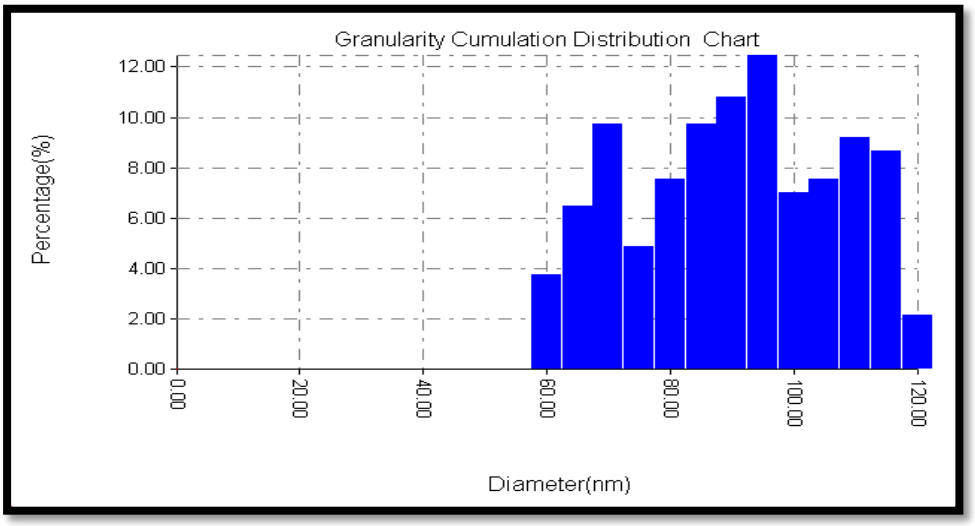

(c)

Fig (4-19) AFM of $(BaTiO_3)_x + (CuFe_2O_4)_{1-x}$ when x= 0.8

4.3.7 Electric properties as a function of frequency

4.3.7.1 Dielectric constant

In figures (4-20 and 4-21) explain real dielectric constant for $(BaTiO_3)_x + (CuFe_2O_4)_{1-x}$ when (x=0 to 1.0).

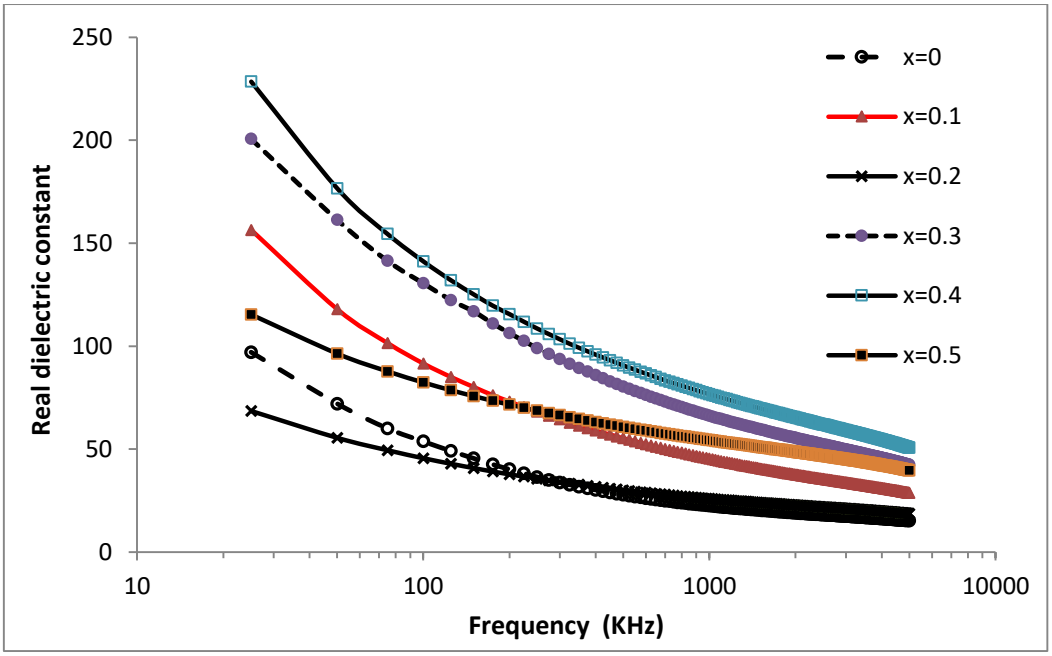

Fig (4-20) Real dielectric constant of $(BaTiO_3)_x + (CuFe_2O_4)_{1-x}$ when (x=0 to 0.5)

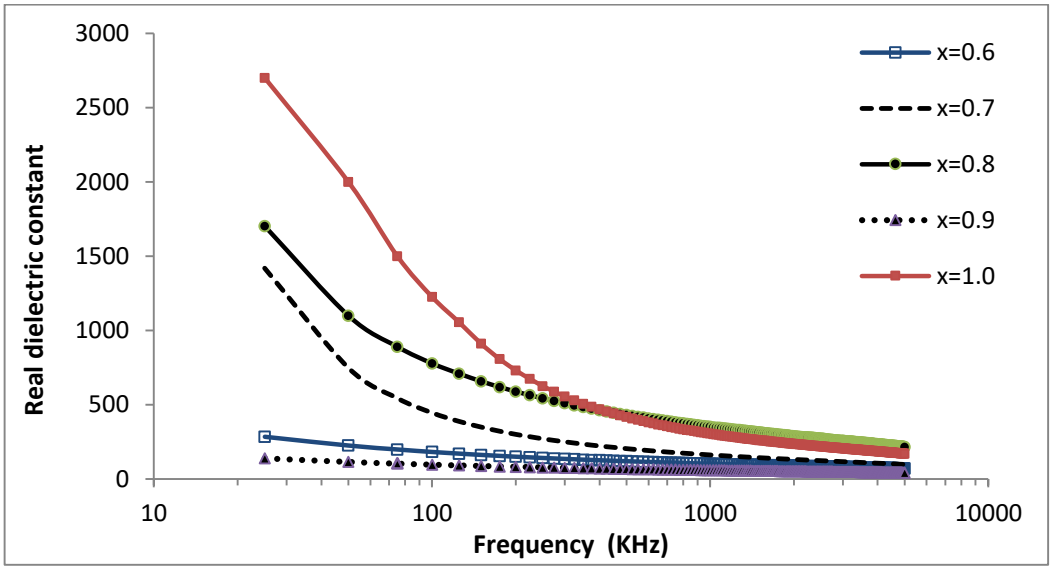

Fig (4-21) Real dielectric constant of $(BaTiO_3)_x + (CuFe_2O_4)_{1-x}$ when (x=0.6 to 1.0)

In figures (4-22) and (4-23) explain imaginary dielectric constant for $(BaTiO_3)_x + (CuFe_2O_4)_{1-x}$ when (x=0 to 1.0) .

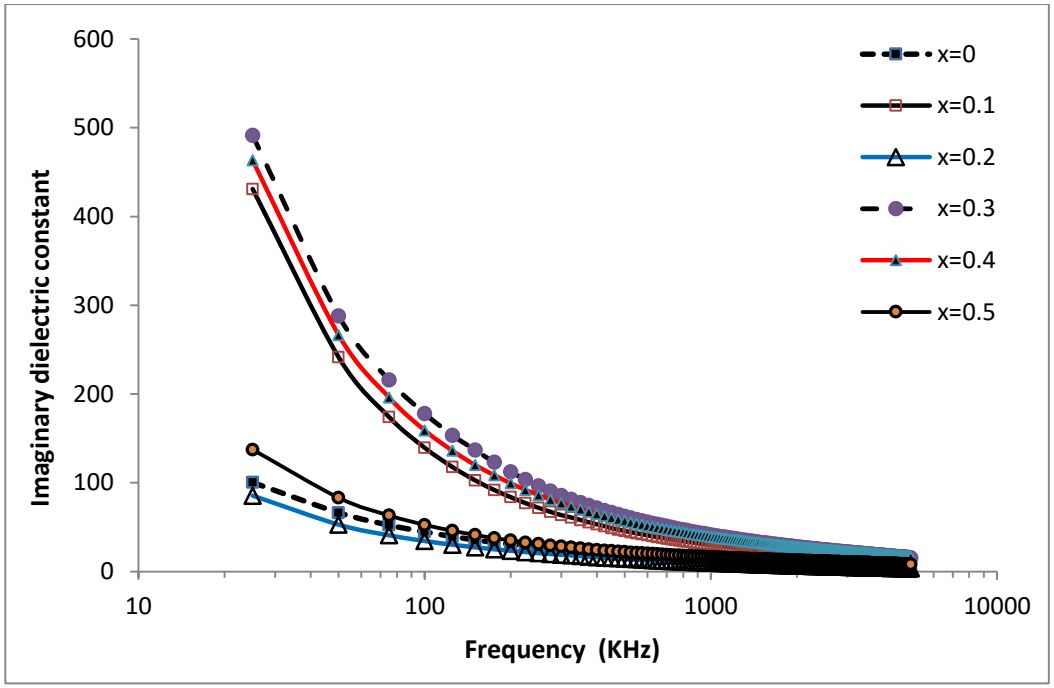

Fig (4-22) Imaginary dielectric constant of $(BaTiO_3)_x + (CuFe_2O_4)_{1-x}$ when (x=0 to 0.5)

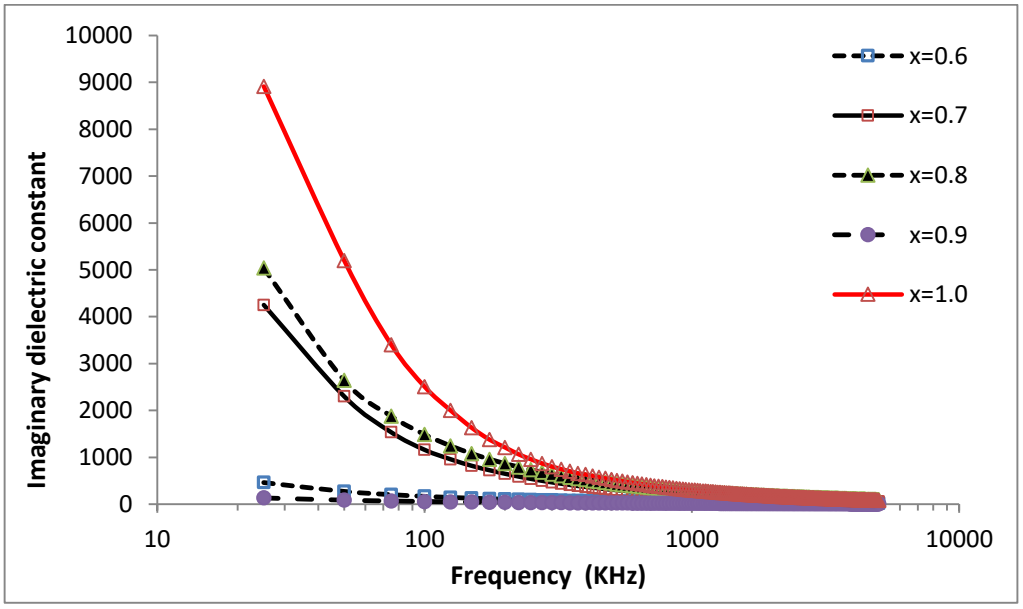

Fig (4-23) Imaginary dielectric constant of $(BaTiO_3)_x + (CuFe_2O_4)_{1-x}$ when (x=0.6 to 1.0)

The dielectric properties of ferrite nanoparticles are influenced mainly by sol-gel. Figures (4-20 to 4-23) displays the variation of dielectric constant (ε) function of frequency at room temperature.Frequency

dependence of the dielectric constant for $(BaTiO_3)_x + (CuFe_2O_4)_{1-x}$ ferrite samples (x=0 to 1.0) sintered at temperature 1200°C. Dielectric constant (ε) decreases with increasing frequency. Because attributed to the fact that the electron exchange between Fe^{2+} and Fe^{3+} ions cannot follow the change of the external applied field beyond certain Frequency, The value of the dielectric constant is very high at lower frequencies and decreases with increasing frequency. At lower frequencies the grain boundaries are more effective than grain electrical conduction. The existence of inertia to the charge movement would cause relaxation of the polarization.

4.3.7.2 Dielectric loss factor

The dielectric properties of ferrite nanoparticles are influenced mainly by sol-gel .Figures (4-24) and (4-25) display the variation of dielectric loss (tan δ) function of frequency at room temperature. Frequency dependence of the dielectric loss for $(BaTiO_3)_x + (CuFe_2O_4)_{1-x}$ ferrite samples (x=0 to 1.0) sintered at temperature 1200^0C.tangent (tan δ) decrease with increase in the frequency of the applied AC field. The values of tangent loss (tan δ) are high at low frequencies and low at high frequencies, at high frequencies this hopping frequency does not follow up the field variation thereby making the relative permittivity a constant. Dielectric polarization in ferrites is due to electron exchange $Fe^{2+} \leftrightarrow Fe^{3+}$, Resistivity electrical properties of ferrites depend upon the conduction phenomenon. Hopping of electron between Fe^{2+} and Fe^{3+} is responsible for this conduction. This hopping is responsible for polarization at grain boundaries due to local charge displacement, where the resistivity is small and the grains are more effective in electrical conduction, a small amount of energy is required for the electrons to be exchanged between Fe^{3+} and Fe^{3+} ions located in the grains .applying an electric field on any material, those suffering

from Article dissipate a certain amount of electrical energy that transformed into heat energy during certain period of time dissipated power resulting because the work done overcome the force of friction dipoles during rotation under the influence of the electric field applied. Called this phenomenon of loss the obtained for the present amples attributed to be more homogeneous. The decrease in dielectric loss tangent with change in the composition and frequency is in accordance with Koops phenomenological.

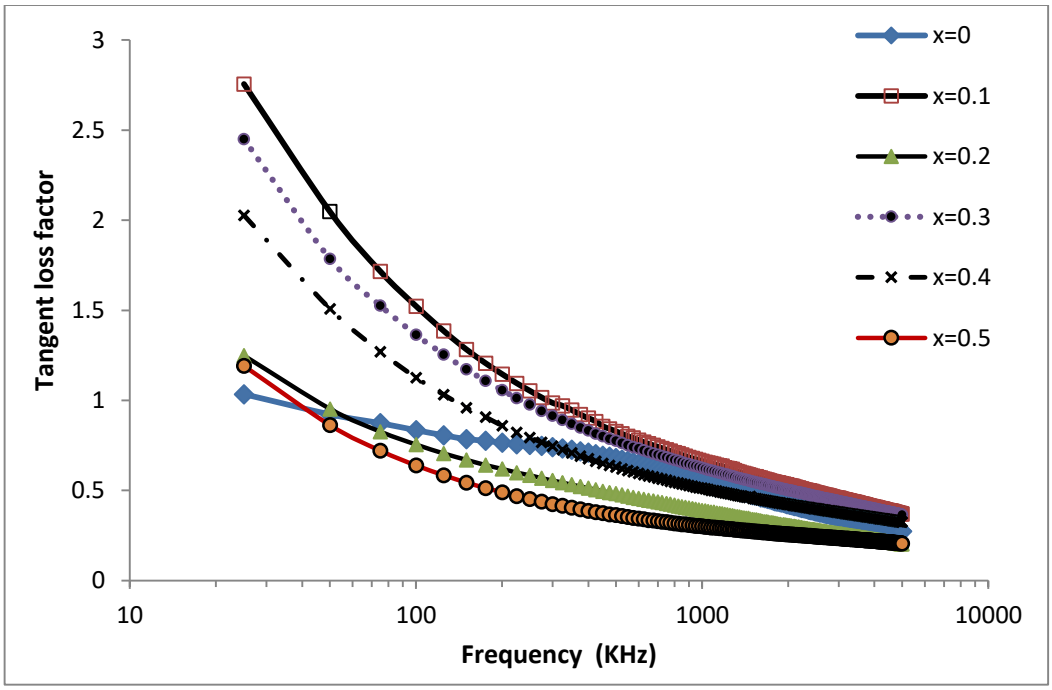

Fig (4-24) Tangent loss factor of$(BaTiO_3)_x + (CuFe_2O_4)_{1-x}$ when (x=0 to 0.5)

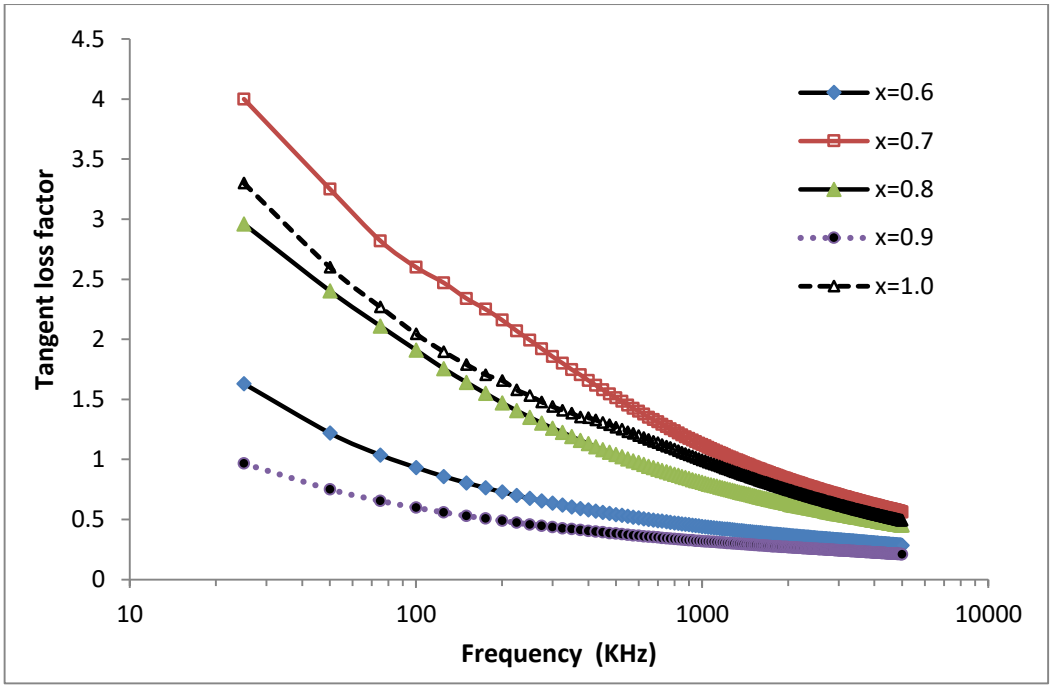

Fig (4-25) Tangent loss factor of $(BaTiO_3)_x + (CuFe_2O_4)_{1-x}$ when (x=0.6 to 1.0)

4.3.7.3 A.C. Conductivity

Figures (4-26) and (4-27) show variation of A.C conductivity σac for all $(BaTiO_3)_x + (CuFe_2O_4)_{1-x}$ ferrite samples (x=0 to 1.0), It was observed that the a.c. electrical conductivity increases with increase in frequency. At lower frequency, the grain boundaries are more active, hence the hopping frequency of electrons between Fe^{3+} and Fe^{2+} ions is less. At higher frequencies, the conductive grains boundaries become more active by promoting the mobility of electrons between Fe^{3+} and Fe^{2+} ions therefore increasing the mobility frequency applied filed increases the conductive grains became more active by promoting the mobility between Fe^{2+} and Fe^{3+} ions, so we observe the increase in conductivity with the increase in frequency.

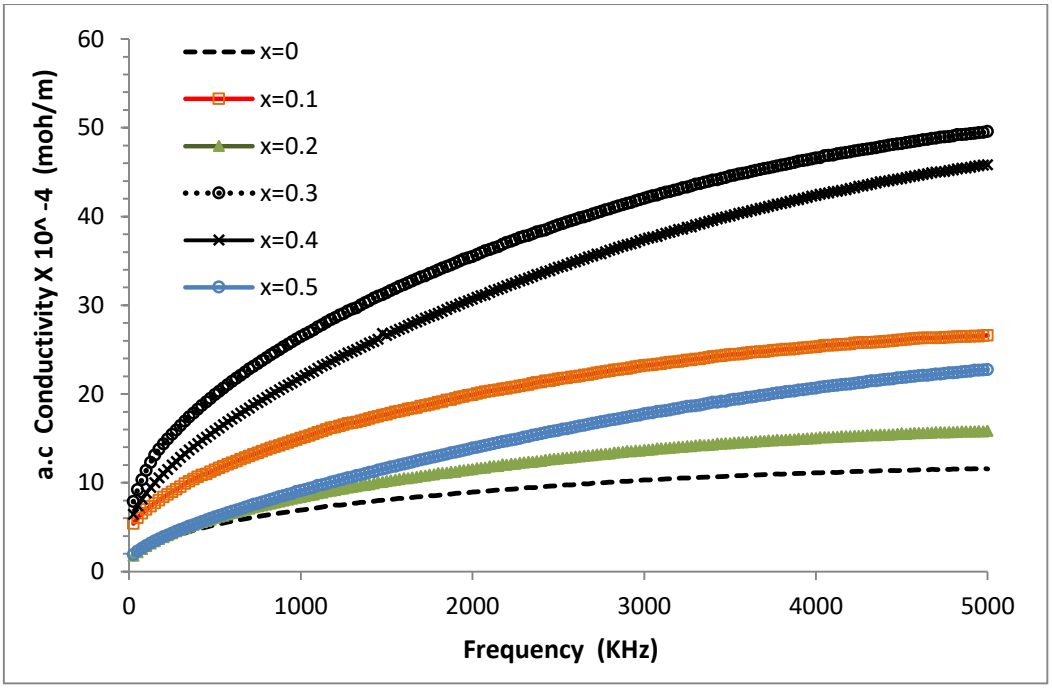

Fig (4-26) A.C. conductivity of $(BaTiO_3)_x + (CuFe_2O_4)_{1-x}$ when (x=0to 0.5)

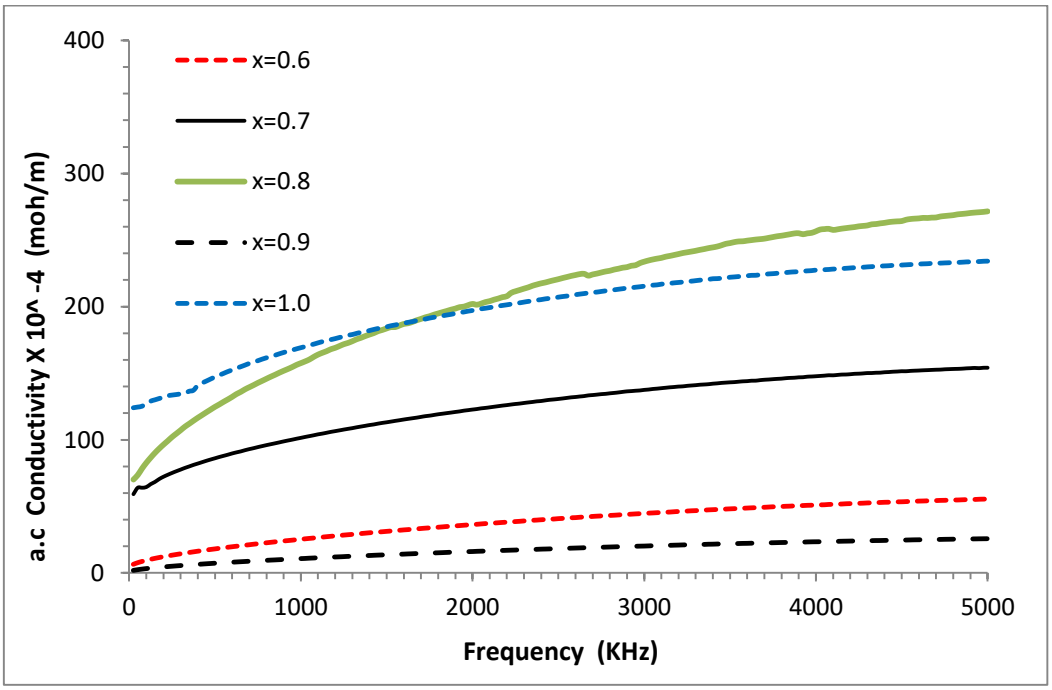

Fig (4-27) A.C. conductivity of $(BaTiO_3)_x + (CuFe_2O_4)_{1-x}$ when (x=0.6to 1.0)

4.3.7.4 A.C.Resistivity

The variation of AC resistivity as a function of applied field frequency in the range 50Hz to 5MHz for all samples shown in figures (4-28) and (4-29) for for all $(BaTiO_3)_x + (CuFe_2O_4)_{1-x}$ ferrite samples (x=0 to 1.0). The AC resistivity with frequency is found to increase with the decrease in applied frequency. The dispersion in the dielectric constant and AC resistivity is observed in the low frequency region, which is analogues to the results predicted by Koop. According to Koop's, at lower frequencies the resistivity is high and the principal effect is of the grain boundaries, therefore the energy required for electron hopping between Fe^{2+} and Fe^{3+} at the grain boundaries is higher and hence the energy losses, And a higher applied frequencies, where the resistivity is small and the grains are more effective in electrical conduction, a small amount of energy is required for the electrons to be exchanged between Fe^{2+} and Fe^{3+} ions located in the grains .

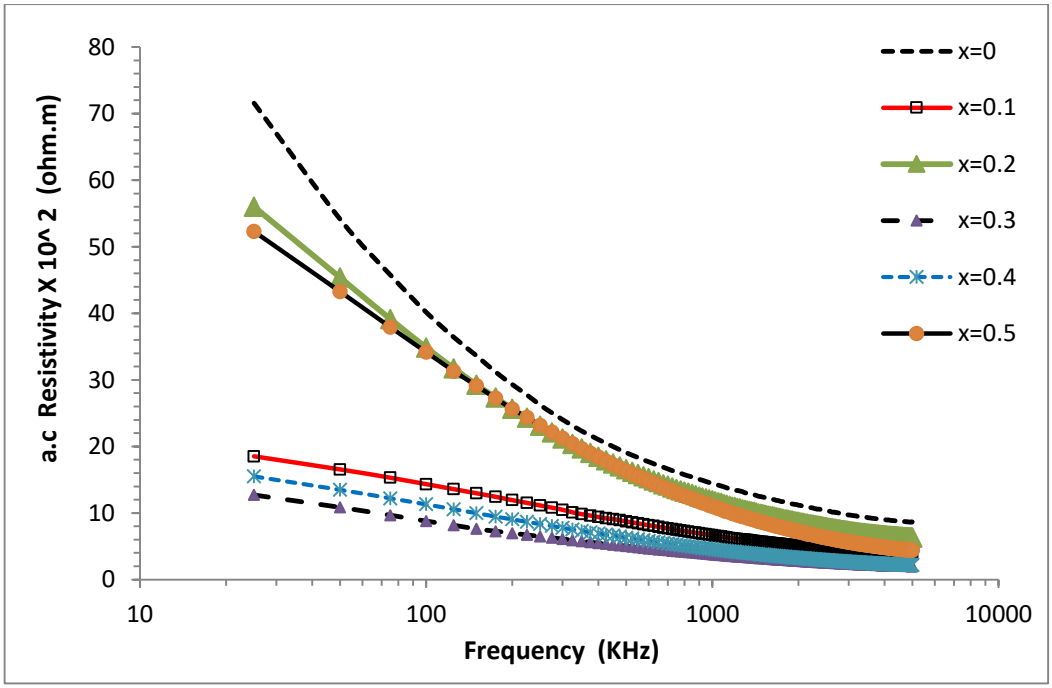

Fig (4-28) A.C. Resistivity of $(BaTiO_3)_x + (CuFe_2O_4)_{1-x}$ when (x=0 to 0.5)

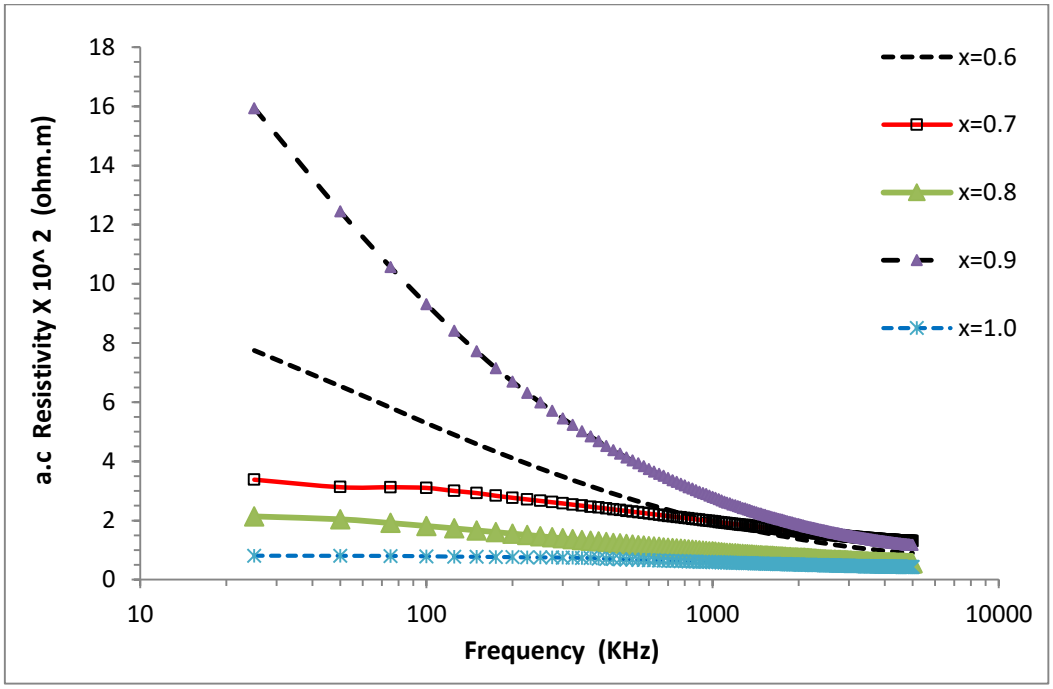

Fig (4-29) A.C. Resistivity of $(BaTiO_3)_x + (CuFe_2O_4)_{1-x}$ when (x=0.6to 1.0)

5.1 Conclusions:

The following derivations are drawn in the current research:

1- The sol-gel auto combustion chemical method was very good to preparation of compositie compounds compared with ceramic bulk methods because of its saving the energy and producing material be in the nano scale.

2- The best sample of powder was obtained at x=0.8 and the worst sample was obtained at x=0.2

3- Debye-Scherrer equations were used to determine of the crystallite size and results were obtained the crystallite size increases with the increase in temperature.

4- The FTIR analysis was obtained the fuctional group that resides in the compounds.

5- SEM images for samples calcined at (1200,400,950 $^{\circ}$C) were showed the $BaTiO_3$, $CuFe_2O_4$ and composite between them powder and obtained the size and shape particles in nano range, also difficulty in the formation of single phase samples, because of few impurities phases which appear.

6- AFM test was proved that the sample calcined at (400,1200 and 950 $^{\circ}$C) in nano range, where in the case of homogeneity.

7- Where we note the dielectric constant , loss factor and a.c.resistivity of samples were increased with decrease frequencies and a.c. conductivity.

8- When increase frequency, electrical resistivity of samples and electrical conductivity are decrease.

9- Phase analysis from XRD patterns displays the formation of spinel cubic – perovskite mixed structure.

10-The calculated particle size decreases as the ferroelectric content increases in the composites due to lower particle size of ferroelectric.

5-2 Future Works:

A set of proposals that can be done in the future and can be summarized in the following:

1- Preparing the same samples by another methods and comparing the results with the results of the sitting work.

2- Calculate the average size of powders by using transmission electron microscope (TEM).

3- Studying the dielectric properties as a function of frequency at different temperatures.

4- Preparing the same sample by the same method but differnet conditions to obtaine that it effect on particle size .

5- Studying other properties of the samples such as structural, electrical, thermal and other mechanical properties.

6- Studying the magnetic properties (hysteresis loop) in order to get a new feature and advantage of it in the modern scientific applications.

References:

[1] Drexler, K., **Engines of Creation: The Coming Era of Nanotechnology**. Doubleday. ISBN 0-385-19973-2, 1986.

[2] Paull, J., and Lyons, K., **Journal of Organic Systems**, Vol. (3), No.1, pp: 3-22, 2008.

[3] Chin, A. B., and Yaacob, I. I. J., of Mater. Process. Techn. 191, 235, 2007.

[4] Drbohlavova, J., Hrdy, R., Adam, V., Kizek, R.; Schneeweiss, O., and Hubalek, J., Sens. 9, 2352, 2009.

[5] Laurent, S., Forge, D., Port, M., Roch, A., Robic, C., Elst, L. V., and Muller, R. N., Chem. Rev. 108, 2064, 2008.

[6] Buzea, C., Pacheco, I. I., Robbie, K. "**Nanomaterials and nanoparticles: Sources and toxicity**". Biointerphases 2 (4): MR17–MR71. doi:10.1116/1.2815690. PMID 20419892, 2007.

[7] S. Sugimoto, K. Okayama, S. Kondo, H. Ota, M. Kimura, Y. Yoshida, H. Nakamura, D. Book, T. Kagotani and M. Homma,“ barium m-type ferrite as an electromagnetic microwave absorber in the GHz range”, Mater. Trans., JIM, Vol. 39, No. 10, P. 1080, 1998.

[8] A. Verma, T.C. Goel, R.G. Mendirattaand R. G. Gupta, “magnetic properties of nickel –zinc ferrites prepared by citrate precursor method”, J. Magn. Magn.Mater,Vol. 192, P.271,1999.

[9] N. Rezlescu, E. Rezlescu, F. Tudorach and P.D. Popa, “MgCunano crystalline ceramic with La^{3+} and Y^{3+} ionic substitutions used as humidity sensor”,J. Opt. Adv. Mater,Vol. 6, P.695, 2004.

[10] X. Chu, B. Cheng, J. Hu, H. Qin and M. Jiang, “semiconducting gas sensor for ethanol based on $LaMg_xFe_{1-x}$ nanocrystals”, Sensors and Actuators B:chemical,Vol. 129,P.53, 2008.

[11] K. Raj, R. Moskowitz and R.Casciari, “advances in ferrofluid technology”, J. Magn. Magn. Mater, Vol. 149, P. 174, 1995.

[12] S.D. Sartale, C.D. Lokhande, M. Muller, Electrochemical synthesis of nanocrystalline CuFe2O4 thin films from non-aqueous (ethylene glycol) medium, Mater. Chem. Phys. 80 (2003) 120–128.

[13] Z. Sun, L. Liu, D.z. Jia, W. Pan, Simple synthesis of CuFe2O4 nanoparticles as gassensing materials, Sens. Actuators, B: Chem. 125 (2007) 144–148.

[14] K.-S. Kang, C.-H. Kim, W.-C. Cho, K.-K. Bae, S.-W. Woo, C.-S. Park, Reduction characteristics of CuFe2O4 and Fe3O4 by methane; $CuFe_2O_4$ as an oxidant for two-step thermochemical methane reforming, Int. J. Hydrogen Energy 33(2008) 4560–4568.

[15] Haruyuki Ohnishi; Teruo Teranishi (1961). "Crystal Distortion in Copper Ferrite-Chromite Series". Journal of the Physical Society of Japan 16: 35–43. Bibcode:1961JPSJ...16...35O. doi:10.1143/JPSJ.16.35.

[16] J. M. Tranquada; S. M. Heald; A. R. Moodenbaugh (1987). "X-ray-absorption near-edge-structure study of La2-x(Ba, Sr)xCuO4-y superconductors". Physical Review B 36 (10): 5263–5274.

[17] William D. Birch. "Who's Who in Mineral Names". RocksAndMinerals.org. Retrieved 13 October 2010.

[18] MIchael Fleischer and Joseph A. Mandarino (1974). "New Mineral Namesx". American Mineralogist. Retrieved 13 October 2010.

[19] S. Castro, M.G. Rivas, J.M. Greneche, J. Mira, C. Rodrlguez, Journal of Magnetism and Magnetic Material 152 (1996) 61–69.

[20] A. Goldman, Modem Ferrite Technology, 2nd edition, Pittsburgh, PA, USA, (1987), p.63-71, ISBN 10: 0-387-29413-9.

[21] J.L. Figueiredo, J.J.M. Orfao, A.F. Cunha, Hydrogen production via methane decomposition on Raney-type catalysts, Int. J. Hydrogen Energy 35(2010)9795-9800.

[22] T. Fujiwara, IEEE Transactions 21 (1985) 1480–1485.

[23] R.K. Selvan, N. Kalaiselvi, C.O. Augustin, C.H. Doh, C. Sanjeeviraja, CuFe2O4/SnO2 nanocomposites as anodes for Li-ion batteries, J. Power Sources 157 (2006) 522–527.

[24] K. Yamamori, T. Suzuki, T.M. Fujiwara, IEEE Transactions 22 (1986) 1188–1190.

[25] S. Roy, J. Ghose, Mössbauer study of nanocrystalline cubic CuFe2O4 synthesized by precipitation in polymer matrix, J. Magn. Magn. Mater. 307 (2006) 32–37.

[26] M. B. Smith, K. Page, T. Siegrist, P. L. Redmond, E. C. Walter, R. Seshadri, L. E. Brus, and M. L Steigerwald, "Crystal Structure and the Paraelectric-to-Ferroelectric Phase Transition of Nanoscale BaTiO3," J. Am. Chem. Soc., vol. 130, pp. 6955 - 6963, 2008.

[27] F. Jona, G. Shirane, Ferroelectric crystals, Dover Publications, INC., New York, 1993.

[28] Van J Suchtelen, *Philips Res Repts*., **27,** 28 (1999) .

[29] Lupeiko T. G. Lopatin S.S, Churikova I. V. and Lopatina I. B. *Inorganic Materials*,**27 (12),** 2300 (1998).

[30] C. J. Brinker and G. W. Sherer, "Sol-Gel Science", Academic Press, San Diego, 1990.

[31] C. J. Brinker, A. J. Hurd, P. R. Schunk, C. S. Ashely, R. A. Cairncross, J. Samuel, K. S. Chen, C. Scotto and R. A. Schwartz, “Sol-Gel Derived Ceramic Films--Fundamentals and Applications”, in: K. Stern (Ed.), Metallurgical and Ceramic Protective Coatings, Chapman & Hall, London, 1996, pp. 112-151.

[32] T. Troczynski and Q. Yang, “Process for Making Chemically Bonded Sol-Gel Ceramics”. U.S. Pat. No. 6,284,682, May, 2001.

[33] T. Olding, M. Sayer and D. Barrow, “Ceramic Sol-Gel Composite Coatings for Electrical Insulation”, Thin Solid Films 398-399 (2001) 581-586.

[34] C. H. Hsueh and P. Miranda, “Modeling of Contact-Induced Radial Cracking In Ceramic Bilayer Coatings on Compliant Substrates”, J. Mater. Res., Vol. 18, No.5, May 2003.

[35] Shaffer, G.D. "An Archaeomagnetic Study of a Wattle and Daub Building Collapse." Journal of Field Archaeology, 20, No. 1. Spring, 1993. 59-75. JSTOR. Accessed 28 January 2007.

[36] "Minerals commodity summary – cement – 2007". US United States Geological Survey. 1 June 2007. Retrieved 16 January 2008.

[37] R P MAHAJAN, K K PATANKAR, M B KOTHALE and S A PATIL," Conductivity, dielectric behaviour and magnetoelectric effect in copper ferrite–barium titanate composites", Bull. Mater. Sci., Indian Academy of Sciences ,Vol. 23, No. 4, pp. 273–279, August 2000.

[38] R. P. MAHAJAN, K. K. PATANKAR, M. B. KOTHALE, S. C. CHAUDHARI, V.LMATHE and S. A. PATIL, " Magnetoelectric effect in cobalt ferrite–barium titanate composites and their electrical properties", P RAMANA, journal of physics, Indian Academy of Sciences, Vol. 58, Nos 5 & 6, pp. 1115–1124,2002.

[39] Arya PR., Jha P., Ganguli AK., *J. Mater. Chem*, 2003, **13**, 415-423.

[40] Xiwei Qi, Ji Zhou, Baorang Li, Yingchun Zhang, Zhenxing Yue, Zhilun Gui and Longtu Li," Preparation and Spontaneous Polarization–Magnetization of a New Ceramic Ferroelectric–Ferromagnetic Composite", Journal of the American Ceramic Society, Volume 87, Issue 10, pages 1848–1852, October 2004.

[41]. Cui Bin., Yu Pengfei., Tian Jing., Guo Huilin., Chang Zhuguo., *Materials Science and Engineering A*, 2007, **454–455**, 667–672

Phys. Lett. 86, 122501, 2005.

[42] ANUJ KUMAR RAY," synthesis and characterization of BaTiO3 powder prepared by combustion synthesis process",thesis B.Sc of technology in ceramic engineering,2007.

[43]. Ramajo L., Parra R., Reboredo M., Zaghete M., Castro M., *Materials Chemistry and Physics*, 2008, **107** 110–114.

[44]. Habib A., R. Haubner., N. Stelzer., *Materials Science and Engineering B*, 2008,**152**, 60–65.

[45] Kenji Kamishima, Yoshitaka Nagashima, Koichi Kakizaki, Nobuyuki Hiratsuka, Kowashi Watanabe, Takaya Mise, Hiroshi Naganuma, and Soichiro Okamura," Simple Process Synthesis of BaTiO3–(Ni,Zn,Cu)Fe2O4 Ceramic Composite", J. Phys. Soc. Jpn. 77, 064801, 4 Pages ,2008 .

[46] M. Venkata Ramana, N. Ramamanohar Reddy, B. S. Murty, V. R. K. Murthy, and K. V. Siva Kumar," ferromagnetic-dielectric Ni0.5Zn0.5Fe1.9O4−δ/PbZr0.52Ti0.48O3 particulate composites electric, magnetic, mechanical, and electromagnetic properties", advances in condensed matter physics, V. 2010, 14 pages ,2010.

[47] Atchara KHAMKONGKAEO, Pongsakorn JANTARATANA , Chitnarong SIRISATHITKUL,Teerapon YAMWONG and Santi MAENSIRI," Frequency-dependent magnetoelectricity of CoFe2O4 − BaTiO3 particulate composites", Trans.Nonferrous Met.Soc.China,21,2438-2442,2011.

[48] M.R.A. Bhuiyan, M.M. Alam, M.A. Momin, M.J. Uddin , M.Islam," Synthesis and Characterization of Barium Titanate (BaTiO3) Nano particle", International journal of Material and Mechanical Engineering,1,21-24,2012.

[49] Joshi, N.J. ; Mater. Res. Cell, Electr. R&D Assoc., Makarpura, India Grewal, G.S. Shrinet, V. Govindan, T.P," Studied Synthesis and Dielectric Behavior of Nano-scale Barium Titanate", Dielectrics and Electrical Insulation, IEEE Transactions on V.19 , Issue: 1, Pp. 83 - 90

[50] D. Bochenek , P. Niemiec , R. Zachariasz , A. Chrobak and G. Ziółkowski," Ferroelectric–Ferromagnetic Composites Based on PZT Type Powder and Ferrite Powder", Archives of Metallurgy and Materials, V. 58, Issue 4, Pages 1013–1017,2013.

[51] Stefanie Haffer, Christian Luder, Till Walther , Roberto Koferstein, Stefan G. Ebbinghaus and Michael Tiemann, " synthesis concept for a nanostructured CoFe2O4/BaTiO3 composite towards multiferroics", Microporous Mesoporous Mater,196,300-304,2014.

[52]Alexander..P.Nosor, Mikhail.A.Semkin,Alexander.E.Teplykh,Sawa.G.Bogdanov et.al," crystal and magnetic state of multiferroic composites (x)MFe2O4 + (1-x)BaTiO3, M = Ni, Co", solid state phenomena ,V.233-234,PP.371-374,2015.

[53]. A. S. Tatarenko, V. Gheevarughese, G. Srinivasan, O. V. Antonenkov and M. I. Bichurin, **J.Electroceram. 24 (1) (2010) 24:5–9.**

M. I. Bichurin, **J.Electroceram. 24 (1) (2010) 24:5–9.**

[54]. T.H. O'Dell, **Electronics and Power 11 (1965) 266.**

[55] S. Priya, R. Islam, S. Dong, D. Viehland, J Electroceram. 19 (2007) 147.

[56] A. D. P. Rao, Nuovo-Cimento B, 20 (1998) 199.

[57] B. K. Das, G. C. Jain, IEEE Transactions on Magnetics, 18 (1982) 2.

[58] P. S. Anil kumar, J. J. Shrotri, S.D. Kulkarni,C. E. Deshpande, S. K. Date, Matter. Lett., 27 (1996) 293.

[59] T. B. Rummery, J. J. Hawton and D. Owen, Corrosion, 33 (1977) 369.

[60] S. W. Cheong and M. Mostovoy, "Multiferroics: a magnetic twist for ferroelectricity" ,Nature Mater.,Vol. 6,P.13, 2007.

[61] Y. Torh, A. Tsuziki, K. Kato, Y. Uwamino, B. H. Choi, M. J. Lee, Mater. Sci., 31 (1996) 2603.

[62] V. Moye, K. S. Rane, V. N. Kamat Dalal, J. Mater. Sci. Mater. Electr., 1 (1990) 212.

[63] P. Lahari and S. K. Sengupta, J. Chem. Soc., Faraday Trans., 91 (1995) 3489.

[64] Wenk, Hans-Rudolf; Bulakh, Andrei (2004). Minerals: Their Constitution and Origin. New York, NY: Cambridge University Press. p. 413. ISBN 978-0521529587.

[65] Carter C. Barry, Norton M. Grant, Ceramic materials – Science and Engineering,Springer, 2007,xxii, 716p.,848 illus.

[66] W. Lu , M. Quilitz, H. Schmidt, ―Nanoscaled BaTiO3 powders with a large surface area synthesized by precipitation from aqueous solutions: Preparation, characterization and sintering‖ , Journal of the European Ceramic Society 27 (2007) 3149–3159.

[67] N. Halder, D. Chattopadhyay, A. Das Sharma, D. Saha, A. Sen, H.S. Maiti, ―Effect of sintering atmosphere on the dielectric properties of barium titanate based capacitors‖ , Materials Research Bulletin 36 (2001) 905–913.

[68]Wadhawan, Vinod K. (2000). ―Introduction to ferroic materials‖ . CRC Press. p. 10. ISBN 9789056992866.

[69] Y. Jung, E. Na, U. Paik, J. Lee, J. Kim, Mater. Res. Bull. 37 (2002) 1633.

[70] Spaldin, Nicola A. (2010). "9. Ferrimagnetism". Magnetic materials : fundamentals and applications (2nd ed.). Cambridge: Cambridge University Press. pp. 113–129. ISBN 9780521886697.

[71] L. Néel, Propriétées magnétiques des ferrites; Férrimagnétisme et antiferromagnétisme, Annales de Physique (Paris) 3, 137-198 (1948).

[72] Jump up ^ Klein, C. and Dutrow, B., Mineral Science, 23rd ed., Wiley, p. 243

[73] C. D. Stanciu, A. V. Kimel, F. Hansteen, A. Tsukamoto, A. Itoh, A. Kirilyuk, and Th. Rasing, Ultrafast spin dynamics across compensation points in ferrimagnetic GdFeCo: The role of angular momentum compensation, Phys. Rev. B 73, 220402 (R) (2006).

[74] Sessoli, Roberta; Tsai, Hui Lien; Schake, Ann R.; Wang, Sheyi; Vincent, John B.; Folting, Kirsten; Gatteschi, Dante; Christou, George; Hendrickson, David N. (1993). "High-spin molecules: [Mn12O12(O2CR)16(H2O)4]". J. Am. Chem. Soc. 115 (5): 1804–1816. doi:10.1021/ja00058a027.

[75] G. F. Goya, H. R. Rechenberg, J. Z. Jiang J. Appl. Phys., 84(1998), p.1101-1108.

[76] S.D. Sartale, C.D. Lokhande, M. Muller, "Electrochemical synthesis of nanocrystalline CuFe2O4 thin films from non-aqueous (ethylene glycol) medium", Mater. Chem. Phys., 80(2003), p.120–128.

[77] Z. Sun, L. Liu, D.z. Jia, W. Pan, "Simple synthesis of CuFe2O4 nanoparticles as gassensing materials", Sens. Actuators, B: Chem. 125 (2007), p. 144–148.

[78] K.-S. Kang, C.-H. Kim, W.-C. Cho, K.-K. Bae, S.-W. Woo, C.-S. Park, "Reduction characteristics of CuFe2O4 and Fe3O4 by methane; CuFe2O4 as an oxidant for two-step thermochemical methane reforming", Int. J. Hydrogen Energy, 33(2008), p.4560–4568.

[79] R.K. Selvan, N. Kalaiselvi, C.O. Augustin, C.H. Doh, C. Sanjeeviraja, "CuFe2O4/SnO2 nanocomposites as anodes for Li-ion batteries'', J. Power Sources, 157(2006), p.(522–527).

[80] S. Roy, J. Ghose, "Mössbauer study of nanocrystalline cubic CuFe2O4 synthesized by precipitation in polymer matrix", J. Magn. Magn. Mater., 307(2006), p. 32–37.

[81] R.K. Selvan, C.O. Augustin, L.J. Berchmans, R. Saraswathi, "Combustion synthesis of CuFe2O4", Mater. Res. Bull., 38(2003), p. 41–54.

[82] M. Sultan, R. Singh, "Magnetization and crystal structure of RF-sputtered nanocrystalline CuFe2O4 thin films", J.Mater. Lett., 63,(2009), p.1764–1766.

[83] W. Ponhan, S. Maensiri, "Fabrication and magnetic properties of electrospun copper ferrite (CuFe2O4) nanofibers", Solid State Sci. 11(2009), p.479–484.

[84] N.Rezlescu and E.Rezlescu, "dielectric behavior of copper ferrite", physica status solidi (a), 23(1974), p.575-582.

[85] S.W.Cheong , Maxim Mostovoy,“Multiferroics : a Magnetic twist for ferroelectricity”, Nature Materials ,Vol.6,p.13 ,2007.

[86] Special issue," Special Sections Containing Papers on Multiferroics and On Multiferroics and Manganites", J. Phys. Condens. Matter .20, 434201–434220 ,2008.

[87] B. B.vanAken et al., Nature Mater.,Vol. 3,p. 164 ,2004.

[88] T. Kimura, T. Goto, H. Shintani, K. Ishizaka, T. Arima and Y. Tokura, “Magnetic control of ferroelectric polarization”, Nature ,Vol.426, p.55 ,2003.

[89] N. Hur et al.,“Electric polarization reversal and memory in a multiferroic material induced by magnetic fields”, Nature. ,Vol.429, p.392, 2004.

[90] T .Arima," Ferroelectricity induced by proper-screw type magnetic order", J. Phys. Soc. Jpn 76, 073702 ,2007.

[91] K. K. Patankar, V. L. Mathe, R. P. Mahajan, S. A. Patil, R. M. Reddy, K. V. SivaKumar, Materials Chemistry and Physics, 72 (2001) 23.

[92] M. B. Kothale, K. K. Patankar, S. L. Kadam, V. L. Mathe, A. V. Rao, B. K. Chougule, Materials Chemistry and Physics, 77 (2002) 691.

[93] W. Eerenstein, N. D. Mathur, and J. F. Scott, Nature 442, 759 (2006).

[94] X. W. Qi, J. Zhou, Z. X. Yue, Z. L. Gui, L. T. Li, and S. Buddhudu, Adv.

Funct. Mater. 14, 920 (2004).

[95] J. Q. Huang, P. Y. Du, L. X. Hong, Y. L. Dong, and M. C. Hong, Adv. Mater. 19, 437 (2007).

[96] J. Ma, J. M. Hu, Z. Li, and C.-W. Nan, Adv. Mater. 23, 1062 (2011).

5H. Zheng, L. Li, Z. J. Xu, W. J. Weng, G. R. Han, N. Ma, and P. Y. Du,

J. Appl. Phys. 113, 044101 (2013).

[97] H. Zheng, L. Li, Z. J. Xu, W. J. Weng, G. R. Han, N. Ma, and P. Y. Du,J. Phys. D: Appl. Phys. 46, 185002 (2013).

[98] K. K. Patankar, V. L. Mathe, R. P. Mahajan, S. A. Patil, R. M. Reddy, and

K. V. SivaKumar, Mater. Phys. Chem. 72, 23 (2001).

[99] X. M. Chen, Y. H. Tang, I.-W. Chen, Z. C. Xu, and S. Y. Wu, J. Appl.Phys. 96, 6520 (2004).

[100] Z. Yu and C. Ang, J. Appl. Phys. 91, 794 (2002).

[101]Y. J. Li, X. M. Chen, R. Z. Hou, and Y. H. Tang, Solid State Commun.137, 120 (2006).

[102] Q. H. Jiang, Z. J. Shen, J. P. Zhou, Z. Shi, and C.-W. Nan, J. Eur. Ceram Soc. 27, 279 (2007).

[103] H. F. Zhang, S. W. Or, and H. L.W. Chan, J. Appl. Phys. 104, 104109 (2008).

[104]H. F. Zhang and P. Y. Du, Solid State Commun. 149, 101 (2009).

14L. P. Curecheriu, M. T. Buscaglia, V. Buscaglia, L. Mitoseriu, P. Postolache, A. Ianculescu, and P. Nanni, J. Appl. Phys. 107, 104106 (2010).

[105]Q. Chen, P. Y. Du, W. Y. Huang, L. Jin, W. J. Weng, and G. R. Han,Appl. Phys. Lett. 90, 132907 (2007).

[106]W. D. Kingery, H. K. Bowen, and D. R. Uhlmann, Introduction to Ceramics (Wiley, New York, 1976).

[107] C. W. Nan, Prog. Mater. Sci. 37, 1 (1993).

[108] Hong-Jian Feng, Fa-Min Liu,Department of Physics, School of Sciences,Beijing University of Aeronautics & Astronautics, Beijing 100083, P. R. China.

[109] Dr. Marta Deri.“Ferrlelectric Ceramics”Maclaren &Sons Ltd. London(1966).

[110] S.O Pallai.“Introduction to solid state physics” Himalaya pulishig House (2008).

[111] B.M. Tareev, N.V.Korotkova, V.M. Petrov , A.A.Preobrazhensky “Electrical and Radio Engineering Materials” MIR Publishers, Moscow (1980).

[112] Francis S.Galasso ”Structure, properties and preparation of pervoskite type compounds”Published by Pergamon press (1969)

[113] Yun Wu , Guozhong Cao,“ Materials Science and Engineering” University of Washington Seattle,Washington 98195(2000).

[114] Zuo-Guang Ye,"Handbook of dielectric, piezoelectric and ferroelectric materials Synthesis, properties and applications ", Wood head Publishing Limited,(2008).

[115] R. Ramesh, N.A. Spaldin, Nat. Mater. 6 (2007) 21.

[116] Tahseen H. Mubarak, Ph. D thesis, University of Technology, (2003).

[117] B.D. Stojanovic, J. Mater. Proc. Technol. 78, 143, (2003).

[118] B. D. Cullity. Elements of x-ray diffraction. 2nd edition. Addison wesley publishing company, canada(1978).

[119] J.A. Gomes, M.H. Sousa, G. J. da Silva, F.A. Tourinho, J. Mestnik-Filho, R. Itrid,G.de M. Azevedo, J. Depeyrot. Cation distribution in copper ferrite nanoparticles of ferrofluids:A synchrotron XRD and EXAFS investigation. Journal of Magnetism and Magnetic Materials, 300, 213–216 (2006).

[120] B. B. He, Introduction to two-dimensional X-ray diffraction, Powder Diffraction, Vol. 18, No2, June 2003.

[121] W. Wang, C. Shi, X. Su, H. Xing, J. Zhang, Mater. Res. Bull. 41, 2018 (2006).

[122] Ponhan W and Maensiri S, Solid State Sci, 11 (2009) 479.

[123] Waldron, R.D., Phy. Rev. 9: 1727 (1955).

الخلاصــة

في هذه الدراسة تم تحضير المواد المركبة ($BaTiO_3+CuFe_2O_4$) باستخدام الطريقة الكيميائية الحديثة (sol-gel auto combustion) التي تكونت من قبل تيتانات الباريوم (BaTiO) بالجمع مع فرايت النحاس ($CuFe_2O_4$) التي صنعت باستخدام أوكسيد التيتانيوم (TiO_2) ،ونترات الباريوم ($Ba(NO_3)_2$)،ونترات الحديديك ($Fe(NO_3)_3.9H_2O$)، حامض الستريك ($C_6H_8O_7.H_2O$)، نترات النحاس ($Cu(NO_3)_2.3H_2O$) ومحلول الامونيا . تيتانات الباريوم أحرقَ عند درجة (800°C) لمدة ثلاث ساعات ثم اخراجها من الفرن وخلطها في موتر مرة اخرى ووضعها في بودقة واحرقَ عند درجة حرارة (1200°C) وتبرد في درجة حرارة الغرفة . فرايت النحاس احرقَ عند درجة حرارة تتراوح مابين (200-220°C) وتبرد في درجة حرارة الغرفة ثم كلسنة عند الدرجة (400°C) درجة حرارة مئوية لمدة ثلاث ساعات. وتكررت هذه العملية للمواد المركبة الفيروكهربائية فيريمغناطيسية $[(BaTiO_3)_x+(CuFe_2O_4)_{1-x}]$ مع اختلاف التراكيز حيث إن (x=0.1,0.2,0.3,0.4,0.5,0.6,0.7,0.8,0.9 and 1) يتم مزج جيد وطحنها معاً ومن ثم يتم حرق كل مزيج عند درجة (800°C) لمدة ثلاث ساعات ومن ثم يطحن الناتج جيداً وبعدها يكبس بقوالب ذات قطر 1.2 سم ويلبد عند درجة حرارة (950°C) لمدة ثلاث ساعات .

تم دراسه الخصائص التركيبية لفرايت النحاس وتيتانيات الباريوم والخصائص التركيبية والكهربائية والعزلية للمواد المتراكبة باستخدام العديد من القياسات مثل(حيود الاشعة السينة (XRD). تحويل فورير للاشعة تحت الحمراء (FTIR)- المجهر الالكتروني الماسح (SEM)- مجهر القوة الذرية (AFM)- وجهاز قياس الخواص الكهربائية والعزلية باستخدام (LCR-meter) .حيث اظهر تحويل فورير للاشعة تحت الحمراء للنموذج تيتانات الباريوم النانوية المحضرة وجود الحزم ضمن نطاق من (522سم$^{-1}$) الى (547سم$^{-1}$) عائدة لرابطة اوكسجين- فلز(تيتانيوم) ، وظهرت حزم ضمن نطاق من (459سم$^{-1}$) الى (584سم$^{-1}$) عائدة الى رابطة اوكسجين – فلز (النحاس) وكذلك ظهرت حزم ضمن النطاق 400-450cm^{-1} and 550-600 عائدة الى رابطة اوكسجين – فلز (تيتانيوم – نحاس).

ان تحليل الطور الكيميائي التي تمت باستخدام جهاز قياس حيود الاشعة السينية XRD يؤكد تكون فيرايت النحاس (سبنل فيرايت)، تيتانيات الباريوم (بيروفسكايت) والمواد المتراكبة بينهما. حيث اظهرت دراسة حيود الاشعة السينية ان حجم البلورة يزداد مع زيادة درجات حرارة الكلسنة لمسحوق فرايت النحاس.بينما

وجد ان حجم البلورة يزداد مع زيادة تركيز تيتانيات الباريوم ونقصـان تركيز فيرايت النحاس وكذلك وجد ان ثابت الشبيكة يتناقص (يقل) مع الزيادة تركيز تيتانيات الباريوم.

صور المجهر الالكتروني الماسحSEM للمساحيق المحضرة تبين بان حجم الجسيمات اقل من 100 نانومتر. اما اشكال مجهر القوة الذرية AFM بينت ان الدقائق صغيرة جدا ضمن المدى حدود النانو.

تم دراســة الخواص الكهربائيه والعزلية لمســاحيق المتراكبة لجميع العينات الملبدة عند 950م^0 بأســتخدام LCR-meter ضمن المدى الترددي (50هيرتز -5 ميكا هيرتز) .وتم قياس المقاوميه كدالة للتردد ولجميع العينات المحضـرة عند 950م^0 حيث وجد ان المقاومية تقل مع ازدياد التردد.ووجد ان ثابت العزل (ε_r') وفقد الظل($\tan\delta$) و فقد العازل (ثابت العزل الخيالي)(ε_r'') من خلال بيانات السـعة اذ يلاحظ بان هذه المعلمات تتناقص مع زيادة التردد.وهذا السـلوك يطابق سـلوك فيرايت. بينما اظهرت النتائج بان التوصـلية الكهربائية تتزايد مع التردد, اما عامل الفقد يقل بزيادة التردد.

جمهورية العراق
وزارة التعليم العالي والبحث العلمي
جامعة ديالى ـــ كلية العلوم

المواد المركبة الفيروكهربائية الفيرو مغناطيسية

رسالة مقدمة

الى

مجلس كلية العلوم – جامعة ديالى

وهي جزء من متطلبات نيل درجة ماجستير علوم في الفيزياء

من قبل

علي احمد حسن

(بكالوريوس علوم فيزياء 2013)

بإشراف

أ. د. تحسين حسين مبارك

أ. م.د .صباح محمد علي

1438 هـ

2017 م